UNIVERSITA' DEGLI STUDI DI PAVIA

FACOLTA' DI INGEGNERIA
DIPARTIMENTO DI INGEGNERIA INDUSTRIALE E DELL'INFORMAZIONE

DOTTORATO DI RICERCA IN BIOINGEGNERIA E BIOINFORMATICA
XXXI CICLO - 2018

UNVEILING THE MOLECULAR MECHANISM OF AUTOLOGOUS MICRO GRAFT-BASED THERAPY FOR SKIN REGENERATION THROUGH A BIOINFORMATIC APPROACH

PhD Thesis by

Martina Balli

Advisor:
Prof. Maria Gabriella Cusella De Angelis

Prof. Maurilio Sampaolesi

Prof. Frederic Lluis Vinas

PhD Program Chair:
Prof. Riccardo Bellazzi

KU Leuven
Biomedical Sciences Group
Faculty of Biomedical Sciences
Department of Development and Regeneration
Stem Cell and Developmental Biology

UNVEILING THE MOLECULAR MECHANISM OF AUTOLOGOUS MICRO GRAFT-BASED THERAPY FOR SKIN REGENERATION THROUGH A BIOINFORMATIC APPROACH

Martina Balli

Jury:

Promoter: Prof. Maurilio Sampaolesi
Co-promoter: Prof. Frederic Lluis Vinas
Chair: Prof. Rik Lories
Jury members: Prof. Michael Casaer
Prof. Jan Vranckx

Dissertation presented in partial fulfilment of the requirements for the degree of Doctor in Biomedical Sciences

January 2019

It's not about perfect. It's about effort.

And when you bring that effort every single day.

That's where transformation happens.

That's how change occurs.

Contents

Contents 2

Acknowledgments 5

List of abbreviations 7

Abstract (English) 11

Abstract (Italian) 13

Chapter 1 15

1.1 The wound healing process, its temporal sequences and its importance ... 16

1.1.a Inflammatory phase 17

1.1.b Proliferative and migratory phase 19

1.1.c Remodelling phase 21

1.2 Impaired wound healing and its consequences 22

1.3 Growth factors, cytokines and related signalling pathways involved in skin wound healing 24

1.3.a The MAPK signalling pathway cascade 27

1.4 Matrix metalloproteinases expression regulated by MAPK signalling pathway and their involvement in wound healing 29

1.5 Use of network and transcriptome analysis for regenerative medicine 32

1.6 Wound care therapies: from conventional to regenerative scar-free treatment 34

1.6.a Autologous micro graft-based treatment in wound healing 35

Chapter 2 37

Chapter 3 40

3.1 Cell culture 41

3.2 Autologous micro graft via Rigenera® protocol 41

3.3 *In vitro* wound healing model - cell scratch assay, imaging and quantification 42

3.4 Cellular viability assay 42

3.5 Cell proliferation assay 43

3.6 Immunostaining of wounded cells/tissues treated with micro graft-based therapy 44

3.7 Protein analysis 44

3.8 Mouse antibody array membrane 45

3.9 Cell migration assay 46

3.10 RNA extraction, cDNA synthesis and gene expression analysis 46

3.11 Transcriptome analysis through RNA sequencing (RNA-seq) analysis 48

3.11.a Single-subject transcriptome analysis (SSA) 49

3.11.b Network-based analysis 52

3.11.c Network Analysis 53

3.12 *In vivo* wound healing assay 54

3.13 Statistical analysis 55

Chapter 4 56

4.1 Autologous micro graft-based therapy increases cell migration and accelerates scratch closure 57

4.2 Soluble AMG fraction improves cell scratch closure acceleration compared to unprocessed micro grafts 63

4.3 Revealing the molecular mechanism of AMG-based treatment through knowledge-based gene association networks 67

4.4 Matrix metalloproteinases regulate AMG-based cell migration in an *in vitro* model of wound healing 79

4.5 Autologous micro graft-based treatment induces ERK signalling pathway activation to promote cell migration 82

4.6 MMPs expression requires ERK signalling pathway activation to promote micro graft-based cell migration 86

4.7 MEK/ERK inhibition impairs *in vivo* AMG-dependent wound healing..... 87

Chapter 5 90

Appendix 100

Literature References 176

Acknowledgments

Sampa Lab thank you for accepting me in the group and for all the great moments that we spent together in these years. I'll never forget them. Dear Giorgia and Natacha I'll never forget what you have done for me when I just arrived. I was lost and your kindness really helped me, thank you!

Hannina mia, thank you for all the help and for all the time you where there with your essential oils to calm me down and to support me, exctacly how you do with all of us.

Dear Jordi, Enrico, Nefele, Domi and Robin thank you for all the moments we spent together.

Thanks to all the Stem Cell Institute Leuven and to make this experience even more unique.

Caro Maurilio, nonostante la nostra relazione sia stata altalenante ci tengo a ringraziarti per avermi portata in Belgio e avermi fatto superare delle paura che mi portavo dentro. Ho sempre pensato ci fosse un motivo per tutto e quando ne ho capito la ragione ho imparato a conoscere una nuova parte di me. Grazie per avermi fatta crescere.

Lluis Lab I don't have enough words to thank you to have adopted me in the group and let me feel part of it from the very beginning. Anchelito thank you for always being there for me and letting me feel supported and protected just how a brother would do. I'll never forget it. Willy even though I'm on your black list I want to thank you for all the great moments (especially for all your cooking skills) and to be always ready to help. I'm sure will be a great team. Jonathan and Youssef thank you for all the laughing. Last but absolutely not least, dear Fredy, I don't have words to thank you for all you have done for me, to have believed in me more than whoever else (even more than myself) and to have guided and mentored me during these years. I wouldn't have achieved all of that without you, THANK YOU!

Cari Mamma e Papà vi prometto che farò di tutto per realizzare tutti i sogni che non avete potuto realizzare perchè troppo impegnati a realizzare i miei. Non vi ringrazierò mai abbastanza per tutti i vostri sacrifici. Vi voglio bene!

Kika mia, abbiamo iniziato con il piede sbagliato da piccole, ma adesso non potrei immaginare la mia vita senza te accanto. Grazie per tutte le volte in cui hai fatto di tutto per farmi distrarre, calmare, rilassare e farmi ricordare che la cosa più importante è la famiglia.

Adrian, ukochany, nie spodziewałam się Ciebie, ale pojawiłeś się, by zmienić wszystko. Dziękuję! Dziękuję za to, że widziałeś naszą przyszłość, zanim ja ją zobaczyłam; za wiarę w nas i za to, że walczyłeś o nas tak mocno. Dziękuję za pokazanie mi swojego wyjątkowego punktu widzenia i niesamowitej perspektywy nas razem. Nigdy nie podziękuję Ci wystarczająco za to, że zawsze jesteś przy mnie, wierzysz we mnie, wspierasz mnie, podczas najgorszych dni mówisz "wszystko będzie dobrze", za nauczenie mnie jak słuchać siebie i przede wszystkim za to, że okazujesz mi miłość w tak fantastyczny sposób. Nie dotarłabym tutaj bez Ciebie. Jest tak wiele rzeczy, które chciałabym Ci powiedzieć... ale zacznę od trzech bardzo ważnych rzeczy:

1. To zaszczyt kochać Ciebie.

2. Kiedy Cię spotkałam, odnalazłam swój brakujący fragment układanki.

3. Rozjaśniasz każdy mój dzień.

Resztę odkryjmy razem, z obietnicą, że zawsze będę przy Tobie. Kocham Cię, z samej głębi mej duszy.

List of abbreviations

WH	Wound Healing
AMG	Autologous Micro Graft
ERK	Extracellular signal-regulated kinase
MAPK	Mitogen-activated protein kinase
MMPs	Matrix Metallopreteinases
ECM	Extracellular Matrix
DAMPs	Damage-associated molecular patterns
PAMPs	Pathogens-associated molecular patterns
TLRs	Toll-like Receptors
NF-κB	Nuclear factor kappa-light-chain-enhancer of activated B cells
M1	Type 1 Macrophages
M2	Type 2 Macrophages
TNF-α	Tumour Necrosis Factor-alpha
ECs	Endothelial cells
EPCs	Endothelial Progenitor Cells
TIMPs	Tissue inhibitor of Matrix Metalloproteinases

EGF	Epidermal Gwh Factor
FGF	Fibroblast Growth Factor
IGF	Insulin-like Growth Factor
KGF	Keratinocyte Growth Factor
PDGF	Platelet-Derived Growth Factor
TGF-β	Transforming Growth Factor Beta
VEGF	Vascular Endothelial Growth Factor
FDA	Food and Drug Administration
EGFR	Epidermal Growth Factor Receport
EMT	Epithelial-To-Mesenchymal Transition
BMPs	Bone Morphogenic Proteins
α-SMA	Alpha-Smooth Muscle Actin
JNK	c-Jun amino-terminal kinase
AP-1	Activator Protein 1
Tcf-4	Transcription Factor 4
HB-EGF	Heparin Binding EGF-like growth factor
ATF	Activating Transcription Factor

NGS	Next Generation Sequencing
RNA-seq	RNA-sequecing
DNA	Deoxyribonucleic acid
cDNA	Complementary DNA
RNA	Ribonucleic acid
GO	Gene Ontology
WHO	World Health Organization
EdU	5-ethynyl-2´-deoxyuridine
PI	Propidium Iodide
PEG	Polyethylene Glycol
IGFBPs	Insulin-Like Growth Factor Binding Proteins
Gapdh	Glyceraldehyde 3 phosphate dehydrogenase
Rpl13a	Ribosomal Protein L13a
RFU	Relative Fluorescence Units
FDR	False Discovery Rate
FC	Fold Change
RWA	Relative Wound Area

SSA	Single-Subject transcriptome Analyses

Abstract (English)

Traumatic acute injuries and chronic wounds, are leading health and economic problems, hindering patient life, requiring long-term hospitalization and contributing to mortality. Eleven million people worldwide require medical attention yearly, the majority belonging to countries lacking proper medical services. A more complete and deep view of the molecular mechanisms involved in the healing process and its failure is required to speed up the discovery of suitable therapies for impaired wound conditions, acute wound repair acceleration and scarring reduction. Improvement of the wound healing (WH) process denotes the goal of the tissue regeneration. Autologous skin micro grafts (AMG)-based therapies have emerged as an advanced and highly effective new treatment for WH repair, although, detailed mechanistic studies explaining their beneficial effect are still missing. Wound repair is composed by an integrated combination of biological and molecular events, which includes cell migration, proliferation and remodelling of extracellular matrix. In this work, we show how soluble AMG fraction is enriched by a myriad of pro-motility growth factors such as epidermal growth factor (EGF), fibroblast like growth factor (bFGF) and transforming growth factor beta (TGF-β). AMG-based treatments increase cell migration and accelerate scratch closure without affecting cell viability or cell proliferation. In accordance, comparative transcriptome analysis of AMG-treated and untreated cells shows enrichment in cell migration pathways. This may be due because AMG-based treatment induces ERK (extracellular signal-regulated kinase) signalling pathway activation and increases significantly metalloproteinase (MMPs) family transcriptional expression and extracellular MMPs enzymatic activity. In addition, MEK/ERK or MMPs activity inhibition significantly reduces either AMG-dependent cell migration and scratch closure *in vitro* as wound healing *in vivo*. Our results demonstrate for the first time that growth factors present in the soluble fraction of AMG drive ERK activation in treated cells, which in turn up-regulates matrix metalloproteinase (MMPs) expression and their enzymatic activity, resulting in accelerated cell migration and faster *in vivo* wound healing.

Therefore, our study sheds light on the molecular mechanisms of AMG-based treatments, which will allow increasing its efficacy in tissue regeneration, accelerating the healing of acute wounds and eventually extending its application to chronic WH disorders.

Abstract (Italian)

Lesioni traumatiche acute e ferite croniche, come ferite e ustioni, rappresentano un grave problema pubblico di salute ed economico, ostacolando la qualità della vita dei pazienti, richiedendo lunghi ricoveri e contribuendo alla mortalità. Undici milioni di persone in tutto il mondo necessitano cure mediche ogni anno e la maggior parte appartengono a paesi poco industrializzati che non dispongono di servizi medici adeguati. Una visione più completa e profonda dei meccanismi molecolari coinvolti nel processo di guarigione delle ferite e dei suoi fallimenti è necessaria al fine di sollecitare la scoperta di nuove efficienti terapie, che siano in grado di stimolare la rigenerazione delle ferite, limitando la formazione di cicatrici. Il miglioramento del processo di guarigione delle ferite (chiamato in inglese *wound healing* - WH) indica l'obiettivo della del campo di ricerca chiamato rigenerazione dei tessuti. Negli ultimi anni, le terapie autologhe di micro-innesti cutanei (AMG) sono emerse come un nuovo ed efficace trattamento per la rigenerazione dei tessuti ed il miglioramento dell'aspetto delle cicatrici, sebbene non siano ancora disponibili dettagliati studi meccanicistici che spieghino il meccanismo molecolare alla base del loro effetto benefico. Il processo di rigenerazione delle ferite è costituito da una combinazione di eventi biologici e molecolari, includenti migrazione cellulare, proliferazione cellulare e il rimodellamento della matrice extracellulare. In questo lavoro, mostriamo in che modo la frazione solubile degli AMG sia arricchita da una miriade di fattori di crescita, incluso il fattore di crescita epidermico (EGF), il fattore di crescita fibroblastico (bFGF) e il fattore di crescita beta trasformante beta (TGF-β), svolgenti ruoli essenziali nella regolazione della migrazione cellulare. I trattamenti basati su AMG stimolano la migrazione cellulare ed accelerano la chiusura delle ferite senza compromettere la vitalità cellulare e non causando cambiamenti a livelli del ciclo cellulare. In accordo, l'analisi comparativa del trascrittoma eseguita su cellule danneggiate sia trattate con AMG che non trattate mostra un arricchimento di processi biologici relativi alla regolazione della migrazione cellulare. Ciò potrebbe essere dovuto al fatto che il trattamento basato su AMG induce l'attivazione della cascata di segnalazione MAPK – RAS,

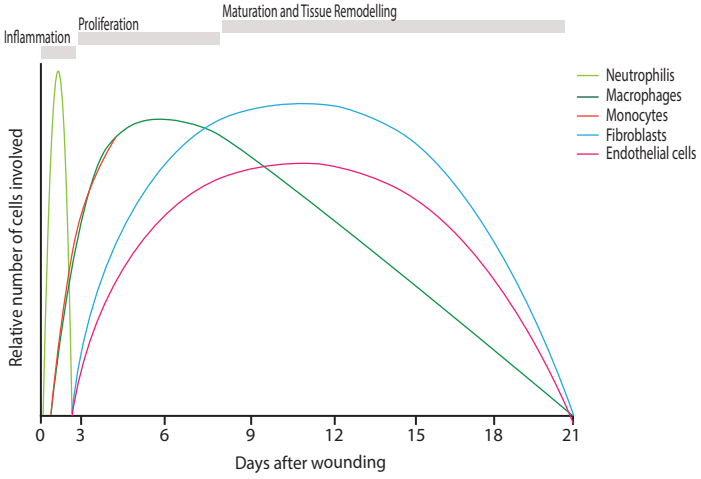
RAF, MEK ed ERK, la quale aumenta significativamente sia l'espressione trascrizionale della famiglia delle metalloproteinasi (MMPs) sia la loro attività enzimatica. Inoltre, l'inibizione dell'attività di entrambe MEK / ERK o MMPs riduce significativamente la migrazione cellulare AMG-dipendente e di conseguenza la chiusura delle ferite sia *in vitro* che *in vivo*. I nostri risultati dimostrano per la prima volta che gli AMG contengono importanti fattori di crescita, i quali ne caratterizzano la frazione solubile e partecipano attivamente all'attivazione della cascata di segnalazione di ERK nelle cellule trattate. Tale regolazione positiva induce a sua volta sia l'espressione sia l'attività catalitica delle metalloproteinasi (MMP), risultando in una migrazione cellulare accelerata e di conseguenza portando ad una più veloce guarigione delle ferite *in vivo*. Pertanto, il nostro studio fa luce sul meccanismo molecolare alla base dei trattamenti basati su AMG, il quale consentirà di comprenderne meglio la funzione ed aumentare la sua efficacia ed applicabilità nella rigenerazione dei tessuti, accelerando la guarigione di ferite acute e, possibilmente, estendendo la sua applicazione a condizione di ferite croniche.

Chapter 1

General Introduction

1.1 The wound healing process, its temporal sequences and its importance

The skin, the largest organ of the body, plays a key role in protection against mechanical forces, infections and fluid/thermal deregulation [1]. However, its functions can be diminished due to skin damages, such as traumatic acute injuries and chronic wound conditions. In the wound healing (WH) process, cells, extracellular matrix (ECM) and growth factors interact together to repair these damages in three overlapping and highly regulated sequential phases: inflammation, cell proliferation and cell migration, in which the epithelialization and the angiogenesis processes take place, and finally the tissue remodelling phase (Figure 1). [2]. Many factors including metabolic disorders (type II diabetes), age, oxygenation, hormones and life style habits can interfere and restrain skin repair (stress, nutrition, smoking) [3]. Without the accurate recovery of wounds, skin functions and in turn life quality of patients is hindered. Although the wound healing process, its molecular mechanism and phases, are widely explored, a deeper understanding of its process with the involvement of essential and new signalling pathways represents a new perspective of the regenerative medicine, supporting the importance of the research in this field.



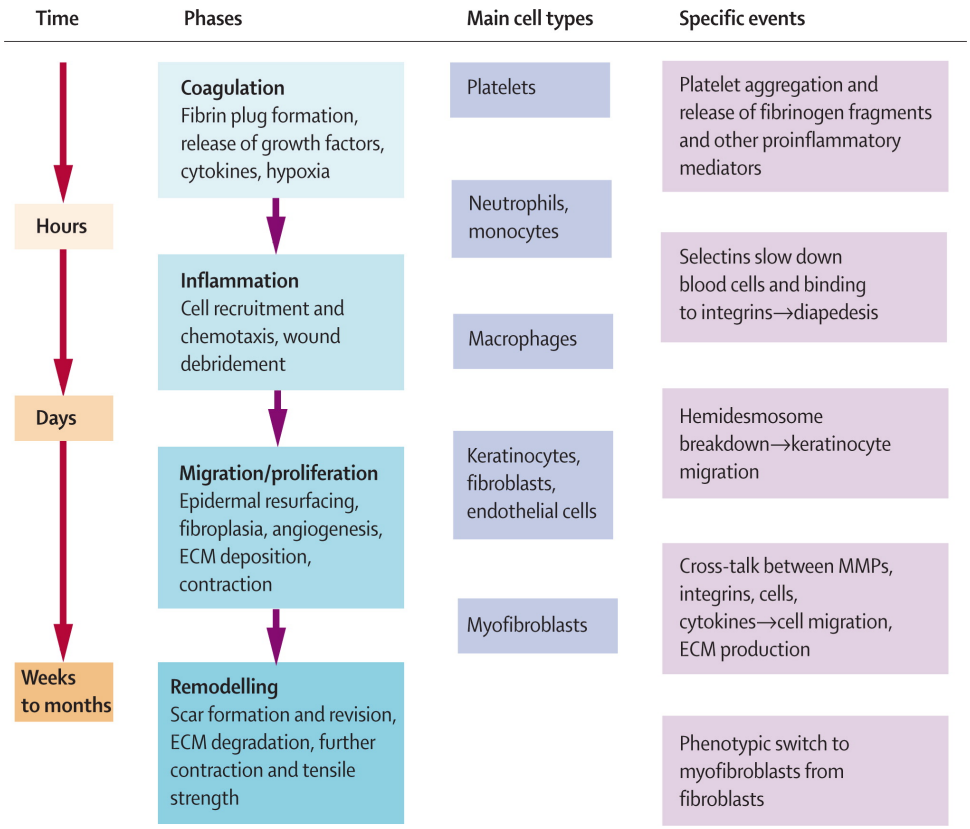


Figure 1: The wound healing process, its physiological stages and related events. The physiological process of the wound healing consists of 3 overlapping and sequential phases, known as inflammatory phase, which include the coagulation phase, proliferative phase and tissue remodelling phase. Cellular components of the immune system and other different cell types, ECM remodelling events and soluble factors interact together leading to the restoration of the tissue damage. Image adapted from [4].

1.1.a Inflammatory phase

When an injury occurs, an orchestrated and synchronized cellular and biological response starts to compensate the damage leading to the wound repair. The first phase of the wound healing process – inflammation - takes place

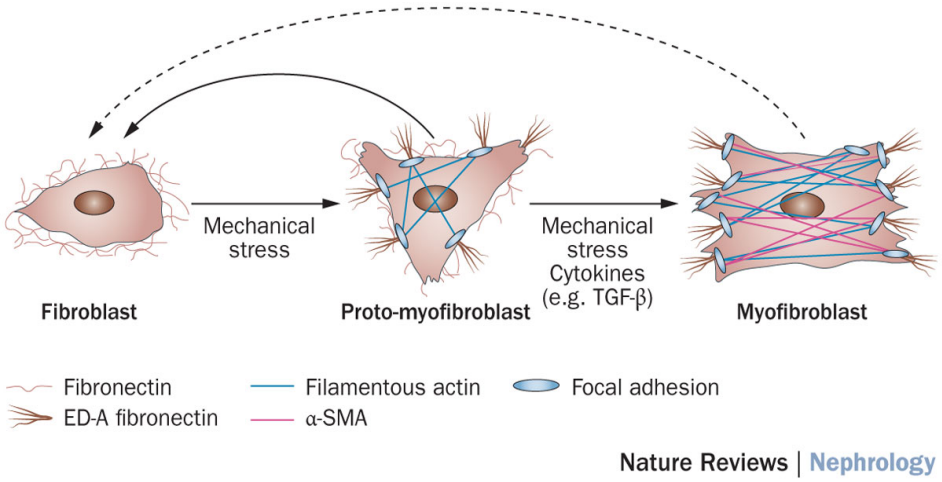
immediately after the creation of the damage. After an injury, upon cytokines, Damage-associated molecular patterns (DAMPs) and Pathogen-associated molecular signals (PAMPs), recognized by specific receptors, including the toll-like receptors (TLRs), several signalling pathways, such as Mitogen-activated signalling pathway (MAPKs) and Nuclear factor kappa-light-chain-enhancer of activated B cells (NF-κB) are activated and synchronized to respond to the damage secreting many cytokines and antimicrobial peptides [5]. In this frame, the coagulation cascade, the inflammatory pathways and the immune system are collectively activated to stop blood/fluid loss and leading to migration of immune cells into the wound site [2]. This essential phase is characterized from the blood clot formation (also known as haemostasis phase), which act as a temporary wound matrix, allowing migration of different cell types. Moreover, in response to the presence of cytokines/chemokines and growth factors, activation of inflammatory cells leads to the phagocytosis of bacteria/cell debris from the injured wound site. Among those, in response to the cytokine gradient and/or to DAMPs, monocytes infiltrate the wound site and differentiate in macrophages to further support the healing process and to promote and resolve the inflammation phase [5] [6]. Many studies on impaired wounds showed that the permanent competition between inflammatory and anti-inflammatory signals represents the cause of the impairment [7]. The essential role of this first phase of the healing process is restraining the infection and cleaning up the wound site, which will lead to the second phase of the process – proliferative/migration phase. Inflammatory cells, such as macrophages are the key regulators of these tasks and, moreover, of the transition from inflammation to proliferation phase, during the wound healing. At the wound site and in response to the cytokines/chemokines gradient, macrophages differentiate into their pro-inflammatory phenotype (also known as M1 macrophages), which lead to cytokines production, such as Il-1, Il-6 and Tumour Necrosis Factor-alpha (TNF-α) in order to support and promote the inflammatory phase of the healing process [6]. However, during the healing process, macrophages can switch from a pro-inflammatory to an anti-inflammatory and pro-tissue repair phenotype (also

known as M2 macrophages). This transition is known to be the key step of the passage to the second phase of the healing process, the proliferative stage. Despite their secretion capacity, M2 macrophages are also known to play an important role in removing immune cells from the wound site by phagocytosis, controlling the progress of the healing process [5].

1.1.b Proliferative and migratory phase

The transition from the inflammatory to the proliferative/migratory phase of the wound healing is an essential step of the entire healing process. Many studies suggested that inflammatory cells are essential during all the phases of the healing process [8]. Inflammatory cells promote angiogenesis, cell growth and extracellular matrix synthesis by secreting many growth factors and proteases. However, factors are also produced by different cell types, such as keratinocytes, fibroblasts and endothelial cells at the wound site [6]. The goal of the wound healing proliferative and migration stage is the closure of the injury itself. This achievement is obtained through activation of several steps, which all take place during this middle phase of the healing process. Angiogenesis, fibroplasia and reepithelialisation are the regulators of the wound closure [9]. Few days after the damage, new connective tissue - the granulation tissue - is generated. Fibroblast cells, migrating from the dermis in response to the cytokines/growth factors gradient, play a fundamental role in the formation of the granulation tissue [5]. These cells, being the most common cell of the connective tissue, play a pivotal role during the wound healing process, especially in the wound contraction, which take place during the proliferative phase [10,11]. Activated contractile fibroblasts, known as myofibroblasts, were first described by Gabbiani *et al.* in 1971 and they were mainly found in the granulation tissue. These cells, stimulated by cytokines, growth factors and ECM signals, produce several extracellular matrix structural proteins in order to build a transitory fibronectin-based matrix, which will help endothelial cells (ECs) to migrate across the ECM and contribute to the generation of new blood vessels [12].

Moreover, these cells play a pivotal role in the healing process, migrating to the wound site and stimulating the formation of the granulation tissue and wound



contraction, which occur during the proliferative phase of the healing process [11].

Figure 2: Myofibroblasts activation and their role in wound healing. Fibroblast cells play a pivotal role in the healing process, stimulating the formation of the granulation tissue. Upon soluble signals such as cytokines and growth factors, fibroblasts become activated acquiring a contractile phenotype. These properties are due to the expression of α-smooth muscle actin in microfilament bundles or stress fibres. Once activated these cells are consequently called myofibroblasts, which play an essential role in the wound contraction [13]. Image adapted from [14].

The angiogenesis, critical step for the wound healing process, supplies nutrients and oxygen to the wound site supporting all events of the healing process, such as cellular proliferation, cellular migration and metabolic activity [15]. However, exactly as all other steps of the healing process, the formation of new capillaries has to be strictly orchestrated by growth factors, membrane proteins, ECM and cellular communications. Altogether, these factors regulate angiogenesis in a perfect balanced activity, obtained by secreting pro-angiogenic and anti-angiogenic molecules [12]. Moreover, *de novo* formation of blood vessels obtained by migration of endothelial progenitor cells (EPCs) from the bone marrow to the wound area (process known as vasculogenesis), is another critical step to

achieve wound revascularization [16]. The reepithelialisation stage takes place through proliferation and migration of epithelial cells – keratinocytes - from the wound edges, which attempt to achieve the closure of the injury. When the injury surface is covered by keratinocytes, the migration capacity ceases and a new stratified epidermis with a basal membrane are restored. ECM deposition and following changes appears in this stage, such as degradation and of the type III collagen fibres and synthesis of new and permanent type I collagen fibres. These events culminate with collagen fibres becoming thick and parallel to the to the wound site, leading to an improvement of the tensile strength for the tissue [9].

1.1.c Remodelling phase

The last step of the wound healing process – the remodelling phase – occurs 2 – 3 weeks after injury and can terminate after 1 year or more. All the discussed process – Inflammation, proliferation, angiogenesis and reepithelialisation - will be completed and will cease, leading to a loss of the majority of the newly formed capillaries, fibroblasts and inflammatory cells from the wound area, by activation of the cell death process [9]. Scar formation denotes this last wound healing phase. Adult skin wounds do not regenerate but undergo through repair. Indeed, normal adult wound healing can be achieved following two different way of healing: repair or regeneration. The first one usually occurs in adults and consist of physiological readjustment of the damage site without aiming at the reconstitution of the original tissue with its total functionality. On the other hand, the goal of the regeneration is the achievement of the total restoration of both tissue morphology and functionality [17]. In conclusion, scar formation denotes the end of the wound healing process in children and adults. Fibroblasts and myofibroblasts both cooperate and play key roles in skin wound contraction. Skin wound contraction is a specific step of the wound healing, in which the length of the scar results much smaller that the original wound area [1].

1.2 Impaired wound healing and its consequences

Successful wound healing is highly dependent on the perfect orchestration of all the processes cited above and it is essential to point out that many factors can interfere and, in turn, modulate the progress of the healing process. In physiological conditions, the repair of an efficient epidermal barrier is generally achieved; however, in humans the response to an injury cannot recapitulate the original functionality of the tissue, which in most of the case heals by fibrosis leading to scar formations. The ability to heal by regeneration instead by repair/fibrosis is highly effective in prenatal development but lost during the adult life [2]. Impaired healing conditions, either linked to traumatic injuries or diseases, are described as barrier defects, which did not progress through a correct healing process and which did not recover architectural and functional integrity of the original tissue [7]. Infections are the leading factor in the development and/or maintenance of an impaired wound environment [7]. Moreover, many other factors including metabolic disorders, age, oxygenation, hormones, life style habits, stress, nutrition and smoking can interfere, leading to non-healing (impaired) wounds and restrain skin regeneration [3], leading to infections and patient psychological and physical discomforts. Likewise, vascular deficiency, metabolic disorders such as type II diabetes [18] and cancer therapies exemplify the common causes of impaired wound healing conditions [19]. In 2014, 422 million people were affected by diabetes worldwide, and this number is estimated to increase to 552 million in 2030. In addition, estimation of 40% to 80% of patients with cancer are susceptible to delayed wound healing [19]. Moreover, million people worldwide are yearly affected by impaired wound conditions after traumatic injuries or post-surgical wounds [7], with the majority belonging to countries lacking proper medical services [20]. The underlying molecular mechanisms that guide the impairment of the wound healing process are still poorly understood and consequently no therapies able to improve endogenous regeneration wound capacity with a scar free outcome are currently

available. Recent evidences showed that the endless competition between pro- and anti-inflammatory signals could represent the cause of the prolonged inflammatory phase of impaired wound conditions. In this frame, the imbalanced environment leads directly to a failure of the correct progress of the wound healing process [7]. Interestingly, foetal wound healing is characterized by low inflammatory response due to the incomplete development of the immune system. Altogether these evidences indicate the involvement of the inflammatory phase in reducing the endogenous regeneration capacity in humans [21]. Moreover, the essential recruitment of endothelial progenitors cells (EPCs) for the microcirculation remodelling, seems to be depleted in condition that contribute to compromised wound healing, such as diabetes [16]. Deregulation of the amount of activated protease and their inhibitor play a pivotal role in the failure of impaired wounds to proceed the healing process. Normal wound healing denotes a strict cooperation between different cell types, bioactive molecules and changes of the extracellular matrix (ECM) integrity, which is obtained by the involvement of tissue proteases under a tight regulation [7]. The appropriate remodelling of the ECM is one of the fundamental events that can lead to a successful healing process. Specific endopeptidases (known as matrix metalloproteinases, MMPs) and their inhibitors (Tissue inhibitor of Matrix Metalloproteinases - TIMPs) can be activated and repressed respectively to contribute to this remodelling and, therefore, to the healing process. In impaired wound conditions, the tight regulation of these proteases is lost, and an excess of protease activity plays an important role in the wound pathogenesis [7]. Without the accurate recovery of wounds, skin functions and life quality of patients is hindered, suffering from pain, immobility, physical discomfort, functional limitations as well as psychological problems [22]. Therefore, there is a need of a substantial medical and public request to enhance therapeutic proposals aimed at improving the endogenous tissue regeneration efficiency. In addition, the improvement of the healing process may contribute to reduce scar formation and, consequently, improve the aesthetic impact on the patient quality life.

Therefore, achieving the restoration of the total tissue functionality remains one of the biggest aims of the clinical wound care [7].

1.3 Growth factors, cytokines and related signalling pathways involved in skin wound healing

When an injury occurs, several signalling pathways are collectively activated and synchronized to respond to the damage. Indeed, the complex process of the wound healing is strictly regulated by an equally complex signalling pathway network in which several growth factors and cytokines are involved [23]. Among these, epidermal growth factor (EGF), fibroblast growth factor (FGF), insulin-like growth factor (IGF), keratinocyte growth factor (KGF), platelet-derived growth factor (PDGF), transforming growth factor beta (TGF-β) and vascular endothelial growth factor (VEGF) are considered to have the broadest spectrum of effects. Following the observation of their importance in all the phases of healing process, the use of growth factors to improve the wound healing is currently widely explored. PDGF, bFGF, IGF and KGF, were investigated in many clinical trials [24]; however, despite their promising effects, only the recombinant human PDGF (becaplermin) is approved by the U.S. Food and Drug Administration (FDA) for use in human medicine [7]. During acute wound healing, these bio-active peptides are massively present in the wound site and play pivotal roles in all the phases of the healing process, such as immune modulation, proliferation, migration, angiogenesis, reepithelialisation, ECM protein production and maturation [25]. The inflammation signalling pathway is the first response to the tissue injury, leading to an increase in vessel permeability and migration of several immune cells. The innate immune system is, indeed, the main contributor to the acute inflammation upon tissue damages [26]. When an injury occurs, the keratinocytes barrier is destroyed and expression of interleukin-1 (IL-1) is the damage signals of the barrier defect [23]. Moreover, injuries cause releasing of important damage signals, such as Ca^{2+}, hydrogen peroxide (H_2O_2) and ATP, leading to changes in the actin cytoskeleton through RHO GTPase-

mediated regulation and stimulation of several signalling pathways [27]. In parallel many DAMPs signals, recognized by pattern-recognition receptors, including the toll-like receptors family (TLRs), stimulate several intracellular signalling pathways, which will drive the healing process during all its overlapping phases [5]. Platelets represent an important source of bio-active peptides, such as epidermal growth factor (EGF), platelet-derived growth factor (PDGF) and Transforming growth factor beta (TGF-β) [23]. PDGF, together with interleukin-1, acts as a chemoattractant for the first immune cells that invade the wound site; TGF-β stimulates the inflammatory phase supporting the monocyte differentiation toward macrophages and the formation of the granulation tissue. VEGF and bFGF induce new blood vessels formation, through proliferation and migration of endothelial cells. FGF, PDGF and TGF-β activation leads to fibroblast migration and lately to their differentiation toward myofibroblasts, which will stimulate the wound contraction [23]. The fibroblasts response during the healing process establishes the outcome of the all tissue repair. In response to the injury, macrophages and fibroblasts secrete growth factors and inflammatory cytokines, which will lead to a further fibroblasts migration toward the wound site [21]. The EGF secreted by platelets, fibroblast and keratinocytes is massively expressed during the earliest phases of healing process [23]. The activated EGFR undergoes to autophosphorylation stimulating signalling cascades regulating many cellular functions, such as cell motility, cell adhesion, cell proliferation [28] and regulating the expression of matrix-degrading proteinases through activation of multiple signal transduction pathways, including MAPK and Akt signalling cascade [29]. Among the growth factors and related signalling pathways involved in the wound healing process, the transforming growth factor beta (TGF-β) cascade is recognized as the signalling pathway with the widest range of effects, being involved in both wound healing and scar formation [30]. The TGF-β plays pivotal roles in all wound healing phases, including immune modulation, proliferation, granulation tissue formation and ECM components production [31]. However, deregulation of TGF-β signalling is implicated in pathological wound conditions and hypertrophic scar formation

[30]. One of the most conserved signalling pathways that is relevant both in development as well as in normal tissue homeostasis is the TGF-β family signalling cascade, which controls the epithelial-to-mesenchymal transition (EMT) [32], cell differentiation, cell cycle progression, cell migration and ECM production. However, the TGF-β family signalling is widely implicated in many fibrotic pathologies, including the formation of hypertrophic scars, where immoderate level of TGF-β lead to an excessive myofibroblast activation with an increase of ECM deposition [32]. TGF-β1, 2, 3, bone morphogenic proteins (BMPs) and Activins are all members of the Transforming Growth Factor Beta family and the three common TGF-β isoforms are all involved in cutaneous wounds. Once these ligands bind the serine-threonine kinase receptors, leading to an autophosphorylation, the intracellular signal transduction will be controlled by the activation of small cytoplasmic molecules, including members of the Smad family [33] and non-smad signalling proteins [34]. Brunner et al. suggested that platelets represent the primary reservoir of activated TGF-β immediately after injury, which in turn will act as a main chemoattractant factors for the stimulation of the inflammatory phase and further for supporting the reepithelialisation phase of the healing process [35]. The TGF-β1 isoform is the main present in cutaneous wound healing, secreted by platelets, immune cells and other different cells type, such as fibroblast and keratinocytes. Moreover, the TGF-β1 isoform is the key regulators of myfibroblast activation, ECM components production and wound contraction [31,35]. Both fibroblasts and their active form (known as myofibroblasts), induced by TGF-β1 signals, play an essential role in the stage of wound contraction, being responsible of the generation of the traction and contractile forces. However, their necessary involvement shows opposite aspects, when an excess of myofibroblast activity and ECM production lead directly to wound pathogenesis [36]. Chitturi RT et al. defined myofibroblasts as modified fibroblasts with smooth muscle like features, which present the ability to contract [10,11]. Darby et al., for the first time, identified that the contractile characteristic is given to these cells by the presence of alpha-smooth muscle actin (α-SMA) stress fibres in their cytoskeleton [37]. The

preeminent function of these cells in the wound healing process is the stimulation of the wound contraction by bringing together the edges of the wounds. After accomplishing their task, myofibroblasts undergo to programmed apoptosis, preventing immoderate contraction activity with development of hypertrophic scars and, in the worst scenario, tissue contracture linked with tissue immobility and loss of tissue function [10,11] [38]. In conclusion, all the factors described work together in a highly regulated manner altering the fate of their cell targets. The positive progress and outcome of the wound healing process is strictly regulated by several bio-active molecules and their signals integration, which will lead at the reconstitution of the tissue through the main phases of the process itself.

1.3.a The MAPK signalling pathway cascade

Cell migration is a cardinal step involved in several physiological processes including embryonic development, differentiation, tumour invasion and wound healing. Among the various inputs that lead to cell motility events, growth factors are considered the main inducers [39]. Glanding et al., in the 1999, demonstrated that activation of the EGFR signalling pathway leads to changing in the cell-substratum adhesion and stimulation of cell migration capacity, through a mitogen-activated protein kinase (MAPK) signalling pathway activation [39]. Several extracellular signals activate the family of serine/threonine protein kinases known as mitogen-activated protein kinase (MAPK). Three different MAPK sub-pathways can be established based on the differences contained in the motif within their activation loops, which characterize the c-Jun amino-terminal kinases (JNKs), extracellular signal–regulated kinases (ERKs) and p38 MAPKs [40].

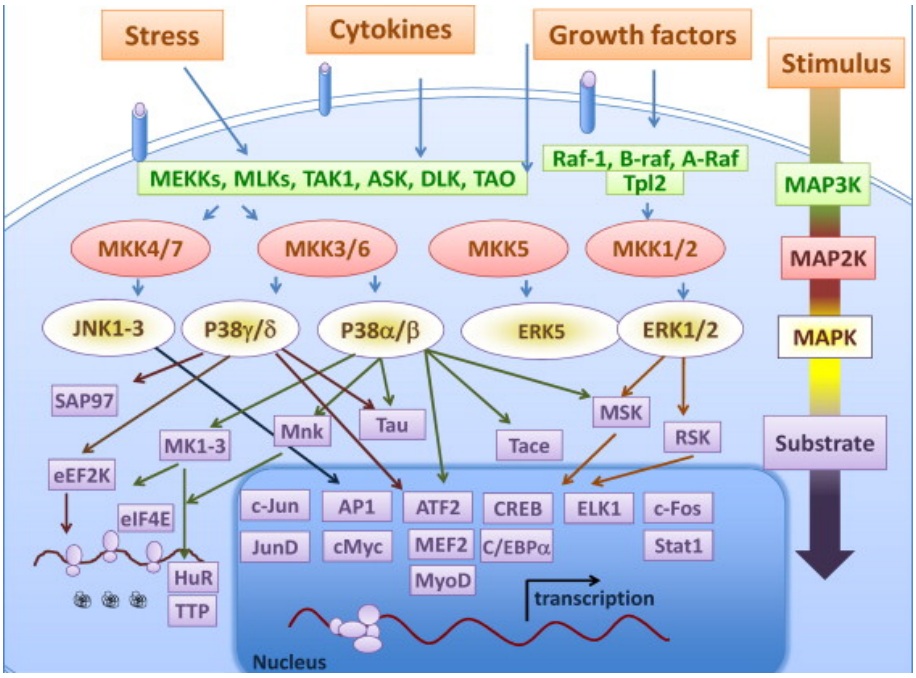


Figure 3: The Mitogen-Activated Protein kinase signalling pathway. A general scheme of the MAPK cascade subgroups, described as ERK (extracellular signal-regulated kinase), JNK (c-Jun N-terminal kinase) and p38. These signalling cascades can be activated by several stimuli, such as growth factors, cytokines and stress signals. Image adapted from [41]

Despite MAPK signalling pathway activities are well-known to play an important role in inducing cell proliferation, differentiation and inflammation, several studies demonstrated the implication of these signalling pathways in stimulating cell motility [40]. The c-Jun amino-terminal kinase (JNK) signalling pathway is known to be widely stimulated by the action of several growth factors and cytokines present at the wound site and by mechanical force as well as environmental stresses [42] and to play important role in cell differentiation and apoptosis [43]. Moreover, evidence indicates the involvement of the JNK subgroup of MAPK signalling pathway in the regulation of cell migration in different cell type, which was well displayed through functional assay where the inhibition of JNK reverts cell migration [40]. Another subgroup of the MAPKs, the extracellular signals-

regulated kinase (ERK) signalling pathway, have been studied in many different physiological processes, including wound healing-mediated cell migration, where improvement of skin wound healing seems to be achieved by ERK1/ERK2 signalling pathway activation [44]. The ERK signalling pathway is stimulated by a broad range of growth factors, such as platelet-derived growth factor (PDGF), epidermal growth factor (EGF) and fibroblast growth factor (FGF), through the Ras-Raf-MEK1/2-Erk signalling transduction, which lead to a changing in cell migration rate [40]. On the other hand, the p38 MAPK signalling subgroup, well known to play a role in cell migration during wound healing in murine models [45]. The involvement of these signal cascades and their cross-talks with other essential signalling pathways appear to be important for the wound healing process and may offer novel drug targets for tissue repair purposes.

1.4 Matrix metalloproteinases expression regulated by MAPK signalling pathway and their involvement in wound healing

The wound healing process is orchestrated by interactions and cross-talk between cells, ECM components, growth factors and, importantly, a family of calcium-dependent zinc-containing enzymes called matrix metalloproteinases (MMPs). In fact, if the wound healing with the total tissue restoration and its functional integrity has to be achieved, the extra cellular matrix (ECM) has to be properly remodelled. Regulators of the ECM remodelling are proteases called matrix metalloproteinases (MMPs), which consist of a family of proteases calcium-dependent, requiring a zinc metal ion for their activity. However, the MMPs role is not limited to the ECM turnover but they are well known to play pivotal roles in several biological processes involving proteolysis, such as developmental processes [46], inflammation and immunity-related processes [47] and physiological processes, including the wound healing [48]. MMPs catalytic activity allows cell migration and produces bio-active substrates, which regulate different signalling pathways [49]. Moreover, MMPs can be transcriptionally regulated by a broad spectrum of cytokines and growth factors, including

epidermal growth factor (EGF), fibroblasts growth factor (FGF), vascular endothelial growth factor (VEGF), platelet-derived growth factor (PDGF-α), keratinocytes growth factor (KGF), transforming growth factor beta (TGF-β) and tumour necrosis factor alpha (TNF- α) [29]. Therefore, several signalling pathways are involved in the regulation of the MMPs expression. MMPs promoter regions hold different binding sites for several trans-activator transcription factors, such as NF-κB, AP-I and β-catenin/Tcf-4 [50].

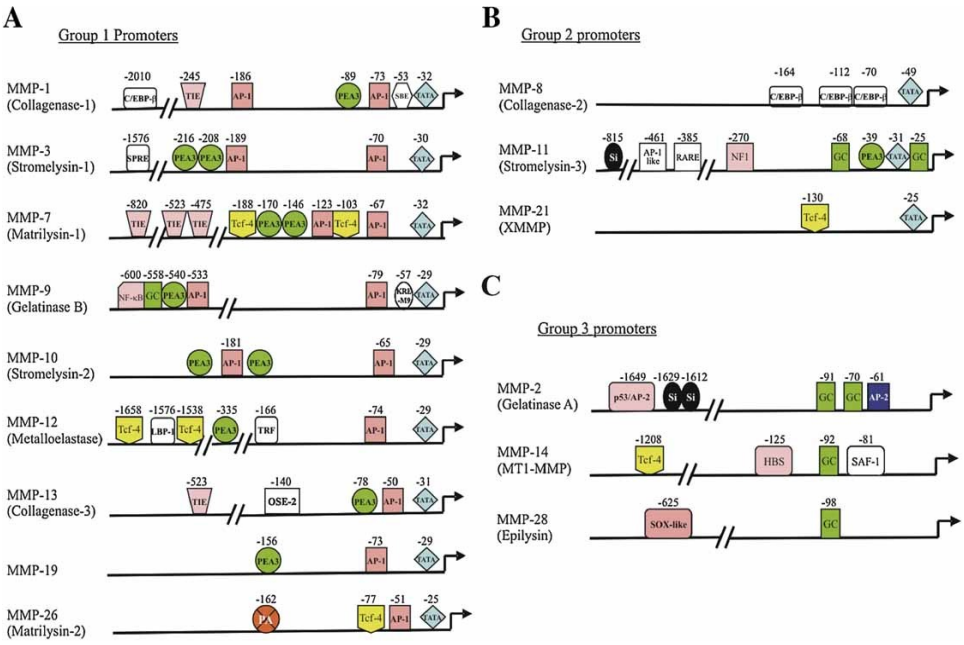


Figure 4: MMPs promoter region. A general scheme of the MMPs promoter regions and its binding sites for several important transcription factors. Image adapted from [50].

Increased MMPs expression via AP-I is chiefly obtained through mitogen-activated protein kinase (MAPK) signalling pathway activation [50]. During the wound healing process, the epidermal growth factor (EGF) represent one of the first cytokines released and involved in the process and interestingly EGF

response is linked to AP-1 transcription factor activity, since both EGF receptor (EGFR) and one of its known ligands (HB-EGF) are AP-I target genes [51]. Moreover, as previously reported, EGF and other transcription factors, like bFGF (basic Fibroblast Growth Factor) trigger cell signalling culminating in trans-activation of MMP promoters by the convergence at the AP-1 sites (Fini et al. 1988). Many studies confirmed that controlled expression of components of the cytokine network, cell surface receptors and proteases, which regulate the wound healing process has been found to depend on AP-1 activity [52]. Evidences show that AP-I involvement in the healing process is mediated by the activation of its sub-units, since Jun, Fos and ATF proteins are activated by signalling pathways initiated by cytokines and growth factors. Moreover, involvement of AP-I transcription factor in wound healing is demonstrated by the fact that specific growth factors, such as EGF, FGF, TGFβ, TNF-α and interleukin proteins stimulate AP-I activity through MAPK signalling pathway activation [52]. Upregulation in gene expression resulting in an enhancement of Jun and Fos protein levels triggers modification in the expression of AP-I target genes, such as matrix metalloproteinases (MMPs) [53]. *In vitro* studies showed the activity of AP-I in coordinating cell migration of the leading cell rows and enhancement of the artificial wounds closure and, if the signal is inhibited, a clear slowing down of the *in vitro* migration/repair process is obtained. AP-1 plays an essential role in the transcriptional activation of the majority of matrix metalloproteinases (MMPs) which are required for cell migration [52]. MMPs are both present in acute and chronic wounds, playing a pivotal role in the ECM turnover and, in turn, in the reepithelialisation phase. However, the uncontrolled expression and activity of MMPs can lead to wound pathogenesis. The timed expression of these enzymes during the healing process is critical for the accomplishment of the wound healing.

1.5 Use of network and transcriptome analysis for regenerative medicine

The wound healing process is one of the most complex mechanisms of the entire human body. When the wound healing process starts, many biological signalling pathways quickly become activated and synchronised to respond to the damage leading to the restoration of the tissue [2]. Therefore, to fully understand the wound healing process, we need to deeply understand all the different signalling pathways involved in this process. Over the past 10 years the possibility to establish the dynamic state of genomes, including both DNA modifications and RNA quantitative and qualitative changes, has been achieved by the introduction of high-throughput next-generation DNA sequencing (NGS) technologies [54]. These methods allow RNA analysis through cDNA sequencing at massive scale (RNA-sequencing - RNAseq), providing a complete knowledge of both quantitative and qualitative aspects of the transcriptome changes in eukaryotes [55]. Transcriptome analysis evaluates quantification of transcripts, including both coding and non-coding RNA, detecting effects of tissue type, regulation, sequence variation, environment and, especially, external stimulation, such as drug treatments [56]. RNA-seq analyses are typically performed on samples belonging to two different conditions (e.g. tumour/control, treated/untreated samples) to assess the effect of one condition. In this way, the analysed the transcriptional state under the conditions where the RNA was collected (e.g. before/after a drug treatment), allowing to establish the biological effect resulting from those conditions [56]. Typically, the analysis of RNA sequencing data leads to the identification of Differentially Expressed Genes (DEGs), i.e. genes whose expression is significantly different between the two conditions. This may finally result in the discovery of, for example, novel biomarkers or treatment targets. In addition, DEGs identification can be coupled with enrichment studies of the biological processes (pathways) overrepresented in the conditions under study. Enrichment analysis can be performed by using public available databases, such as the Gene Ontology (GO) [57], that associates genes to the pathways they belong to. As a result, enrichment analysis can lead

to a better understanding of the several physiological and pathological processes underpinning the analysed conditions. All these analyses can contribute to the discovery of novel therapeutics for complex diseases. For this reason, RNAseq techniques have currently spread well beyond the genomics community and have become a standard part among the methods used by the life sciences research field [58]. Different techniques can be applied to analyse RNAseq data and extract DEGs, examples are edgeR [59], DEseq [60], and NOIseq [61]. Other RNA-seq techniques directly performs their statistics at the pathway level giving as output the Differentially Expressed Pathways (DEPs) across the two conditions, one example is the N-of-1 pathways MixEnrich method [62]. However, the mathematical approach at the basis of these techniques requires well-powered cohort of patients or replicates (N>3) to extract significant DEGs or DEPs. Despite these transcriptome analytic tools are wide used to establish effect of new treatments and predict positive or negative clinical outcomes, they are not designed to address the single-subject transcriptome analyses (SSA) [62]. SSA analysis aims at detecting the differential status of the genes or the pathways across paired samples drawn from the same subject. In this case, standard analyses are underpowered since no replicates are available. Nowadays, with the arrival of precision medicine, a more individual view of both physiological and pathological process and response to new treatments is required. These SSA methods can have many advantages, such as allowing revealing bidirectional and deregulated pathways one subject at the time, detecting gene expression changes reflective of individual physiological reaction, disease and physiological process progression and response to new therapies [62]. SSA approaches comprises the N-of-1 pathways [62-64], RankComp [65] and DNB [66] These methods are particularly suggested in absence of large cohort and when only pair samples from a single subject are available since they can provide biologically and clinically interpretable results of altered expression. In this work, we decided to use the N-of-1 pathways MixEnrich method recently developed and validated [62] since it computes directly the DEPs between two single-subject samples providing signalling pathways candidates for a better

understanding of the individual profile of a single subject under the studied conditions [62].

1.6 Wound care therapies: from conventional to regenerative scar-free treatment

The restoration of skin integrity is the goal of the wound healing process and represents one of the biggest challenges of the regenerative medicine field. The skin, as the largest organ of the body, plays essential roles in the maintenance of the physiological processes and in the protection against mechanical stresses and infections [1]. However, traumatic injuries and impaired wound conditions affect millions of people yearly, leading to a widespread public health and economical problem [7,67], which has been recognized as a worldwide issue from World Health Organization (WHO) in the 2010 [20]. Healing by fibrosis instead of regeneration represents the critical outcome of the wound healing process, leading to anaesthetic scars and loss of tissue function, which, in turn, hinders patient quality of life. Despite the fact that the wound healing process and its principal players, such as cells, ECM components, growth factors and signalling pathways are well understood, the incomplete understanding of the fundamental molecular basis of the wound healing and its breakdown, as well as the lack of proper animal model recapitulating the human wound healing conditions has led to a lack of proper therapeutic approaches able to improve endogenous regenerative capacity. Enhancing the healing capacity, aiming at the total restoration of the tissue functional integrity and reducing the aesthetic impact on the patient with scarless wound healing represents the goal of the clinical wound care. When taking new therapeutic strategies for wound healing into account, it is important to realize that the impaired healing is caused by uncontrolled stages of the physiological healing process. Many factors can interfere with the previously reported wound healing phases, leading to a delay in the wound repair achievement and, in turn, to chronic wound conditions [3]. Studying the wound healing process will lead to a deeper knowledge of the wound repair in

humans and may identify new treatments or signalling pathways which will play an essential role in the restoration of the lost regenerative capacity. Skin wound therapies can be classified as conventional/traditional or modern/regenerative. Traditional strategies include the debridement of the necrotic tissue, the topical use of several dressings and the use of natural compounds obtained from animals, fungi, plants or minerals, which are widely used in Asia and Africa (from the 80% of the population), whit an increment of number of people using of these therapies in Europe, Canada and United States [68]. Despite their potential healing capacity, the conventional therapies generally lead to scar formation and, in turn, to enormous aesthetic and functional-related impairment [17]. On the other hand, the modern/regenerative skin wound therapies represent a novel and developing field of the biomedical research with the purpose of enhancing wound healing, restoring functional integrity of original tissues and minimizing scar formations. However, it is necessary to remind that regenerative strategies should to be considered complementary of the conventional one [17]. Regenerative therapies include the use of soluble bio-active molecules, such as growth factors, biomaterials, engineered devices, stem cell-based treatment, tissue engineering, laser therapy, cell reprogramming, *ex vivo* cell and gene therapy, transplantation of skin substitutes and transplantation of transgenic epidermal cultures [69].

1.6.a Autologous micro graft-based treatment in wound healing

Among these modern strategies a new emerging treatment able to improve skin wound condition and its related consequences (scars and nonhealing wounds) is described as autologous micro graft technique. In 1869, for the first time, Reverdin described the method of grafting small pieces of skin in order to enhance the reepithelialisation stage of the wound healing process [70]. Today, the micro graft techniques have been reconsidered and improved in order to support and improve the healing of wounds, minimizing scar formation. Many

recent studies reported the effectiveness of autologous micro graft obtained by mechanical disaggregation of a small piece of tissue biopsy in ameliorating the repair of dehiscent wounds [71], traumatic wounds associated with hypertrophic skin/cardiac scars [72,73]. Due to the high rate of success of the micro graft technique, many devices have been developed and are based on this concept. An ideal graft has to be immediately available, non-immunogenic and with low morbidity to the patient. This micro graft concept is retained in one of the most used clinical and experimental protocol, called Rigenera®. The protocol achieves all the micro graft characteristics due to the fact that it is autologous (thus avoiding rejection case) and allows wound coverage by using a minimal amount of donor tissue. From the 1869 until today, considerable studies used the autologous micro graft technique supporting their positive involvement in the improvement of the wound healing process. However, the molecular mechanism behind the autologous micro graft treatment and their connection with the wound healing process are still not understood. From early understanding of the physiology and pathophysiology of the healing process and from clinical trial experiences, it became unequivocal that the best therapy approach for wound healing improvement has to minimize the systemic causes of the healing impairment, successfully providing the correct timing of all its necessary phases and implementing combinatorial treatments. It is doubtful that the replacement of a single molecule, such as the administration of a single growth factor, will lead to the optimal clinical outcome. Therefore, future studies will be needed to prove the functionality of these autologous micro graft-based treatments for supporting and improving *in vivo* tissue regeneration; both in physiological and pathological wound healing conditions.

Chapter 2

Aims and Objectives

Successful wound healing requires tight regulation of several biological and molecular events, which need to be coordinated in an appropriate and sequential manner. These phases include haemostasis and inflammation, cell proliferation, migration, angiogenesis and tissue granulation formation, reepithelialisation and ECM remodelling [2]. The complexity of the healing process and the failure of one of these essential steps leads to wound impairment with a prolonged inflammation phase and high risk of infections. Moreover, impaired healing and progression of infections are the result of a decreased oxygenation of the damaged tissues [74], as well as other different factors that can interfere and restrain the regeneration capacity [3]. The number of patients suffering of impaired wound conditions is today reaching high demographic level, resulting in a burden health/economical public problem and in a leading cause of mortality [7]. Improvement of the healing process enhancing the endogenous regeneration capacity, minimizing scar formation and physical and psychological patient discomfort denotes the goal of the tissue regeneration. Autologous micro graft-based (AMG) therapies represent *in situ* and immediate new treatments for WH with promising clinical outcomes [72,73].

Surprisingly, detailed mechanistic studies explaining their beneficial effects are still missing. Within this thesis we aim at shedding light on the molecular mechanisms of AMG treatment, which will allow to increase its efficacy in tissue regeneration and eventually to extend its application to chronic WH disorders. **The aims of this project are: (i) to understand the molecular mechanism behind the beneficial effect of AMG treatment and (ii) to establish its connection with the *in vivo* WH process. The final goal is to enhance the endogenous tissue regenerative capacity reducing scar formation, which can eventually be applied to impaired wound conditions.**

To achieve the aim, four main objectives have been formulated.

Objective 1: Define the effectiveness of AMG treatment at the cellular level, evaluating *in vitro* cell viability, induction of cell proliferation and cell migration upon AMG stimulation on an in vitro wound healing model.

Objective 2: Establishing the molecular composition of the AMG and separately testing their potential on an *in vitro* model of wound healing through evaluation of the cell migration capacity. This objective will allow to address the question of which is the main driver of the AMG positive outcome?

Objective 3: Detecting transcriptome profile changes of wounded murine fibroblasts on an *in vitro* wound healing model upon AMG treatment. Alteration in signalling pathways, already known and possibly new, will lead to a deeper understanding of the molecular mechanism behind this new wound treatment. Altogether, the results will allow improving the use of AMG-based treatments in different clinical settings and supporting their use in patients suffering of impaired wound conditions, such as diabetic and cancer patients.

Objective 4: Validation of the established *in vitro* molecular mechanism on an *in vivo* wound healing model. The effect of AMG therapy will be assess through *in vivo* excisional wound healing assays combined with functional experiments. The results will lead to a confirmation of the molecular mechanism behind the AMG treatment, and in turn, improving the functionality of these treatments for translational purposes.

Chapter 3

Materials and Methods

3.1 Cell culture

Mouse primary fibroblasts were used in all the experiments. The cells were isolated from the end of the tail (0,5 cm) of C57BL/6 mouse model under anaesthesia (isoflurane). Tails were placed in sterile 1X phosphate buffered saline (PBS) with 1:10 of antibiotics (penicillin-streptomycin-gentamycin) and transferred to the laboratory for cell extraction. Tails were disaggregated by collagenase IV digestion for 40 minutes at 37°C in agitation. Cells were cultured with GlutaMax media (Ca No. 61965-026, Gibco, Grand island, NY, USA) supplemented with 10% of fetal bovine serum, 1% of penicillin-streptomycin, 1% of L-glutamine, 1% of sodium pyruvate and 1% of nonessential amino acids (Growth medium) at 37°C in 5% of CO_2 and maintained in culture until obtaining the correct level of confluence (90%) to perform the cell scratch assay. All the experiments were performed in accordance with the Ethics Committee at KU Leuven university (ethical approval code P056/2017).

3.2 Autologous micro graft via Rigenera® protocol

Due to high success rate in the clinical setting, our attention is dedicated to Rigenera®, a new CE-certified medical device [72]. AMG were obtained using the provided sterile tissue disruptor, called Rigeneracons®, in which murine skin biopsies (1 cm^2) were placed. Through a method of disruption, autologous micro grafts (AMG) solution (1 mL) with a dimension of approximately 50 microns was obtained. Skin murine samples (1cm²) (C57BL/6) were collected and immediately deposited in a sterile falcon tube containing PBS and 1% of antibiotics (1:10 of penicillin-streptomycin-gentamycin). Skin samples were then cut using a scalpel and further disaggregated with 1 ml of PBS under sterile conditions (vertical laminar flow hood) using the sterile biological tissue disruptor - Rigeneracons - for 4 minutes. The AMG suspension obtained (1 ml) was applied in different dilutions (1:5, 1:10 and 1:20) on murine primary fibroblasts on an *in vitro* model of wound healing (cell scratch assay).

3.3 *In vitro* wound healing model - cell scratch assay, imaging and quantification

Mouse primary fibroblasts were plated at a density of 3500 cell/cm^2 on 24 multi-well culture plates. Cells at passages 4 to 6 were used in this study. The cells were cultivated *in vitro* until a confluent cell layer was obtained to perform the scratch assay. The *in vitro* cell scratch assay represent an easy and cost-effective technique to measure cell migration *in vitro*. The method consists of the creation of an artificial wound in a cell monolayer using a pipette tip. After the creation of the damage, debris were washed out using sterile PBS (phosphate-buffered saline) and images were taken at the beginning (T0) and at regular intervals until the closure of the *in vitro* artificial wounds was achieved. The comparison between the images allowed quantifying the cell migration rate. The experimental procedure carried out through cell isolation and *in vitro* cultivation until obtaining the correct level of cell confluence was obtained to perform the scratch assay. AMG obtained from murine skin tissue, as previously reported, were applied on the scratched cells with different dilutions (1:5, 1:10 and 1:20) and for different time of treatment (1h, 5h, 12h and 24h). ERK signalling MAPK sub-pathway and MMPs enxymatic activity were inhibited using respectively MEK inhibitor PD0325901 (1 μM) and Actinonin (20μM) in an *in vitro* model of wound healing.

3.4 Cellular viability assay

The XTT cell viability protocol was used to measure metabolic activity and micro graft-related sensibility in primary murine fibroblasts treated with the autologous micro graft-based therapy, following manufacturer instructions (purchased from Thermo Fisher Scientific). In brief, mouse primary fibroblasts were plated at a density of 10^5cell/well, in 96 multi-well culture plate, in 100 µL of Growth medium, in which AMGs obtained by Rigenera® protocol were diluted (1:5, 1:10 and 1:20). Cultures were incubated for the different time period of treatments

(1h, 5h, 12h and 24h). At the end of each time period, cell culture media were replaced with 100µL of XTT/PMS (Phenazine methosulfate) (1 mg/ml; 10 mM) solution. Cells were incubated for 2 hours at 37°C. The absorbances were read at 450 nm by Nanodrop 1000 spectrophotometer (Thermo Fisher Scientific). Analysis was performed using Excel. Absorbance values are normalized to the control, plotted using GraphPad Prism 6 and presented ad a FoldChange.

3.5 Cell proliferation assay

Cell proliferation was assessed using the EdU proliferation assay. The EdU - 5-ethynyl-2'-deoxyuridine – (purchased from Thermo Fisher Scientific), as an analog of the thymidine nucleoside can be incorporated into newly synthesized DNA and detected by flow cytometry application. Scratched and unscratched cells were treated with the diluted micro graft-based therapy (1:10; for 1h, 5h, 12h and 24h of treatment) or untreated with vehicle (PBS). After each time point, cells were incubated with EdU 10 μM for 2 hours and were incubated at 37°C. Cells were harvested with Trypsin-EDTA 0,25% (Ca No. 25200056, Gibco, Grand island, NY, USA), washed with PBS 2% FBS and pelleted. Samples were fixed with 4% PFA for 20 minutes at RT, washed with PBS 2% FBS, permeabilized with Triton-X100 0,5% in PBS for 20 minutes at RT and washed again with PBS 2% FBS. 250 μL of cocktail solution (containing PBS 1X, $CuSO_4$ 100 mM, Sodium Ascorbate 1M, Azide Alexa Fluor 647) was applied on the cells which were incubated for 10 minutes at RT in the dark, followed by two washes with PBS 2% FBS and pelleted. 500 μL of PBS 2% FBS was finally added on the cells supplemented with 1 μL of Propidium Iodide (PI) and RNase 250 μg/mL for 30 minutes at RT. The samples were then acquired by Flow Cytometry (BD-Biosciences) and analysed by FlowJo software.

3.6 Immunostaining of wounded cells/tissues treated with micro graft-based therapy

Murine primary fibroblasts were plated at a density of 20^5cell/well on 24 multi-well culture plates. The cells were cultivated *in vitro* until a confluent cell layer was obtained to perform the scratch assays. Cells were fixed with 4% PFA for 20 minutes at RT, permeabilized with 1% BSA, 0,2% Triton-X in PBS for 30 minutes at RT, washed repeatedly with PBS and blocked with donkey serum 1:10 in PBS (blocking solution) for 40 minutes at RT. The primary antibodies were diluted in 1% BSA, 0,2% Triton-X and PBS and incubated overnight at 4°C. Primary antibodies used in this study were Mouse monoclonal anti-actin α-Smooth Muscle - Cy3™ (1:200, C6198, Sigma Aldrich), CD31 (1:500, 557355, Pharmingen). The following day, after PBS washes, the cells were incubated with secondary-AlexaFluor antibody for 1h at RT and washed repeatedly with PBS. Hoechst 33342 (1:10000) was used for the nuclear counterstaining, samples were washed three times with PBS and wells/slides with cells were mounted using FluorSave™ mounting medium (EDM Millipore). The images were taken using Nikon Eclipse Ti Microscope and NIS-Elements AR 4.11 software. Pictures were analysed, quantified and merged using ImageJ software (NIH).

3.7 Protein analysis

Scratched and unscratched murine fibroblasts treated with AMG-based therapy for 1h, 5h, 12h and 24h or untreated cells were washed with PBS 1X and were lysate in RIPA Buffer containing 0,5 mM Sodium Orthovanadate, 1:100 Protease inhibitor cocktail and 1mM Phenylmethanesulfonyl Fluoride. Equal amount of protein extracted from each samples (30 μg) were heat-denaturated in sample-loading buffer (50 mM of Tris-HCl, pH 6.8, 100mM DTT, 2% SDS, 0.1% Bromophenol Blue, 10% Glycerol), resolved by SDS-PAGE and transferred to nitrocellulose membranes (GE Healthcare Bio-Sciences, Pittsburg, USA).

Membranes were then stained with Ponceau S dye (Sigma-Aldrich) and then were blocked with non-fat dry milk 5% in TBS (Tris-Buffered Saline) supplemented with Tween 0.05% for 1 hour at RT. The membranes were then incubated overnight at 4°C in agitation with primary antibodies: rabbit α-Smooth Muscle actin (1:800, ab15734, Abcam), mouse p-ERK (1:1000, sc-7383, Santa Cruz), rabbit ERK (1:1000, sc-94, Santa Cruz), mouse CD9 (1:250, 10626D, Invitrogen), mouse CD63 (1:250, 10628D, Invitrogen), mouse Tubulin-alpha (1:1000, T5168, Sigma Aldrich). The following day, membranes were incubated with secondary horseradish peroxidase (HRP-)conjugated antibodies (1:5000, Santa Cruz Biotechnology, CA, USA), in TBS 0.05% tween and non-fat dry milk 2,5%. Analyses were performed using the ChemiDoc XRS+ detection system (BioRad, Temse, Belgium) in combination with chemiluminescent HRP substrates SuperSignal West Pico PLUS and SuperSignal West Femto (Thermo Fisher Scientific). Relative densitometry was obtained normalizing all samples to the housekeeping Tubulin-alpha, using both the QuantityOne software and ImageLab software (BioRad).

3.8 Mouse antibody array membrane

Simultaneous detection of several growth factors within the autologous micro grafts was analysed using Mouse Growth Factor Antibody Array Membrane containing 30 targets (RayBiotech, AAM-GF-3-2). The membranes (spotted with 30 different antibodies) were blocked using the provided blocking buffer for 30 minutes at RT, then incubated with 1 mL of autologous micro grafts for an equal amount of protein 30 μg (1:10 diluted in blocking buffer) overnight at 4°C. The following day, membranes were washed repeatedly with the provided washing buffer I and II (1X) and incubated overnight at 4°C with provided Biotinylated Antibody Cocktail. The membranes were washed, incubated with HRP-conjugated Streptavidin (1X) for 2 hours at RT and washed again. Chemiluminescent detection was obtained using the provided detection buffers.

Relative densitometry was obtained using the QuantityOne software (BioRad) and normalizing all signals to the positive controls signals of each membrane.

3.9 Cell migration assay

Murine primary fibroblasts were detached using 0,25% Trypsin-EDTA, washed with PBS (1X) and pelleted. Transwell Multiple Well Plate with Permeable Polycarbonate Membrane Inserts (Cat No. 3422, Thermo Fisher Scientific) were used for this study. 10^5cell were plated on the upper layer of the transwell in a maximum volume of 100 μL of cell culture media. 600 μL of autologous micro grafts 1:10 diluted in Growth medium or 600 μL of AMG soluble fraction 1:10 diluted in complete GlutaMax media were added in the lower part of the chamber. A well containing 10^5cell and 600 μL of complete GlutaMax media were used as a control. Different incubation times were evaluated in this study, such as 5h and 24h of treatment. After each incubation time, transwell inserts were removed from the chemo-attractant factors, cleaned from remaining media and not migrated cells using a cotton-tipped applicator and submerged in 600 μL of 70% ethanol for 10 minutes at RT. After the fixation time, membranes were left to dry for 15 minutes at RT, stained with 0,1% of crystal violet for 10 minutes at RT, cleaned from remaining staining solution using a cotton-tipped applicator and washed twice in distilled water. After the staining time, membranes were again left to dry for 15 minutes at RT, detached from the transwell inserts, deposited on slides and mounted using DPX. Picture of the membranes were taken with Axiovert 40 CFL connected with Axiocam MRc5 (Zeiss) and analysed using ImageJ software.

3.10 RNA extraction, cDNA synthesis and gene expression analysis

Total RNA was purified using PureLink® RNA Mini Kit (Cat No. 12183018A, Life Technologies™) according to the manufacturer's instructions. cDNA was generated using 0,5 μg of RNA and obtained by the Superscript III Reverse Transcriptase First-Strand Synthesis SuperMix (Invitrogen). Quantitative real-

time PCR (qRT-PCR) was performed using the Platinum® SYBR® Green qRT-PCR SuperMix-UDG (Cat No. 11733038, Thermo Fisher Scientific) on a ViiA™ 7 Real-Time PCR System with 384-well plate (Cat No. 4453536, Applied Biosystems). Gene expression values were normalized based on the *Gapdh*, *B actin*, *Rpl13a* house keeping genes. All primers that were used were purchased from IDT technologies, Leuven, Belgium and are reported in table 1.

Table 1: Murine Primers for qRT-PCR

Gene	FORWARD SEQUENCE	REVERSE SEQUENCE
Gapdh	AGGAAGGCGATATTGTGCTCTCC	TGGCTGGAAAGTGTGAGCAAGC
B actin	GCAGTTGTGGAAGATGCCATCG	CCATCAAATGTGTAGAGGTCACC
Rpl13a	TGCTGCCTATGAGGCTCACAAC	GGAGGAAAACCGAGAGTGTGGA
αSMA	GTCCCAGACATCAGGGAGTAA	TCGGATACTTCAGCGTCAGGA
Mmp1a	AGGAAGGCGATATTGTGCTCTCC	TGGCTGGAAAGTGTGAGCAAGC
Mmp1b	GCAGTTGTGGAAGATGCCATCG	CCATCAAATGTGTAGAGGTCACC
Mmp10	TGCTGCCTATGAGGCTCACAAC	GGAGGAAAACCGAGAGTGTGGA

Mmp9	GGACCCGAAGCGGACATTG	CGTCGTCGAAATGGGCATCT
Mmp12	CACACTTCCCAGGAATCAAGCC	TTTGGTGACACGACGGAACAGG
Mmp13	GATGACCTGTCTGAGGAAGACC	GCATTTCTCGGAGCCTGTCAAC

3.11 Transcriptome analysis through RNA sequencing (RNA-seq) analysis

RNA samples were purified using PureLink® RNA Mini Kit (Cat No. 12183018A, Life Technologies™) according to the manufacturer's instructions, quantified with Nanodrop 1000 spectrophotometer (Thermo Fisher Scientific) and RNA integrity was evaluated using Bioanalyzer (Agilent 2100) combined with Agilent RNA 6000 Nano Kit (Ca No. 5067-1511). RNA samples were then processed by the Genomics Core (KU Leuven – UZ Leuven, Belgium). Library preparation was performed with the Illumina TruSeq Stranded mRNA Sample Preparation Kit, according to the manufacturers protocol (48 samples, Cat No. 20020594). Denaturation of RNA was performed at 65°C in a thermocycler and cooled down to 4°C. Samples were indexed to allow for multiplexing. Sequencing libraries were quantified using the Qubit fluorometer (Thermo Fisher Scientific, Massachusetts, USA). Library quality and size range was assessed using the Bioanalyzer (Agilent Technologies) with the DNA 1000 kit (Agilent Technologies, California, USA) according to the manufacturer's instructions. Libraries were diluted to a final concentration of 2nM and sequenced on Illumina HiSeq4000 sequencing system, according to the manufacturer's recommendations. 50 bp single-end reads were generated. An average of 20 million reads were obtained from all samples. Quality control of raw reads was performed with the FastQC v0.11.5. The adapters were filtered with ea-utils v1.2.2.18. The splice-aware alignment was performed with TopHat v2.0.13 against the mouse genome

mm10. The number of allowed mismatches was 2. Reads that mapped to more than one site to the reference genome were discarded. The minimal score of alignment quality to be included in count analysis was 10. Resulting SAM and BAM alignment files were handled with Samtools v0.1.19.24. Quantification of reads per gene was performed with HT-Seq count v0.5.3p3. Count-based differential expression analysis was done with R-based (The R Foundation for Statistical Computing, Vienna, Austria) Bioconductor package DESeq. Reported p-values were adjusted for multiple testing with the Benjamini-Hochberg procedure, which controls false discovery rate (FDR). List of differentially expressed genes were selected at a adjust p-value < 0,05, used to perform Gene Ontology (GO) analyses (via Panther classification system) and enriched biological processes and pathways were selected at FDR < 0,05 and presented using GraphPad Prism 6. Among these list, selected GO terms were then used to obtained either specific cell migration/cell motility signature genes or ERK/MAPK signature genes, which were then presented as heatmaps (via R studio software).

3.11.a Single-subject transcriptome analysis (SSA)

The N-of-1 pathway MixEnrich is an approach designed to analyse gene expression data from paried samples drawn from the same subject [62]. N-of-1 pathway MixEnrich gives as a results a list differentially expressed pathways (DEPs) resulting from two different condition on two samples of the same subject. We applied this technique to the paired samples (treated vs untreated tissue) drawn from the same animal at different times (1h, 5h, 12h, and 24h). This produces a total of 8 pairs of samples that were analysed using N-of-1 MixEnrich method [62].

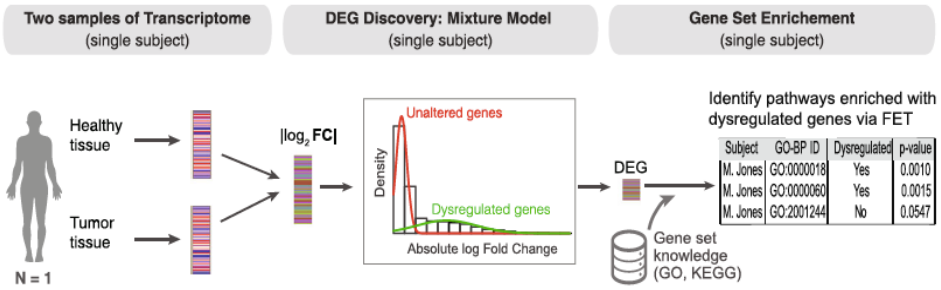


Figure 1: N-of-1 pathways MixEnrich method. Single-subject paired transcriptome profiles (wounded and unwounded murine primary fibroblasts both untreated and treated with AMG for different time period – 1h, 5h, 12h and 24h) have been used to perform the clustering technique reported in the central panel. The mRNAs have been classified in two separate groups, revealing unaltered and dysregulated mRNAs. The group including the dysregulated mRNAs have been subsequently analysed for pathways enrichment by using the Fisher's Exact Test (FET). Image adapted from [62].

In detail, two groups (wounded and unwounded murine primary fibroblasts both untreated and treated with autologous micro grafts for different time period – 1h, 5h, 12h and 24h) were used in this study to explore the changes in the gene expression profile induced by the autologous micro graft-based treatment. For each transcriptome sample the absolute value of log transformed fold change - $|\log_2 FC|$ - was obtained as $|\log_2(U/T)|$where U is the expression level of the mRNA in the Untreated condition and T is the mRNA expression level in the Treated condition (in both unwounded and wounded conditions). mRNAs were then clustered in dysregulated mRNAs (*cluster a*) and non-dysregulated (unaltered) mRNAs (*cluster b*), based on the $-|\log_2 FC|$value. The clusters members have been assigned using a Bernoulli trial (Eq.1)

$$\pi_k = p(Z_i = k), \sum_{k=1}^{2} \pi_k = 1 \quad i = 1, \cdots, G; \; k = 1,2$$

where Zi the latent variable and G is the total number of mRNAs detected in the transcriptome. The clusters formation was then followed by evaluation of the probability that each mRNA belongs to the assigned cluster, evaluated by posterior probability by using Bayes rule (Eq. 4)

$$p(z_i = k \mid x_i, \mu_1, \sigma_1, \mu_2, \sigma_2) = \frac{\pi_k \phi(x_i, \mid \mu_k, \sigma_k^2)}{\sum_{j=1}^{2} \pi_j \, \phi(x_i \mid \mu_j, \sigma_j^2)}$$

Dysregulated mRNAs have been defined by a posterior probability above 0.5, where this cluster is defined as the cluster with the larger mean. After allocating the mRNAs to specific clusters, the enriched pathways, related to each time period of treatment (in both unwounded and wounded conditions), were obtained using a Fisher's Exact Test (FET). After assigning mRNAs to clusters, N-of-1 pathway MixEnrich performs a second Fisher's Exact Test (FET) to detect the gene sets (pathways) enriched with the previously identified dysregulated mRNAs. The FET is computed according with the contingency table:

Dysregulated mRNAs	**Unaltered mRNAs**	**Row sums**	
mRNAs in target pathway	*d*	*M – d*	*M*
mRNAs not in target pathway	*D - d*	*N - M - D + d*	*N-M*

Dysregulated mRNAs	Unaltered mRNAs	Row sums	
Column sums	*D*	*N - D*	*N*

assuming one pathway consists of *M* mRNAs among which *d* mRNAs are dysregulated; while the entire genome consists of *N* mRNAs among which *D* mRNAs are dysregulated. Thanks to this procedure, pathway dysregulation is determined relative to the dysregulation of the entire transcriptome as the background. Since different pathways may not be independent due to overlapping mRNAs between them, the p-values resulting from FETs are adjusted for multiple hypothesis testing using Benjamini and Yekutieli approach that accounts for correlated p-values.

3.11.b Network-based analysis

The Protein-Protein Interation (PPI) network, related to the DEGs identified through RNA sequencing analysis and thus representing the wound healing process, has been obtained by using the public PPI repository STRING. From STRING, we extracted all the protein interactor of the proteins codified by the DEGs. Note that, PPIs in STRING can come from different types of evidence, including Neighborhoods, Gene Fusion events, Co-occurrence events, Co-expression data, Experimental data, Database information, and Text-mining associations. Altogether these sources of evidence are measured and adjusted against previous knowledge. Through this kind of methods STRING attribute a *confidence score* to each known or predicted association. The score ranges from 0 to 1 and it determines the association quality based on the related type of evidence (low confidence: scores <0.4, medium confidence: 0.4 to 0.7, and high

confidence: >0.7)[75] . The interaction pattern among nodes is delineated according to the STRING interactions considering the *confidence score*.

When buildind our network, in order to restrict the edge set to the most trustworthy STRING associations, we introduced two restrictions on the extracted PPIs: (1) PPIs must be derived from Experimental and Database evidence, (2) STRING *confidence score* must be higher than 0.7 (high-confidence score association). Note that *confidence scores* have been also integrated into the network model as weights on the network edges.

3.11.c Network Analysis

One the network has been constructed, we analyse it to gather more information on the proteins and biological processes represented by the network. In detail, we first identify hub nodes, i.e. nodes with a high number of neighbors, and secondly we computed the clustering of the network. Finally, for each group of gene we performed the Gene Ontology (GO)[76] enrichment analysis.

Hub nodes

The network hubs have been identified by selecting the top 10% of the highest degree nodes. This threshold was suggested by other studies [77]. This allowed to identify nodes that have an important role in the network and therefore in the wound healing process.

Network Clustering

To gather a more detailed interpretation of the biological pathways underling the constructed network we first performed the clustering of the network and subsequently, the enrichment of the nodes in each cluster. In this way, we could study the behaviours of group of genes clustered together based on their topological properties. It is known that topological clusters corresponds specific biological functions or biological processes [78]. In our study, we performed the clustering using the Cytoscape [79] plugin ClusterONE, because of its reliability

and because considers network weights (i.e., STRING confidence scores) and it allows cluster overlapping [80]. Statistically significant clusters are identified by a *p*-value, also provide by ClusterONE through a one-sided Mann-Whitney U test performed on the in-weights and out-weights of cluster vertices. A low *p*-value indicates that the in-weights are highly larger than out-weights, leading to a reliable cluster which is not the result of random fluctuations. To distinguish significant clusters from not statistically significant ones, authors suggest a *p*-value threshold of 0.05 [80].

Enrichment analyses

Finally, for both hub nodes and nodes belonging to each cluster, we performed GO enrichment analysis to establish a biological interpretation of the proteins. We detected the enrichment on the basis of GO terms with a significant *p*-values corrected with a false discovery rate (FDR). Statistically significant processes and terms are identified considering adjusted *p*-values < 0.001. Subsequently, the significant pathways were compared to reference lists GO terms of biological processes known to be involved in the wound healing process. The GO enrichment analysis allowed selecting possible new candidate genes, signalling pathways and proteins, which have a relevant role in the AMG molecular mechanism.

3.12 *In vivo* wound healing assay

20 females C57BL/6 mice 12 weeks old were used in this study. Excisional wound splinting mouse model was performed [81], [82]. C57BL/6 (12 weeks old) mice were shaved, sterilized with betadine and ethanol and full-thickness wounds (0,5 cm diameter) were made in the shaved dorsal skin under ketamine/xylazine anaesthesia with a 5-mm biopsy punch. In order to avoid wound closure caused by skin contraction, silicone rings were sutured to the

skin around the wounds. Wounds were then topically treated with thirty microliter of AMG (DMSO, 1:3), obtained from the 0,5 cm of skin biopsy following the Rigenera® protocol [72] [71]. A second group (n=5) was topically treated with the AMG-based therapy supplemented with a specific MEK inhibitor – Trametinib (0.2 mg, Cat No. HY-10999, MCE). Trametinib was dissolved in dimethylsulfoxide (DMSO) to a concentration of 20 mg/ml and 10 μL of the mixture (corresponding to 0.2 mg) was added topically together with the autologous micro grafts. A third group (n=5) was topically treated with the MEK inhibitor – Trametinib (0.2 mg, Cat No. HY-10999, MCE) (1:3 in PBS). The control group was treated with DMSO 1:3 in PBS as vehicle. Wounds were covered with Tegaderm™ dressing (3M, Maplewood, USA) to protect the wound area and to prevent the area from drying out. Every other day (day 2,4, 6 and 8), digital images were taken using a Nikon D1 camera, treatments were re-applied topically to the wound site and dressings were renewed. Wound contraction was calculated by comparing RWA (relative wound area) during the time. The analyses were performed using ImageJ software (NIH, Baltimore, Maryland). RWA of each mouse was expressed as a percentage normalized to the relative wound area at the beginning of the experiment (day 0). Animals were sacrificed at day 8 after wounding and wound skin fractions were collected to be further processed for paraffin embedding and gene expression analyses. Stainings were performed on 5 μm microtome sections. Animals procedures were performed in accordance with the Ethics Committee at KU Leuven (Belgium) under the ethical approval code P036/2018.

3.13 Statistical analysis

GraphPad Prism (version 6) was used to graph the data and GraphPad Prism software (San Diego, CA, USA) was used to analyse all the experiments of this study. Significant differences were determined by one-way or two-way analysis of variance (ANOVA) statistical tests and unpaired t test. Data are presented as mean ± standard error of mean (SEM).

Chapter 4

Results

4.1 Autologous micro graft-based therapy increases cell migration and accelerates scratch closure

Autologous micro grafts (AMG) have shown in recent years to be a new, cost-effective and alternative wound healing self-treatment that avoids immune rejection. Despite the considerable potential of this technique, neither the cellular nor the molecular mechanisms behind AMG treatment are still understood, limiting significantly our knowledge of this therapy and its future improvement. First, we aimed to understand the cellular effects exerted by AMG on wound healing. By mimicking cell migration during *in vivo* wound healing, the *in vitro* scratch assay is particularly suitable for wound healing research studies [83]. Murine primary adult fibroblasts were isolated from tail's tips and *in vitro* cultivated until obtaining the correct level of cell confluence to perform the cell scratch assay. The artificial wounds/scratches were created on cell monolayers and images were taken at the beginning (T0) and at regular intervals (T1, T5, T12 and T24) until closure of the *in vitro* wounds. Scratched cells were treated with AMG, being applied on the wounded cells with different dilutions (1:5, 1:10 and 1:20) and for different time period of treatment (1h, 5h, 12h and 24h) (Figure 1a).

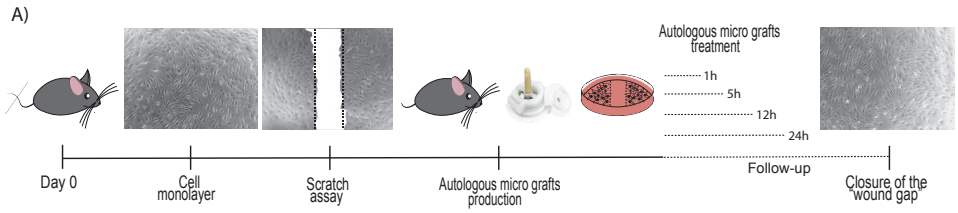
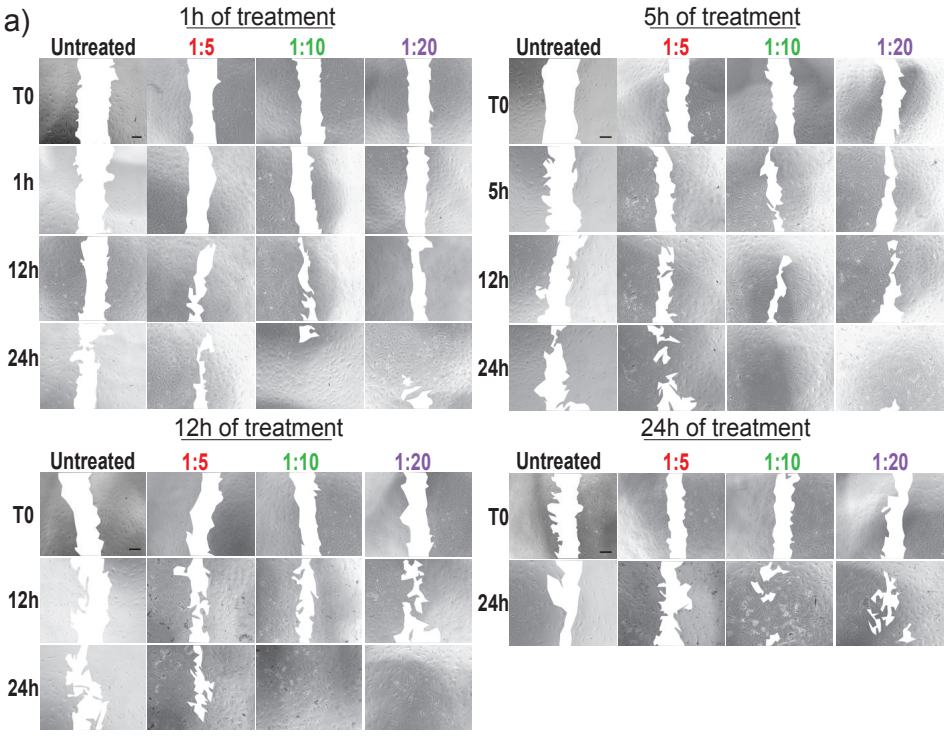


Figure 1: a) Schematic representation of the in vitro wound healing study performed using murine primary fibroblasts (obtained from tail tips of C57BL/6 mice).

Untreated scratched cells showed a reduction of scratch closure fewer than 50% at 24h after *in vitro* wounding. Interestingly, our results showed that, independently of timing and concentration, all AMG treatments were able to

increase cell migration rate and to accelerate scratch closure compared to untreated cells. Particularly, cells exposed to dilution 1:10 for 5 and 12 hours exhibited the highest significant enhancement scratch-closure of the *in vitro* artificial wounds (Figure 2a and b) with a scratch closure of 78%±26% and 84%+20% respectively 24 hours after AMG treatment.



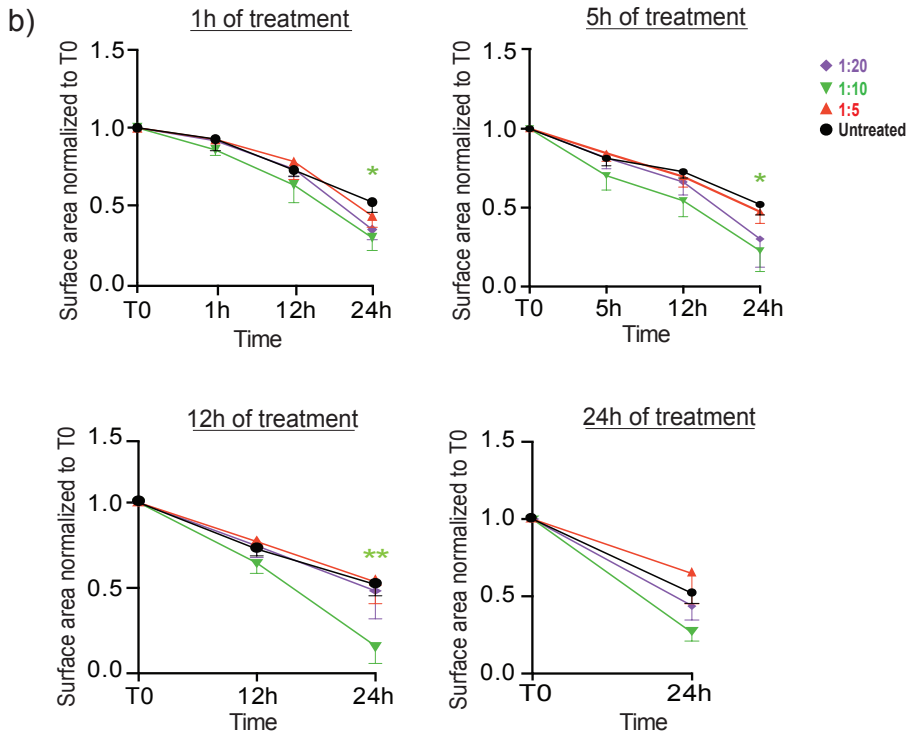


Figure 2: AMG-based cell treatment increases migration rate of murine primary fibroblasts after scratch assay. (a) Representative images of scratch assay on a monolayer of fibroblasts. AMG were applied on wounded cells with different dilutions (1:5, 1:10 and 1:20) and for different time periods (1, 5, 12, 24h). Images were taken at the beginning (T0) and at regular intervals until the closure was achieved. Comparisons of the images allowed quantifying the cell migration rate. **(b)** Quantification average of 4 biological replicates for each time of treatment. Data are presented as mean ± SEM (standard error mean). Significant differences *vs* control are calculated with two-way ANOVA (n=4) and indicated as * $P < 0.05$; ** $P < 0.01$.

Moreover, cell viability assays showed no differences in the number of viable cells after AMG treatment compared to untreated cells, indicating that AMG treatment has no effect on increasing cell survival of wounded cells (Figure 3).

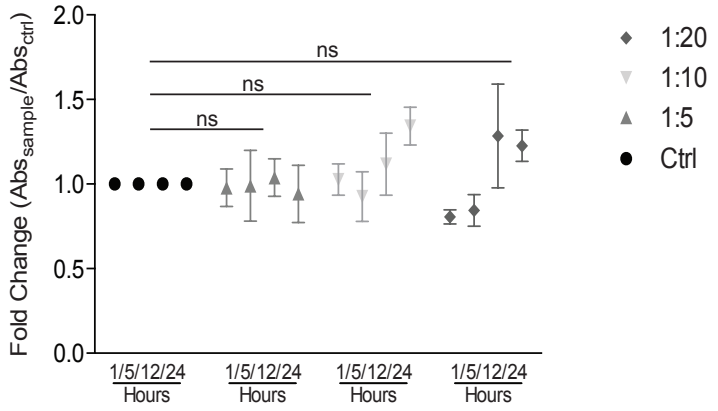


Figure 3: Effect of the autologous micro graft treatment on cellular viability. XTT assays were used to measure metabolic activity and drug sensibility of murine primary fibroblasts exposed to different dilutions of the AMG-based treatment. Different dilutions showed comparable responses in cell viability. Each dilution absorbance value (read it at 450 nm) was normalized to the control group (untreated). 450 nm absorbance values were then expressed as a fold change and significant differences were evaluated by two-way ANOVA (5 biological replicates).

We then hypothesized that accelerated scratch closure after AMG treatment could be due to an increase in cell proliferation or an enhancement of cell migration. First, cellular proliferation was evaluated by performing the EdU proliferation assays. EdU (5-ethynyl-2´-deoxyuridine) is a thymidine nucleoside analog that is incorporate in the DNA during the S-phase of the cell cycle. Wounded cells were incubated with the AMG-based treatment for different time periods (1h, 5h, 12h and 24h) and subsequently incubated with EdU (10 μM) for 2 hours at 37°C. The presence of the Propidium Iodide (PI) allowed following the cell cycle phase progress. Unwounded cells were used to assess the effect of the treatment on the proliferation rate in a “wild-type” environment. No differences in the cell cycle at any exanimated cell cycle phase (G1, S and G2/M) were observed in any treated or untreated group (Figure 4a and 4b), dismissing any possible effect on cell proliferation in AMG-mediated acceleration of scratch closure.

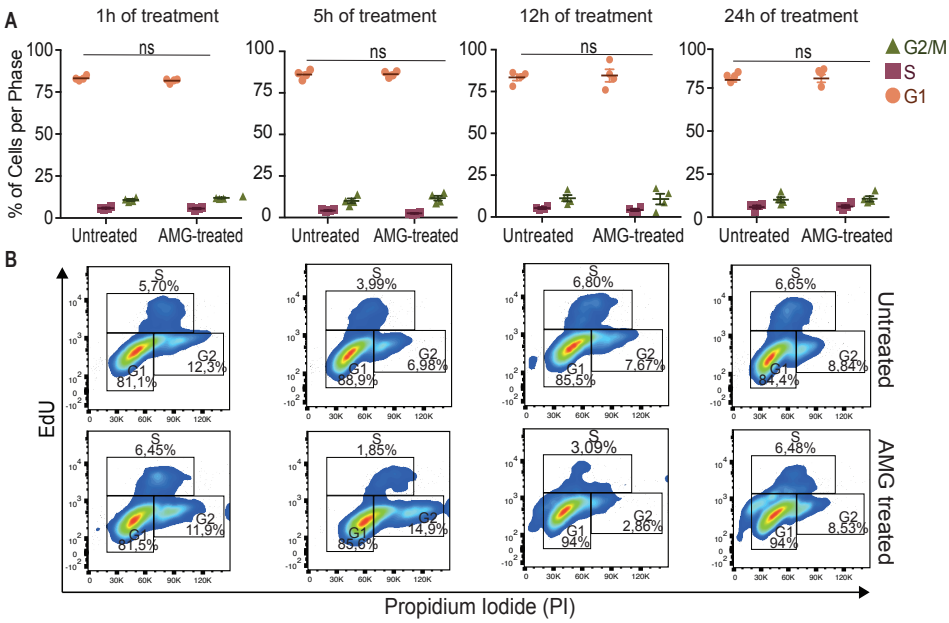


Figure 4: Micro graft-based treatment does not trigger cell proliferation on an *in vitro* wound healing model. (**a)** FACS analyses of wounded and unwounded murine primary fibroblasts AMG-treated for 1h, 5h, 12h and 24h. Data is a representative experiment of 4 biological replicates. (**b)** Quantification average of 4 biological replicates is reported. Data are presented as mean ± SEM (standard error mean). Significant differences were calculated with two-way ANOVA.

Next, effect of AMG treatment on cell migration was evaluated by transwell migration assay. Fascinatingly, AMG-treated cells showed a significant increase in the migration rate upon AMG-based treatment compared to untreated cells (Figure 5a). Importantly, alpha-Smooth Muscle Actin *(αSMA)* protein, a marker of activated contractile fibroblasts (also known as myofibroblasts), detected by immunofluorescence and western blotting was highly increased in cells treated with autologous micro grafts. (Figure 5b and 5c).

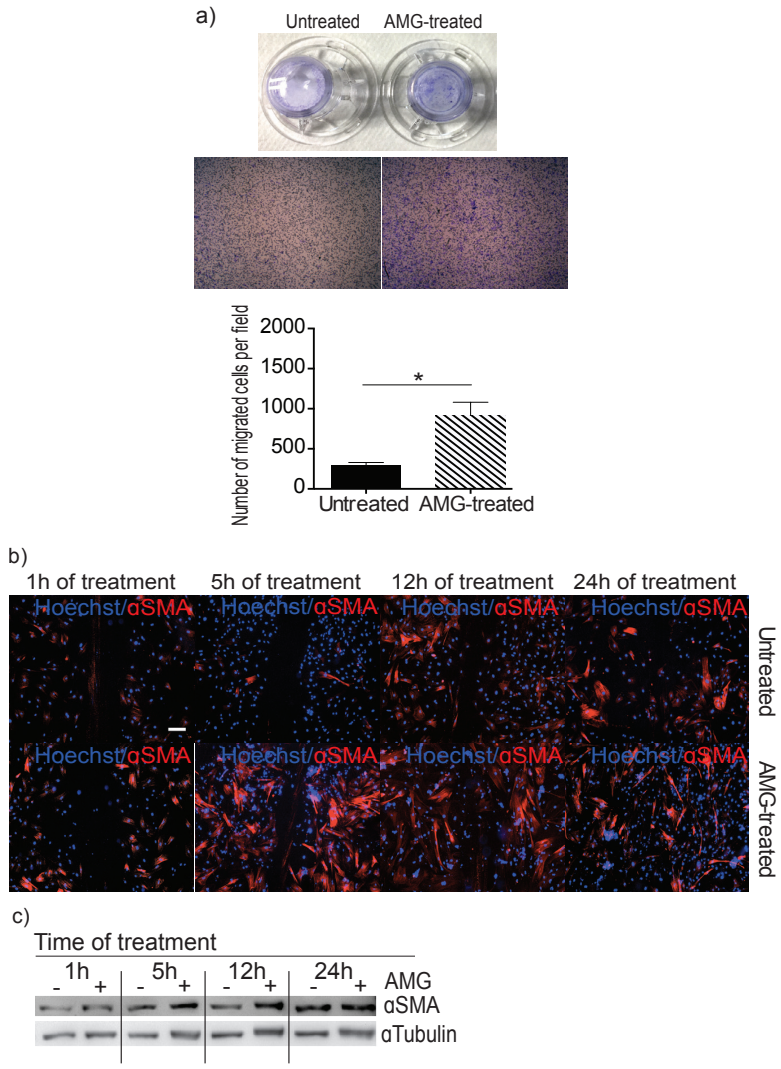


Figure 5: AMG-based treatment boosts cell migration and *α-SMA* protein level in an *in vitro* model of wound healing. (a) Macro- and microscopic observation of transwell chambers untreated and AMG-treated. Migrated cells were stained with alpha Smooth Muscle Actin (Cy3 conjugated) (1:200, C6198, Sigma) and observed under a light microscope and analysed using ImageJ software. Data are presented as mean ± SEM. P-values were calculated using student t test (4 biological replicates) * $P < 0.05$. (**b)** Representative immunofluorescence for *α-SMA* protein localization (in red). Nuclei were stained with Hoechst (blue). Scale bar = 200 µm. **(c)** Representative western blotting showing *α-SMA* protein level extracted from wounded murine fibroblasts AMG-treated (+). Group of unwounded cells were used as controls (-).

In conclusion, our results show that AMG treatment accelerates cell scratch-closure in an *in vitro* model of wound healing. This effect is mediated by increased capacity of cell migration as showed by the transwell assay and increased a-SMA protein level in treated cells. Interestingly, AMG treatment has no effect on cell cycle which discard a proliferation-mediated effect on the accelerated scratch closure.

4.2 Soluble AMG fraction improves cell scratch closure acceleration compared to unprocessed micro grafts

To gain knowledge about the mechanisms by which AMG treatment enhances cell migration and scratch closure we centred our attention in the putative components present within the AMG solution. We hypothesized that micro grafts support the healing process either by providing a **soluble fraction** containing essential growth factors and/or cytokines or an **insoluble fraction** containing intra and extra cellular vesicles. Using a polyethylene glycol (PEG)-based vesicles enrichment method, the insoluble fraction of the autologous micro grafts was collected by tying up cellular vesicles out of solution. Insoluble fractions were collected by a short, low-speed centrifugation. Fractions were then deeply analysed and compared to the total AMG (unprocessed). Mouse antibody array membranes were used to unveil the presence of soluble growth factors within the soluble fraction of the autologous micro grafts (Figure 6a). Among the soluble growth factors, we observed the presence of high level of insulin-like growth factor (IGF-1), insulin-like growth factor binding proteins (IGFBPs), epidermal growth factor (EGF) and basic fibroblast growth factor (bFGF) (Figure 6b). On the other hand, the insoluble fraction was evaluated by Nanosight and immunofluorescence analyses (figure 6c and d), which confirmed the presence of a high range of cellular vesicles within the autologous micro grafts.

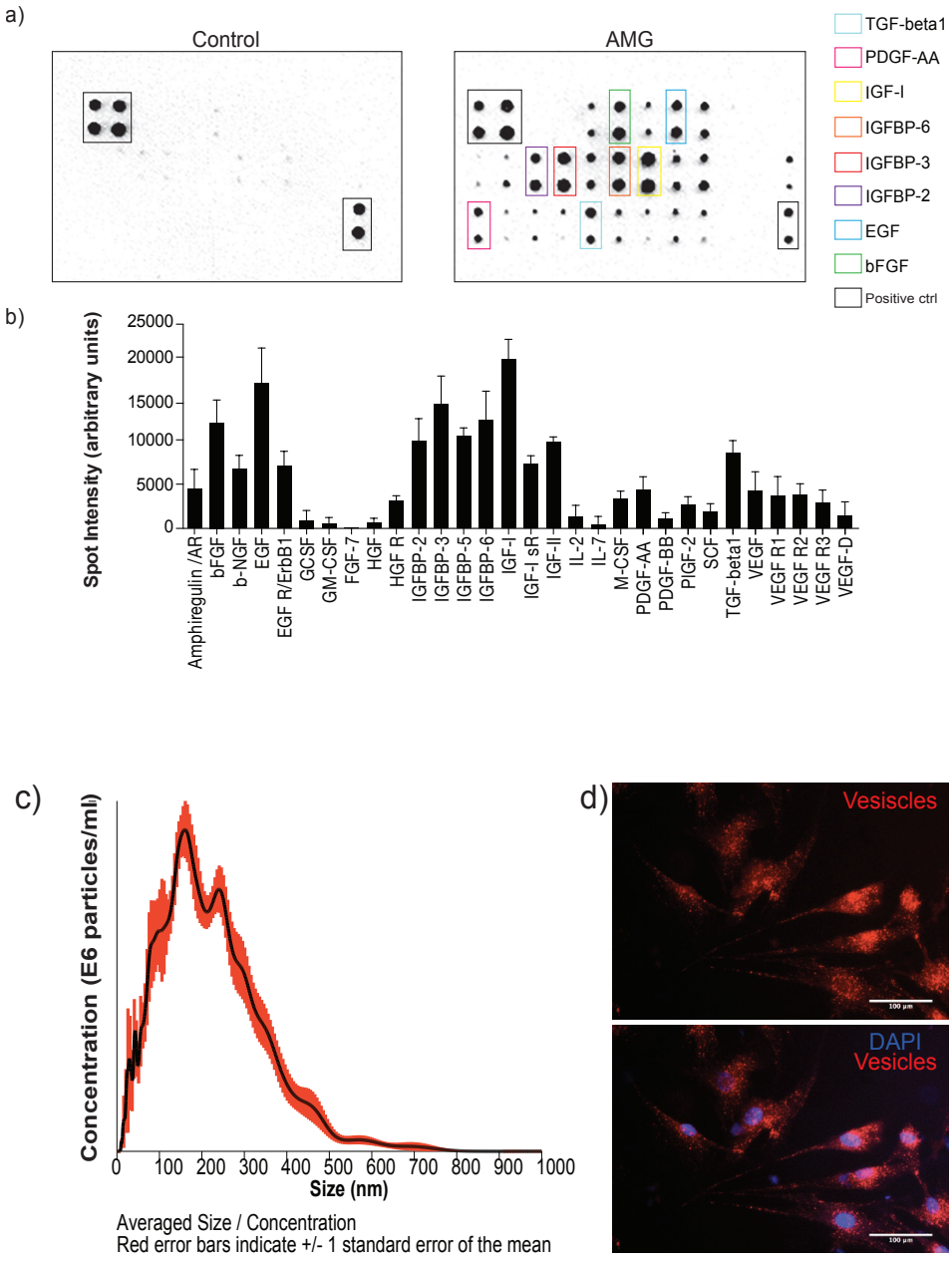


Figure 6. Characterization of the AMGs molecular fractions. (a) Representative images of antibody array membrane showing presence of several growth factors within the AMG soluble fraction (right panel) compared to the PBS-vehicle (left panel) (4 biological replicates). **(b)** Analysis of

the increase in spot intensity (in arbitrary units) is shown in the graph. Vesicles were isolated from the insoluble fraction of the AMG using a polyethylene glycol (PEG)-based vesicle enrichment technique (average of 4 biological replicates is shown). **(c)** Nanosight analyses indicating vesicle average size and concentration within the AMG insoluble fraction. **(d)** Representative immunofluorescence of vesicles labelled using Exo-Glow™ fluorescent label. Scale bar= 100 µm. (n=1).

Subsequently, adult fibroblasts were treated with the unprocessed AMG, insoluble and soluble AMG fractions separately on an *in vitro* wound healing model (cell scratch assay). Intriguingly, all soluble fraction treatments showed a complete scratch closure capacity 12h after *in vitro* wounding proving to significantly accelerate even further *in vitro* scratch-closure compared to unprocessed AMG treatment (Figure 7a and 7b). Soluble fraction also granted an enhanced cell migration capacity confirmed by Transwell migration assay (Figure 7c). These results show that soluble fraction increases the efficiency of the *in vitro* scratch-closure. Therefore, it may serve as a potential way to improve the AMG regenerative effect. Soluble fraction shows presence of several growth factors such us IGF, IGFBPs, EGF and bFGF. Importantly, either EGF as bFGF have been previously involved in cell migration and wound healing [40].

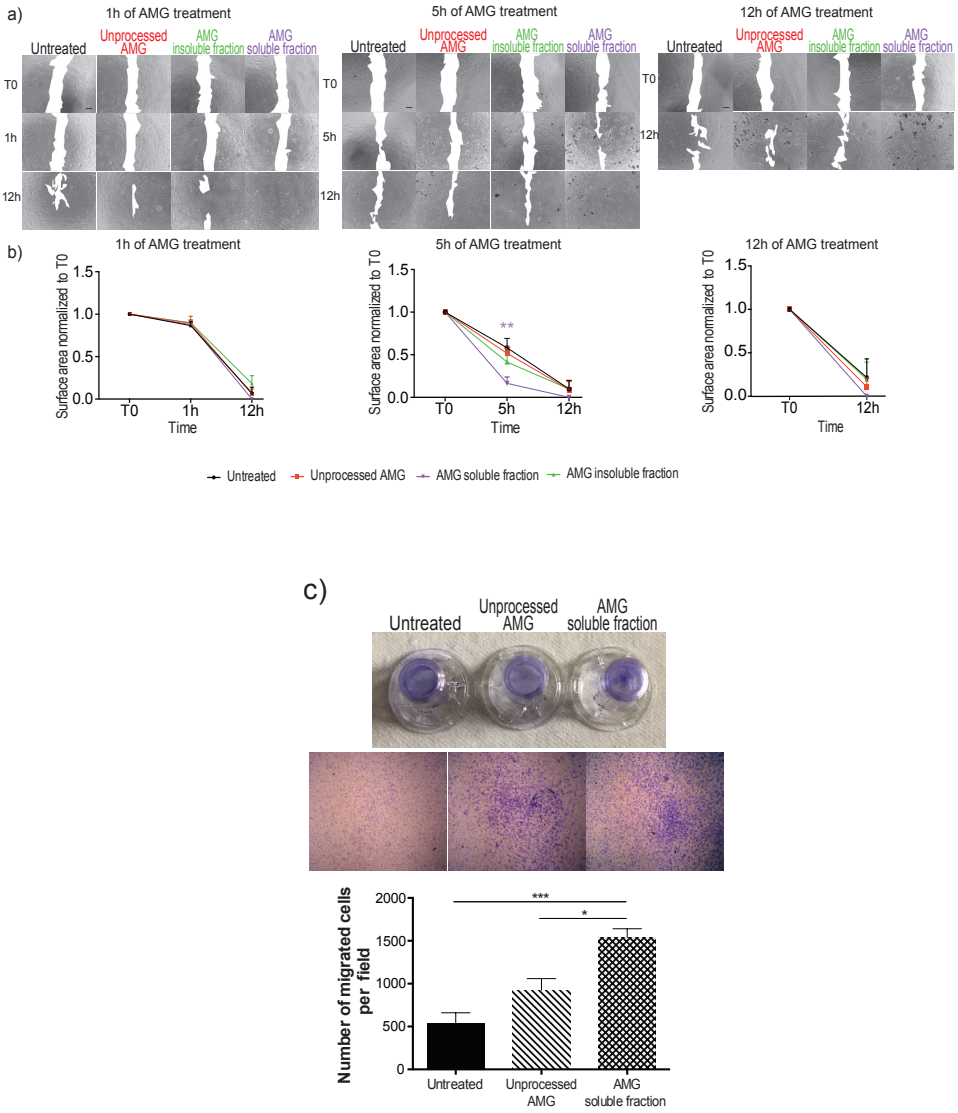


Figure 7: The soluble fraction of the AMG-based treatment increases the migration rate of murine primary fibroblasts. (a) Representative image of scratch assay on a monolayer of AMG treated murine primary fibroblasts (unprocessed, insoluble and soluble fraction) and for different time periods (1, 5, 12, 24h). Scratched untreated cells were used as a control. Images were taken at the beginning (T0) and at regular intervals until the closure was achieved. **(b)** Quantification average for each time of treatment. Data are presented as mean ± SEM (standard error mean). Differences are calculated with two-way ANOVA (4 biological replicates) and indicated as *** $P < 0.005$. **(c)**

Observation of transwell chambers after stimulation with the AMG-based treatment. Migrated cells were stained with crystal violet 0,1%, observed under a light microscope and analysed using ImageJ software. Data were presented as mean ± SEM. Differences are calculated using unpaired student t test (4 biological replicates) and indicated as * P < 0.05; *** P < 0,005.

4.3 Revealing the molecular mechanism of AMG-based treatment through knowledge-based gene association networks

To shed light on the molecular mechanism of micro graft-mediated wound healing acceleration we studied the changes in the transcriptome of wounded murine primary adult fibroblasts exposed to different time period of AMG treatment (1h, 5h, 12h and 24h) compared to untreated cells. RNA samples were collected after each time of treatment and analysed by RNA sequencing (HiSeq 4000 sequencing system - Illumina). Effectiveness of the AMG treatment was assessed by analysing the gene expression differences related to each time of treatment. Moreover, in order to obtain individual transcriptome profiling and individual biological interpretation we used the N-of-1-pathways MixEnrich methods [62]. This strategy allowed us to compare single-subject paired mRNAs (e.g. AMG-treated and untreated cells). The pilot RNA sequencing showed that both treatment and time of treatment have an effect on the transcriptome profile, irrespective of the presence of the artificial wounds, as shown by the principal component analysis (Figure 8a). The results showed that the number of enriched pathways is increasing over the time, even that the high number of pathways enriched at 12 and 24 hours of treatment is probably due to secondary/feedback effects (Figure 8b). Therefore, we focused subsequent analyses on the 5h of treatment, which more likely represents the early direct effect of the micro-graft treatment on wounded cells transcriptome. Importantly, enrichment of important pathways that play roles in the healing process, such as positive regulation of cell migration and cell motility and regulation of inflammatory response was assessed (Figure 8c).

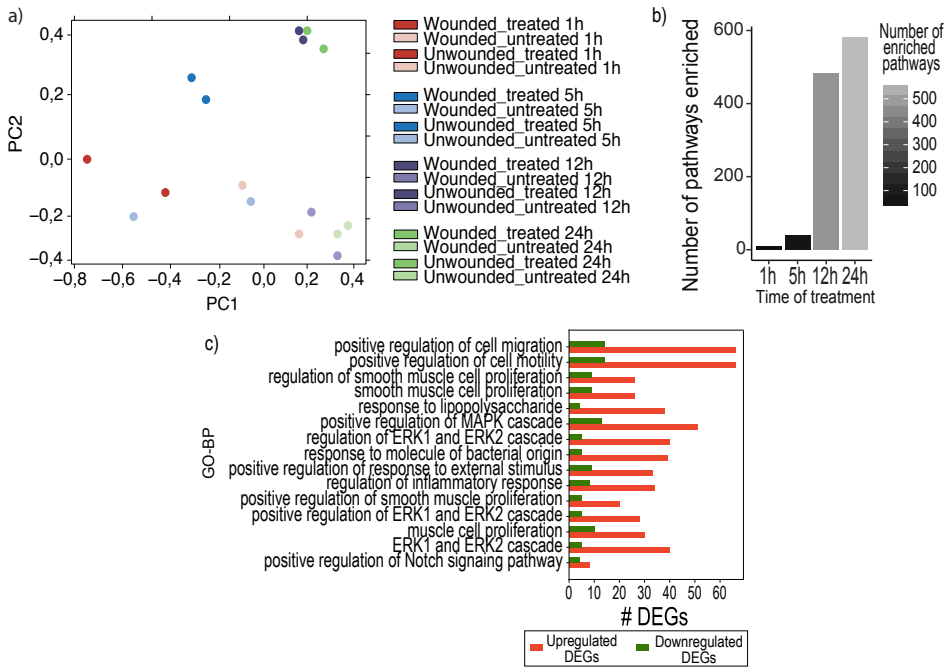


Figure 8: Transcriptome changes in murine primary fibroblasts exposed to the AMG-treatment, a pilot study. (a) Principle component analysis was performed in order to evaluate transcriptome differences caused by the AMG-based treatment. **(b)** GO (Gene Ontology) analysis based on N-of-1-pathways MixEnrich methods. Dysregulated mRNAs were used to perform the gene ontology analysis (p-value < 0,05). **(c)** Top 20 enriched pathways upon autologous micro graft-based treatment (5h of stimulation). Red bars indicate up-regulated genes and green bars indicate down-regulated genes (p-value < 0,05).

The N-of-1-pathways MixEnrich method allowed us to select the condition that likely best represents the effect of the treatment on the transcriptome level. Therefore, we subsequently expanded our biological cohort within this condition and set out to comprehensively explore the transcriptome changes caused by the micro graft treatment. Firstly, we validated that the differences in the transcriptome level inferred from the N-of-1 analysis are retained, as shown by the principal component analysis plot. The principal component 2 clustered samples treated and untreated separately (Figure 9a). These changes are linked with important biological process related with response to stimulus, cell migration and inflammatory response. Interestingly, Gene Ontology (GO)

analysis of biological processes associated with the differentially expressed genes stimulated by the AMG treatment, showed enrichment of important pathways related to positive regulation of cell migration and cell motility (Figure 9b). Heatmap of selected genes involved in positive regulation of cell migration and cell motility clearly showed the changes in the transcriptome profile of samples exposed to the treatment, compare to the untreated samples (Figure 9c). This supports our hypothesis that the increasing of the migration rate plays a key role in the molecular mechanism of the autologous micro graft-based treatment. Moreover, a high number of differentially expressed genes were found up-regulated upon the treatment. Fascinatingly, among those, several members of matrix metalloproteinases (MMPs) were found to be transcriptionally up-regulated in micro-graft treated cells compared to untreated cells, as shown by the volcano plot (Figure 9d). MMPs play an essential role in the wound healing reepithelialisation phase, orchestrating degradation and new synthesis of extracellular matrix [29].

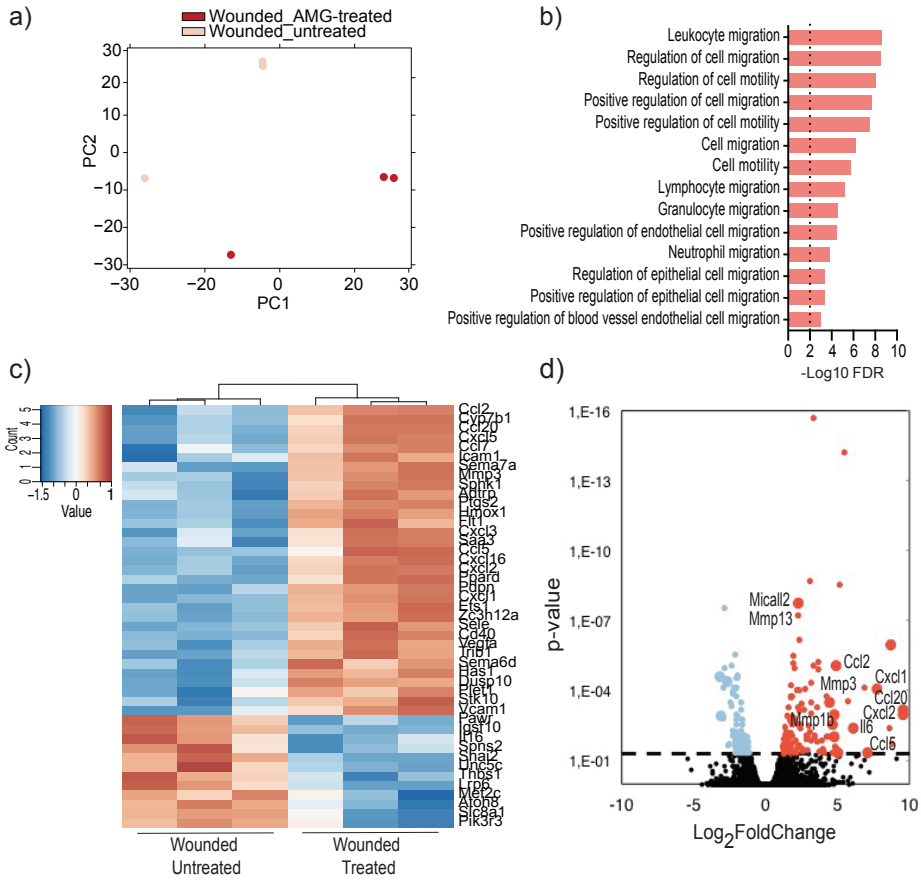


Figure 9: Autologous micro based-treatment triggers cell migration in murine primary fibroblasts in an *in vitro* model of wound healing. (a) Principle component analysis was performed in order to evaluate transcriptome differences caused by the autologous micro graft-based treatment (3 biological replicates for each condition). **(b)** Enriched GO terms biological process stimulated by the AMG-based treatment (5h of treatment; False Discovery Rate (FDR) < 0,05). **(c)** Heatmap showing differentially expressed genes associated with selected biological process related with cell migration and cell motility (GO:0030334, GO:0030335, GO:0016477, GO:0010632, GO:0010634, GO:2000145, GO:2000147 and GO:0048870). **(d)** Volcano plot showing up-regulated (red dots) and down-regulated (light blue dots) genes altered by the autologous micro grafts treatment (5h of stimulation). Gene values are reported as a Log2FoldChange (p-value < 0,05).

Subsequently, significant increased expression of Mmp1a, Mmp1b, Mmp9, Mmp10, Mmp12 and Mmp13 at mRNA level in micro graft treated cells for 5, 12 and 24 hours was confirmed. Interestingly, MMPs enzymatic activity was higher in micro-graft treated fibroblast cells compared to untreated cells (Figure 10a and 10b).

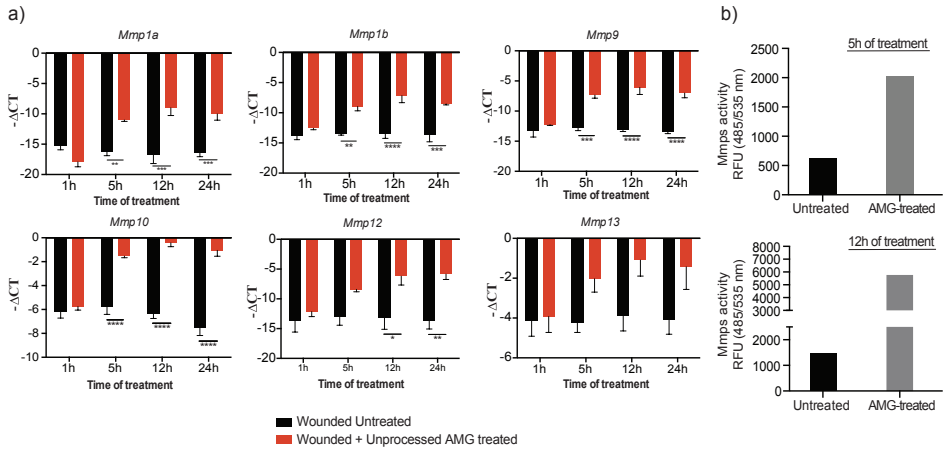


Figure 10: Autologous micro based-treatment triggers Mmps expression and protein activity in murine primary fibroblasts in an *in vitro* model of wound healing. (a) MMPs gene expression evaluated by RT-qPCR. Expression values are expressed as a -ΔCT normalized on the expression of *Gapdh, B-actin and Rpl13a* housekeeping genes (3 biological replicates).. Differences are calculated with two-way ANOVA (3 biological replicates) and indicated as * P < 0.05; ** P < 0.01; *** P < 0.005; ****P < 0.001. **(b)** Enzymatic activity of all MMPs members present in cell supernatant was fluorometrically detected. Data are presented as RFU (Relative Fluorescence Units). Signals were evaluated 30 minutes after starting the reaction using a microplate reader with a filter set of Ex/Em = 485/535. The fluorescence signal obtained from each sample was normalized on the substrate control.

RNA sequencing analysis led assessing the involvement of important genes and biological process involved in the regulation of the wound healing phases, such as genes related with the inflammation and remodelling phases. Pro-inflammatory cytokines including *Il-6* were found up-regulated upon the micro grafts treatment. *Il-6* is shown to play a pivotal role in initiating the healing

response [23]. Moreover, *Ccl2, Ccl20, Ccl5, Cxcl1, Cxcl2* chemokines are considered active participants in the wound healing process, enhancing cell migration of different cell types. Among those, the CXC family member - *Cxcl1* - is known to be up-regulated in acute wounds, having a pivotal role during the remodelling phase by stimulating cell migration [23]. On the other hand, matrix metalloproteinases were found increased in both mRNA and protein level upon the treatment, indicating their involvement in the molecular mechanism of the autologous micro graft-based treatment. Interestingly, transcriptome samples obtained from unwounded murine primary fibroblasts stimulated with the autologous micro grafts showed the same pattern. Samples are differently clustered upon the treatment, as shown in the principal component analysis (Figure 11a). Gene Ontology (GO) analysis showed that biological process related with regulation of response to external stimulus, inflammatory response and regulation of cell migration/motility were enriched upon the treatment (Figure 11b; False Discovery Rate, FDR < 0,05). Heatmap showed an up-regulation of selected genes involved in biological process related with cell migration and cell motility upon treatment (Figure 11c). Among those, cytokines, chemokines and matrix metalloproteinases were found strongly up-regulated upon autologous micro graft-based treatment, as showed in the volcano plot (Figure 11d).

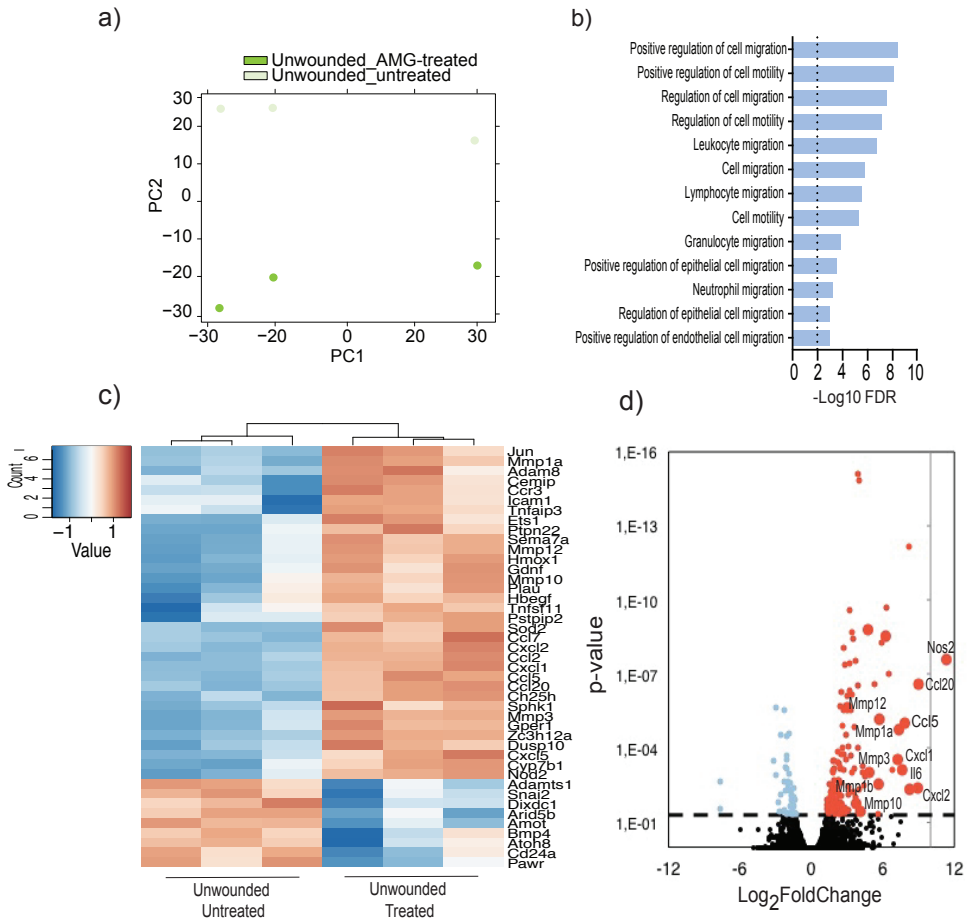


Figure 11: AMG-based treatment triggers cell migration and motility in wild-type murine primary fibroblasts. (a) Principle component analysis was performed in order to evaluate transcriptome differences caused by the autologous micro graft-based treatment (3 biological replicates for each condition). **(b)** Enriched GO terms biological process stimulated by the AMG-based treatment (5h of treatment; FDR < 0,05). **(c)** Heatmap showing differentially expressed genes associated with selected biological process related with cell migration and cell motility (GO:0030334, GO:0030335, GO:0016477, GO:0010632, GO:0010634, GO:2000145, GO:2000147 and GO:0048870). **(d)** Volcano plot showing up-regulated (red dots) and down-regulated (light blue dots) genes altered by the autologous micro graft treatment (5h of stimulation). Gene values are reported as a Log2FoldChange (p-value < 0,05).

The obtained results confirmed the involvement of specific biological process related with cell migration and cell motility as key points in the effect of the AMG-based treatment. On the other hand, the results allowed excluding a direct effect on the transcriptome changes caused by the creation of the “artificial wound”.

To better understand the biological mechanisms highly associated with the AMG treatment and the wound healing process we construct the wound healing network using the list of differentially expressed genes (DEGs) obtained from the RNA sequencing analyses. In detail, we used the repositories STRING to extract the protein interactors associated with the proteins codified by the DEGs [84]. This led to the construction of a Protein-Protein Interaction (PPI) network, in which network nodes represent proteins and network edges correspond to possible biological interactions between them (Figure 13). To build the network we selected from STRING only PPIs with high confidence score (>0.7) and recruited from experimental and database evidences (considered more reliable if compared to, for example, text-mining). Subsequently, we performed a topological network analysis that allowed detecting essential nodes, called hub nodes, which play pivotal roles in the likeds (Figure 13). Consequently, these nodes are considered fundamental for a better understanding of critical biological and molecular mechanisms [85]. The network has been further studied by dividing the network in clusters using the highly precise and reliable clustering software named ClusterONE [80], which allow studying complex protein systems starting from PPI networks (Figure 14). Here, nodes and edges represent proteins and interactions respectively. Moreover, proteins play different roles being crucial in several biological processes and, in turn, belonging to different modules (clusters). The advantage of ClusterONE is the ability to easily detect overlapped proteins and, in turn, cluster overlapping [80] (overlapping nodes presented as Δ - Figure 14). Afterwards, clusters have been enriched with GO terms, allowing to find new candidate genes, proteins and signalling cascades involved in the AMG molecular mechanism. A total of 107 clusters have been identified as possible target of the AMG treatment and all being essential events involved in the wound healing process (Figure 14). The results of the Network

analysis support our previously showed RNA sequencing data, linking together cell migration, positive regulation of the immune system and stimulation of the MAPK signalling pathways through ERK1/2 activation as indispensable factors of the AMG-mediated beneficial effect.

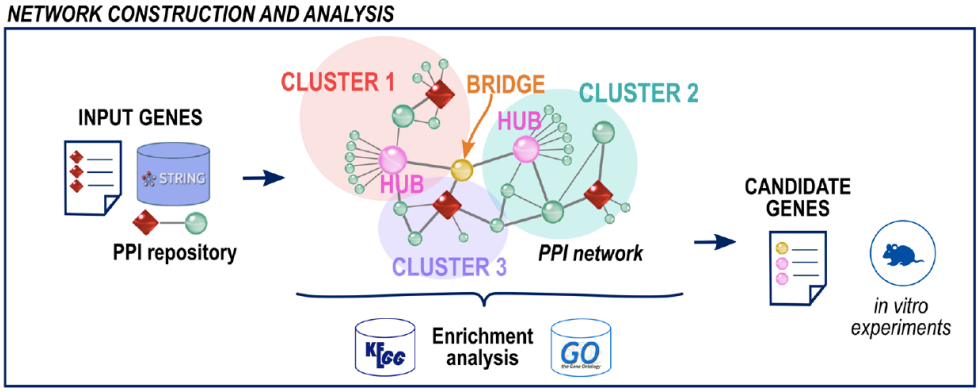


Figure 12: Overview of the Network analysis: The Protein-Protein Interaction Network (PPI) referred to the list of differentially expressed genes (DEGs) observed upon AMG treatment exposition and obtained through RNA sequencing was constructed using the STRING repository. Topological network analysis allowed obtaining important targets nodes, which more likely play important roles in the AMG-mediated effect in the wound healing process. Gene Ontology (GO) enrichment analysis has been then performed on the obtained clusters. Candidate protein, genes and signalling pathways regulated by the AMG treatment are shown as clusters. Image adapted from [85].

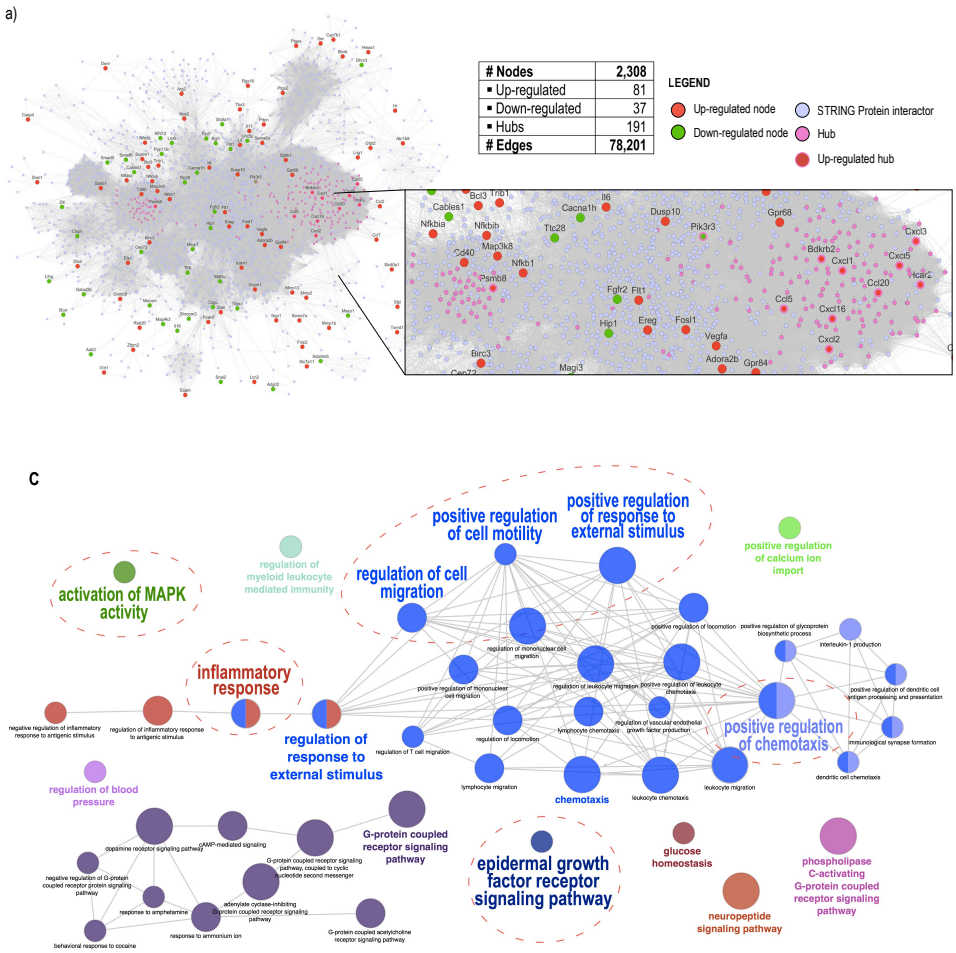
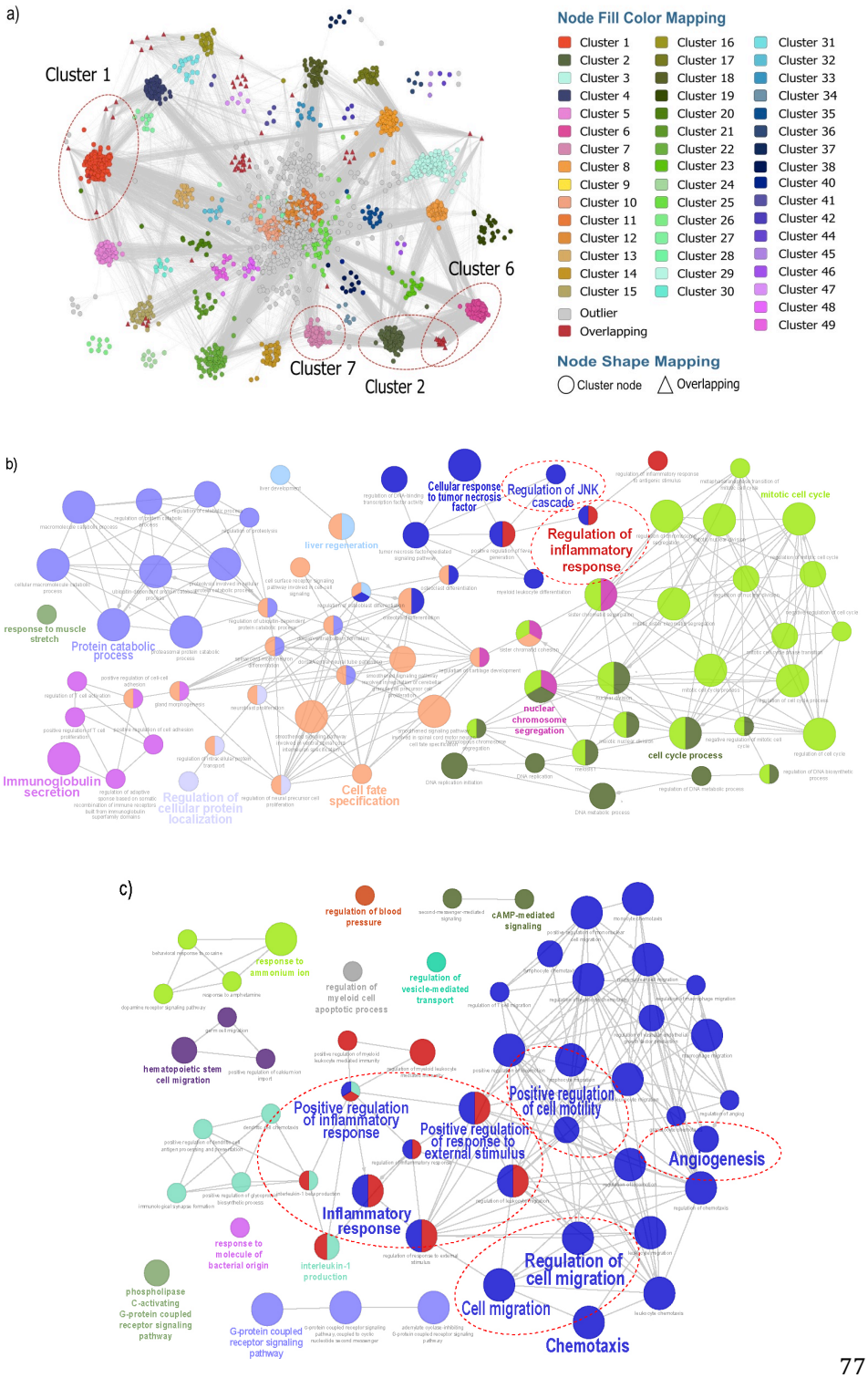


Figure 13: Protein-Protein Interaction network stimulated upon AMG treatment: (a) The Protein-Protein Interaction Network (PPI) referred to the list of differentially expressed genes (DEGs) observed upon AMG treatment and obtained by the STRING repository. DEGs are represented as red and green nodes of the network, based on their up-regulated or down-regulated expression respectively. Hub nodes are presented as purple nodes, sknown in an enlarged view. **(b)** Hub related GO enrichment analysis with selected biological process playing essential roles in the wound healing process.


a)
Cluster 1
Cluster 6
Cluster 7
Cluster 2
Node Fill Color Mapping
Cluster 1
Cluster 2
Cluster 3
Cluster 4
Cluster 5
Cluster 6
Cluster 7
Cluster 8
Cluster 9
Cluster 10
Cluster 11
Cluster 12
Cluster 13
Cluster 14
Cluster 15
Cluster 16
Cluster 17
Cluster 18
Cluster 19
Cluster 20
Cluster 21
Cluster 22
Cluster 23
Cluster 24
Cluster 25
Cluster 26
Cluster 27
Cluster 28
Cluster 29
Cluster 30
Cluster 31
Cluster 32
Cluster 33
Cluster 34
Cluster 35
Cluster 36
Cluster 37
Cluster 38
Cluster 40
Cluster 41
Cluster 42
Cluster 44
Cluster 45
Cluster 46
Cluster 47
Cluster 48
Cluster 49
Outlier
Overlapping
Node Shape Mapping
Cluster node
Overlapping
b)
Cellular response to tumor necrosis factor
Regulation of JNK cascade
Regulation of inflammatory response
mitotic cell cycle
liver regeneration
response to muscle stretch
Protein catabolic process
nuclear chromosome segregation
cell cycle process
Immunoglobulin secretion
Regulation of cellular protein localization
Cell fate specification
c)
regulation of blood pressure
cAMP-mediated signaling
response to ammonium ion
regulation of myeloid cell apoptotic process
regulation of vesicle-mediated transport
hematopoietic stem cell migration
Positive regulation of inflammatory response
Positive regulation of response to external stimulus
Positive regulation of cell motility
Angiogenesis
Inflammatory response
response to molecule of bacterial origin
interleukin-1 production
Regulation of cell migration
Cell migration
Chemotaxis
phospholipase C-activating G-protein coupled receptor signaling pathway
G-protein coupled receptor signaling pathway

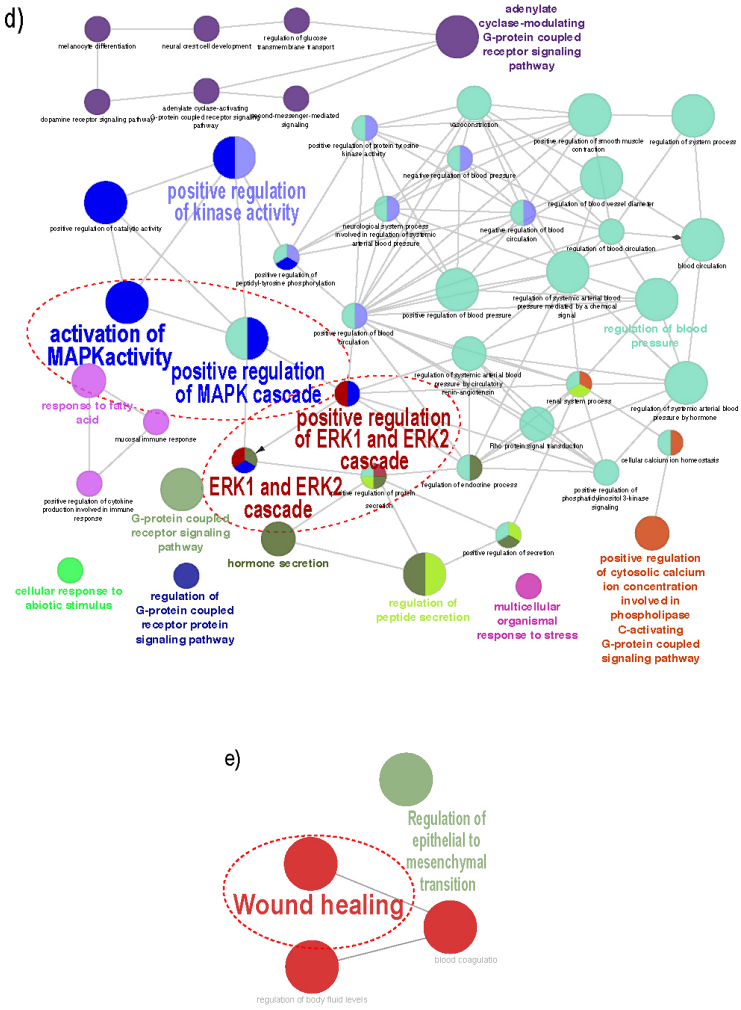


Figure 14: Network clustering: **(a)** Clusters have been obtained through ClusterONE and presented with different colours. Clusters including important wound healing-related biological processes have been selected and presented separately. **(b)** Cluster 1: Positive regulation of the inflammatory response, including regulation of the JNK cascade, tumour necrosis factor-mediated signalling pathways as well as regulation of DNA-binding transcription factor activity have been found as candidate of the AMG treatment. **(c)** Cluster 2: Positive regulation of locomotion, cell migration, chemotaxis, angiogenesis and regulation of vascular endothelial growth factor production have been identified as candidate of the AMG treatment. **(d)** Cluster 3: Positive regulation of kinase activity, including positive regulation and activation of both the MAPK activity and ERK1/2 cascade has been

assessed as target of the AMG treatment. **(e)** Cluster 9: Regulation of the wound healing process is also referred as candidate of the AMG treatment.

4.4 Matrix metalloproteinases regulate AMG-based cell migration in an *in vitro* model of wound healing

If a proper wound healing has to be achieved, the extra cellular matrix (ECM) has to be remodelled correctly. Key regulators of the ECM remodelling process are endopeptidases called matrix metalloproteinases (MMPs), which consist of a family of proteases calcium-dependent, requiring a zinc metal ion for their activity. The MMPs role is not limited to the ECM turnover but also they play a pivotal role in biological processes involving proteolysis, such as developmental processes [46], inflammation and immunity-related processes by monitoring cytokines/chemokines activities [47] and tissue preservation function processes, including the wound healing [48]. MMPs catalytic activity allows cell migration and produces bio-active substrates, which regulate different signalling pathways [49]. RNA sequencing analysis after treatment with the autologous micro grafts (5h of exposure) led identifying MMPs as important targets. Among those, we found highly expressed Mmp1a, Mmp1b (known as collagenase-1), Mmp3 (known as stromelysin-1), Mmp9 (known as gelatinase B), Mmp10 (known as stromelysin-2), Mmp12 (known as metalloelastases) and Mmp13 (known as collagenase-3). (details showed in Table 1).

Table 1

Member	Substrates	GO Biological process	Source
Mmp1a (Collagenase-1)	Cleaves collagens of types I, II, and III at one site in the helical domain. Also cleaves collagens of types VII and X (By similarity). Able to degrade synthetic peptides and type I and II fibrillar collagen	Collagen catabolic process GO:0030574, positive regulation of fibroblast migration GO:0010763, positive regulation of smooth muscle cell migration GO:0014911,proteolysis GO:006508	UniProtKB-Q9EPL5 (MMP1A_MOUSE). GO annotation on QuickGO
Mmp1b (Collagenase-1)	Cleavage of the triple helix of collagen at about three-quarters of the length of the molecule from the N-terminus, at 775-Gly-|-Ile-776 in the alpha-1(I) chain. Cleaves synthetic substrates and alpha-macroglobulins at bonds where P1' is a hydrophobic residue.	Collagen catabolic process GO:0030574	UniProtKB - Q9EPL6 (MMP1B_MOUSE). GO annotation on QuickGO
Mmp3 (stromelysin-1)	Can degrade fibronectin, laminin, gelatins of type I, III, IV, and V; collagens III, IV, X, and IX, and cartilage proteoglycans. Activates procollagenas	Cellular response to amino acid stimulus (GO:0071230), collagen catabolic process (GO:0030574), negative regulation of protein kinase B signaling (GO:0051898), positive regulation of cell migration (GO:0030335), positive regulation of oxidative stress-induced cell death (GO:1903209), protein catabolic process (GO:0030163), proteolysis (GO:006508), regulation of cell migration (GO:0030334)	UniProtKB - P28862 (MMP3_MOUSE). GO annotation on QuickGO
Mmp9 (gelatinase B)	Could play a role in bone osteoclastic resorption. Cleaves type IV and type V collagen into large C-terminal three quarter fragments and shorter N-terminal one quarter fragments. Cleavage of gelatin types I and V and collagen types IV and V.	Cellular response to cell-matrix adhesion (GO:0071460), cellular response to reactive oxygen species (GO:0034614), collagen catabolic process (GO:0030574), embryo implantation (GO:0007566), extracellular matrix organization (GO:0030198), leukocyte migration (GO:0050900), negative regulation of apoptotic process (GO:0043066), negative regulation of fibroblast proliferation (GO:0048147), positive regulation of angiogenesis (GO:0045766),positive regulation of epidermal growth factor receptor signaling pathway (GO:0045742), positive regulation of keratinocyte migration (GO:0051549), positive regulation of leukocyte migration (GO:0002687), positive regulation of protein phophorylation (GO:0001934), proteolysis (GO:0006508), response to drug (GO:0042493), tissue remodelling (GO:0048771)	UniProtKB - P41245 (MMP9_MOUSE). GO annotation on QuickGO
Mmp10 (stromelysin-2)	Can degrade fibronectin, gelatins of type I, III, IV, and V; weakly collagens III, IV, and V. Activates procollagenase.	Collagen catabolic process (GO:0030574), regulation of cell migration (GO:0030334)	UniProtKB - O55123 (MMP10_MOUSE). GO annotation on QuickGO
Mmp12 (metalloelastase)	May be involved in tissue injury and remodeling. Has significant elastolytic activity. Hydrolysis of soluble and insoluble elastin. Specific cleavages are also produced at 14-Ala-|-Leu-15 and 16-Tyr-|-Leu-17 in the B chain of insulin.	Positive regulation of epithelial cell proliferation involved in wound healing (GO:0060054), positive regulation of gene expression (GO:0010628), positive regulation of type I interferon-mediated signaling pathway (GO:0060340), protelysis (GO:0006508), wound healing, spreading of epidermal cells (GO:0035313)	UniProtKB - P34960 (MMP12_MOUSE). GO annotation on QuickGO
Mmp13 (collagenase 3)	Plays a role in the degradation of extracellular matrix proteins including fibrillar collagen, fibronectin, TNC and ACAN. Cleaves triple helical collagens, including type I, type II and type III collagen, but has the highest activity with soluble type II collagen. Can also degrade collagen type IV, type XIV and type X. May also function by activating or degrading key regulatory proteins, such as TGFB1 and CTGF. Plays a role in wound healing, tissue remodeling, cartilage degradation, bone development, bone mineralization and ossification. Required for normal embryonic bone development and ossification. Plays a role in the healing of bone fractures via endochondral ossification. Plays a role in wound healing, probably by a mechanism that involves proteolytic activation of TGFB1 and degradation of CTGF. Plays a role in keratinocyte migration during wound healing. May play a role in cell migration and in tumor cell invasion.	Bone morphogenesis (GO:0060349), cartilage development (GO:0051216), collagen catabolic process (GO:0030574), extracellular matrix disassembly (GO:0022617), proteolysis (GO:0006508)	UniProtKB - P33435 (MMP13_MOUSE). GO annotation on QuickGO

In order to study if MMPs and its enzymatic activity play a deterministic role in AMG-dependent accelerated scratch-closure, we inhibited MMPs activity in an *in vitro* cell scratch assay. First, the effect of the MMPs activity and its inhibition (using the MMPs inhibitor -Actinonin) [86] was evaluated in three different conditions – Untreated cells, unprocessed AMG treated cells and cells treated with the AMG-derived soluble fraction. As shown in Figure 15a, unprocessed AMG and soluble fraction treated cells showed a notable increase in MMPs enzymatic activity. As expected, treatment of cells with Actinonin inhibitor

reduced MMPs enzymatic activity. Scratch assays combined with inhibition of the MMPs catalytic activity decreased the migration rate, leading to a significant delay in the closure of our artificial wounds, demonstrating that matrix MMPs enzymatic activity is involved in AMG-dependent accelerated scratch closure (Figure 15b and 15c).

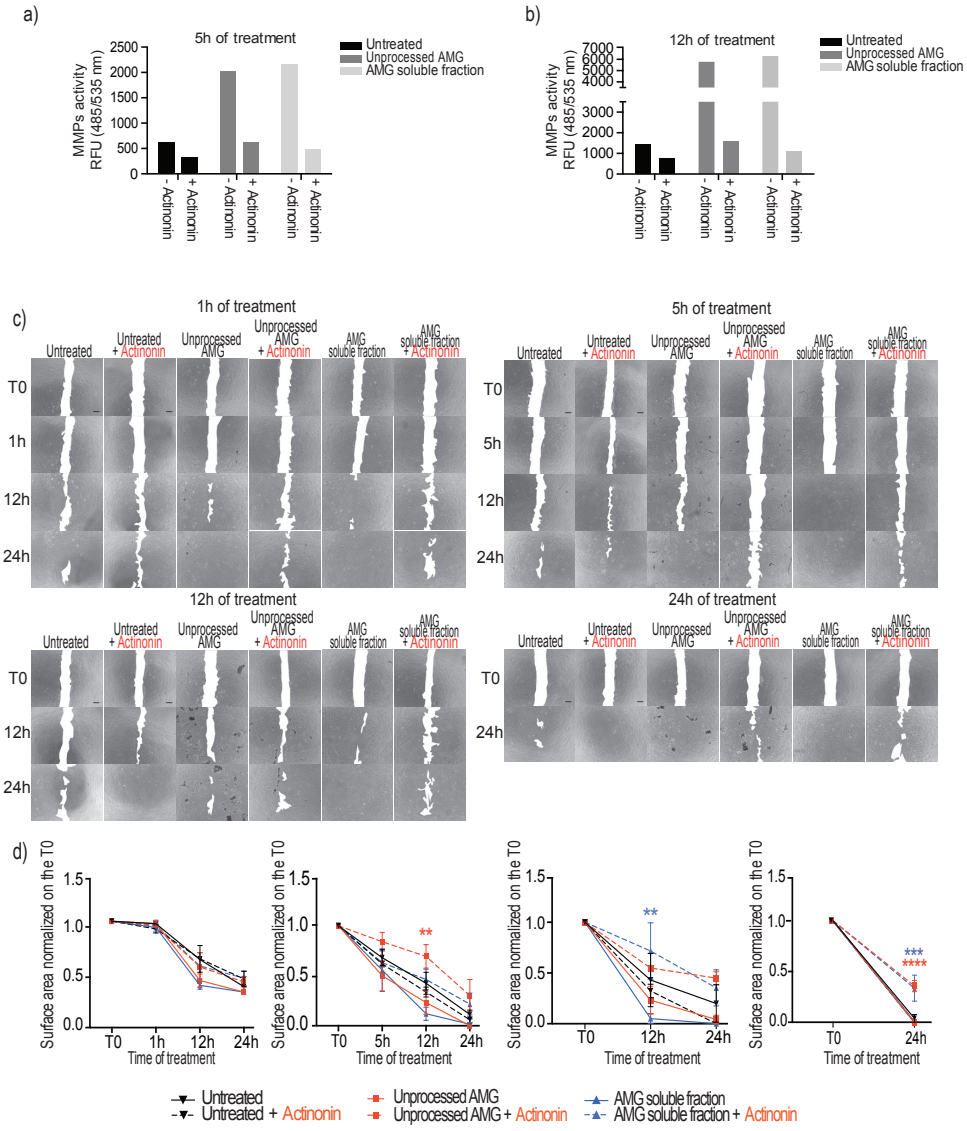


Figure 15: Inhibition of matrix metalloproteinases activity delays artificial wound closure in an *in vitro* model of wound healing. **(a)** Mmps extracellular activity in the biological samples exposed to the micro graft treatment was detected using the MMP activity assay kit - fluorometric green. Data are presented as RFU (Relative Fluorescence Units). The signals were evaluated 30 minutes after starting the reaction using a microplate reader with a filter set of Ex/Em = 485/535. The fluorescence signal obtained from each sample was normalized on the substrate control. **(b)** Representative images of scratch assay on a monolayer of murine primary fibroblasts. Autologous micro grafts were applied on wounded cells with different conditions (1:10 micro grafts dilution and its soluble fraction) and for different time periods (1, 5, 12 and 24h). Each group was or not incubated with the MMPs inhibitor – Actinonin – 20μM. Groups of wounded cells did not receive any treatment and were used as a control. Images were taken at the beginning (T0) and at regular intervals until the closure of the artificial wounds was achieved. Comparisons of the images allowed quantifying the cell migration rate. **(c)** Quantifications of AMG-treated cells with or without Actinonin are reported next to the image panels. Data were presented as mean ± SEM (standard error mean). Differences were calculated with two-way ANOVA (4 biological replicates) and indicated as ** $P < 0.01$; *** $P < 0.005$; ****$P < 0.001$.

4.5 Autologous micro graft-based treatment induces ERK signalling pathway activation to promote cell migration

RNA-sequencing analysis and Network-based analysis after autologous micro graft-based treatment identified important target genes and signalling pathways involved in the regulation of the Mitogen-activated protein kinase (MAPK) signalling pathway. Interestingly, Gene Ontology (GO) enrichment analysis associated with the differentially expressed genes stimulated by the AMG treatment, showed enrichment of important pathways related to regulation of Mitogen-activated protein kinase (MAPK) cascade and positive regulation of the extracellular signal-regulated kinase (ERK1, ERK2 cascade), both in the wounded and unwounded condition (Figure 16a and 16b).

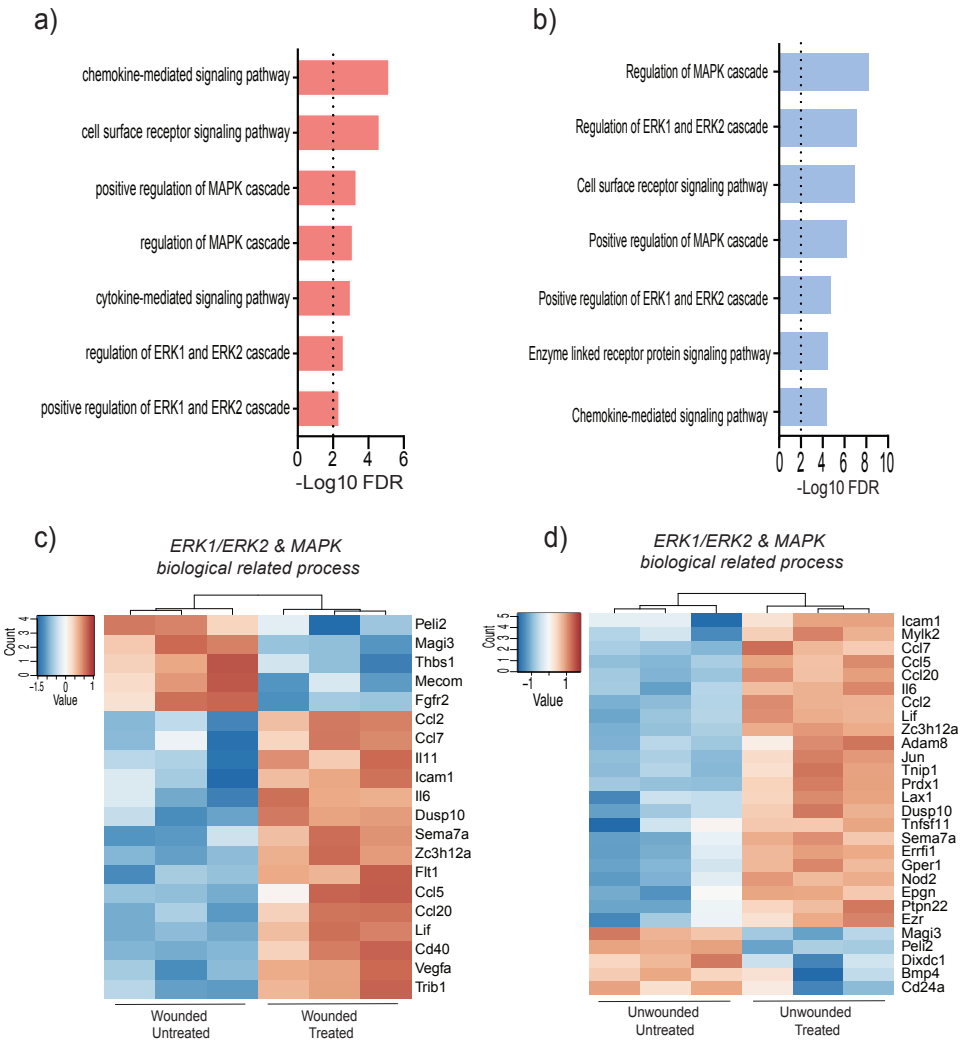


Figure 16: ERK/MAPK signalling pathway specifically activated by the autologous micro based-treatment. (a) Pathway enrichment analysis from selected GO terms (FDR<0,05). **(b)** Pathway enrichment analysis from selected GO terms (FDR<0,05). **(c)** Heatmap showing up-regulation of selected genes involved in biological process related with ERK1/ERK2 and MAPK (GO:0070372, GO:0070374, GO:0043410, GO:0043408). **(d)** Heatmap showing up-regulation of selected genes involved in biological process related with ERK1/ERK2 and MAPK from unwounded murine primary fibroblasts exposed to the treatment (GO:0070372, GO:0070374, GO:0070373, GO:0043410, GO:0043408, GO:0043409, GO:1903753, GO:0032872, GO:0043405).

In particular, exposure to the AMG-treatment induced up-regulation of important elements of the ERK1-ERK2 and MAPK signalling pathways, both in the wounded and unwounded condition, as shown from the heatmaps (Figure 16b and 16c).

Furthermore, among the soluble growth factors founded within the autologous micro graft-based treatment, insulin-like growth factor (IGF-1), insulin-like growth factor binding proteins (IGFBPs), epidermal growth factor (EGF) and basic fibroblast growth factor (bFGF) were the most enriched (Figure 2a). These growth factors exploit their function by activating different signalling pathways [23], such as ERK/MAPKs. Mitogen-activated protein kinases (MAPKs), including the ERK sub-pathway, are well described in playing critical role in cell proliferation, inflammation and response to stress. Moreover, many studies showed evidences that MAPKs play pivotal role in cell migration [40]. We aimed to evaluate whether the AMG-treatment was inducing activation of ERK1/2 signalling pathway and consequently enhancing acceleration of scratch closure. Western blotting analyses confirmed increased phosphorylation of ERK1/ERK2 mediators at 1 hour upon the AMG-based treatment (Figure 17a and b). ERK phosphorylation was maintained for 5 and 12 hours upon AMG-treatment. Scratch assays in AMG-treated cells combined with inhibition of the MAPKs pathway, obtained using the MEK inhibitor PD0325901, delayed significantly the capability of the cell to migrate compared to AMG-treated cells (Figure 18a and b). Our results show that activation of MEK/ERK pathway upon AMG-treatment plays an essential role in accelerated scratch closure.

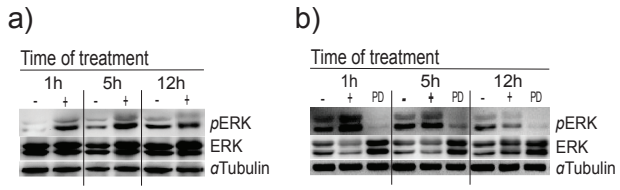


Figure 17: ERK phosphorylation upon autologous micro graft-based treatment in an in vitro model of wound healing. (a) Representative western blotting out of three biological replicates

showing the protein level of phosphorylated and total ERK1/ERK2 obtained from wounded and unwounded murine primary fibroblasts exposed to the micro graft-based treatment for different time periods (1, 5 and 12h). **(b)** Representative western blotting showing protein level of phosphorylated and total ERK1/ERK2 obtained from wounded and unwounded murine primary fibroblasts exposed to the micro graft-based treatment and in which we induced the inhibition of the MAPK signalling pathway (using the MEK inhibitor PD0325901 - 1 μM) for different time periods (1, 5 and 12h).

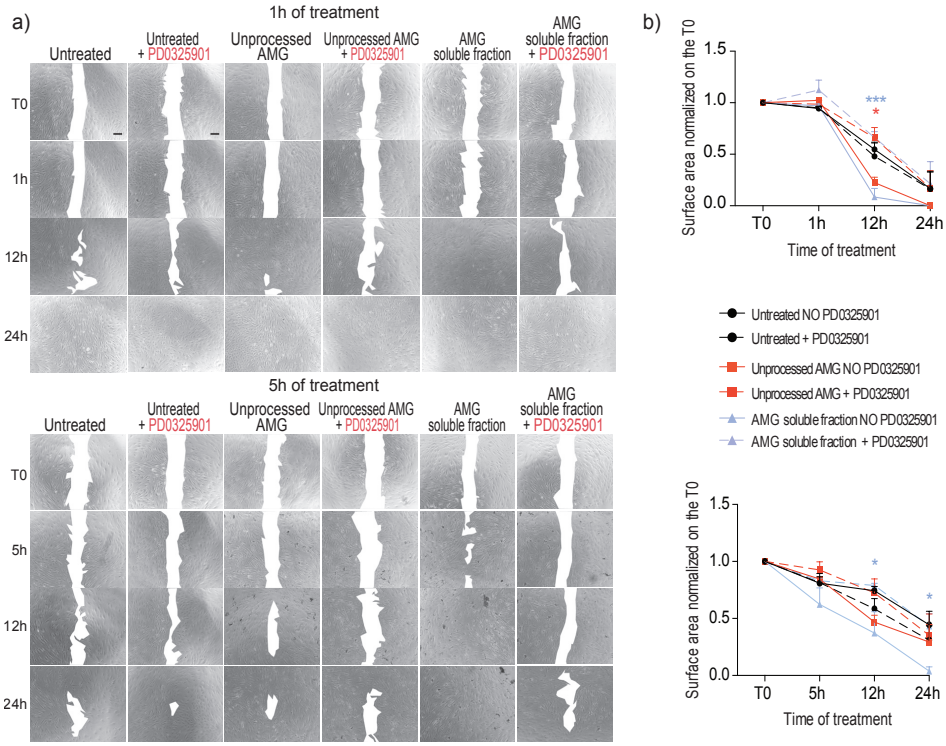


Figure 18: Inhibition of ERK signalling pathway activation delays in vitro wound closure. (a) Representative images of scratch assay on a monolayer of murine primary fibroblasts. Autologous micro grafts and their soluble fraction were applied on wounded cells for different time periods (1, 5, 12 and 24h). Each group was also incubated with the MAPKs MEK inhibitor –PD0325901– 1μM. Groups of wounded cells did not receive any treatment and were used as a control. Images were taken before the starting of the treatment (T0) and at regular intervals until the closure of the artificial wounds was obtained. **(b)** Quantifications of each time of treatment were reported next to the image panels. Data were presented as mean ± SEM (standard error mean). Significant differences *vs*

control were calculated with two-way ANOVA (4 biological replicates) and indicated as * P < 0.05; ** P < 0.01; *** P < 0.005; ****P < 0.001.

4.6 MMPs expression requires ERK signalling pathway activation to promote micro graft-based cell migration

MAPK signalling pathway, via ERK activation, is associated with positive regulation of cell migration and cell motility both *in vitro* [40] and *in vivo* [87]. Moreover, we have also shown, upon AMG-based treatment, an increase of MMPs gene expression and their enzymatic activity (Figure 10a and 10b). MMPs gene expression is fine-tuned regulated at the transcriptional level and its enzymatic activity is essential for tissue regeneration given that allows cell motility and migration.

Interestingly, all MMPs upregulated upon AMG-treatment possess in its promoter region binding sites for the AP-1 transcription factor [50]. Moreover, several cytokines and growth factors, including EGF (Epidermal Growth Factor) and b-FGF (basic Fibroblast Growth Factor) [29] trigger cell signalling culminating in trans-activation of MMP promoters by the convergence at the AP-1 sites (Fini et al. 1988). Increased trans-activation through AP-1 is achieved largely through mitogen-activated protein kinase/ERK pathway [88] (Yan et al 2006). Here, we hypothesised that the MMPs expression might be determined by ERK signalling pathway via AP-1 transcription factor activation upon AMG-treatment. In order to test our assumption, we combined scratch assay, *in vitro* inhibition of the ERK signalling pathway and gene expression analysis. Our results showed that inhibition of MEK/ERK pathway was able to significantly revert increased MMPs expression of Mmp1a, Mmp1b, Mmp9 and Mmp10 exerted by AMG-cell treatment (Figure 19a). Interestingly, Mmp12 expression, which was also upregulated upon AMG-cell treatment, showed no differential expression following MEK/ERK pathway inhibition, suggesting that other alternative pathways could be involved in AMG-mediated Mmp12 expression.

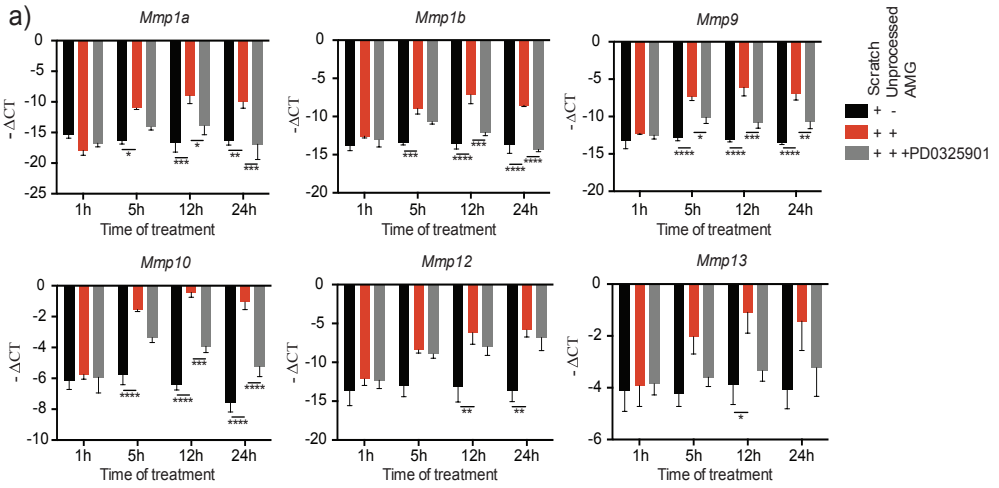


Figure 19: Inhibition of ERK signalling avoids AMG-dependent MMPs gene expression. (a) MMPs gene expression evaluated by RT-qPCR. Gene expression values are expressed as a -ΔCT normalized on the expression of *Gapdh, B actin and Rpl13a* housekeeping genes (3 biological replicates). Differences were calculated with two-way ANOVA and indicated as * P < 0.05; ** P < 0.01; *** P < 0.005; ****P < 0.001.

In conclusion, we established the contributions of the MMPs gene expression in the AMG effect and, in particular, the link between matrix metalloproteinases expression and ERK pathway activation.

4.7 MEK/ERK inhibition impairs *in vivo* AMG-dependent wound healing

In order to confirm the beneficial effect of the AMG-based treatment, an excisional wound splinting mouse model, using C57BL/6 mice, was performed [81], [82]. 0,5 cm full-thickness round wounds were made on the back of the animals, under xylazine/ketamine anaesthesia. In order to avoid wound closure caused by skin contraction, silicone rings were sutured to the skin around the wounds. Wounds were then treated with thirty microliter of AMG (DMSO, 1:3), obtained

from the 0,5 cm of skin biopsy following the Rigenera® protocol [72] [71]. In order to avoid the wound area from drying out, Tegaderm™ dressing (3M, Maplewood, MN, USA) was applied immediately after the creation of the wound and starting of treatment. AMG (DMSO, 1:3) and vehicle control (DMSO in PBS, 1:3 as vehicle control) were freshly applied on the wounds every other day. General scheme of the *in vivo* wound healing is reported in Figure 20a. AMG-treated mice (n=5 mice per group) significantly increased the wound closure compared with vehicle-treated controls. Topical administration of the MEK inhibitor – Trametinib (0.2 mg, Cat No. HY-10999, MCE) - in addition to the AMG significantly delayed the wound closure compared with the vehicle-treated mice and especially compared with the autologous micro graft-treated group alone (Figure 20b). To exclude any impairment correlation due to the presence of the MEK inhibitor, a group of animal (n=5 mice per group) was treated with Trametinib (0,2 mg). Trametinib on its own delayed the wound closure, being faster then combinatory treatment AMG + trametinib. Analyses of the % of wound contraction were performed using ImageJ software (NIH, Baltimore, Maryland). % wound contraction was calculated following the formula:

$$\%\ of\ wound\ contraction = \frac{Healed\ Area}{Total\ Wound\ Area}\ x\ 100$$

The healed area corresponds to the original wound area (day 0) – the present wound area [89]. Animal procedures were performed in accordance with the Ethics Committee at KU Leuven (Belgium) under the ethical approval code P036/2018.

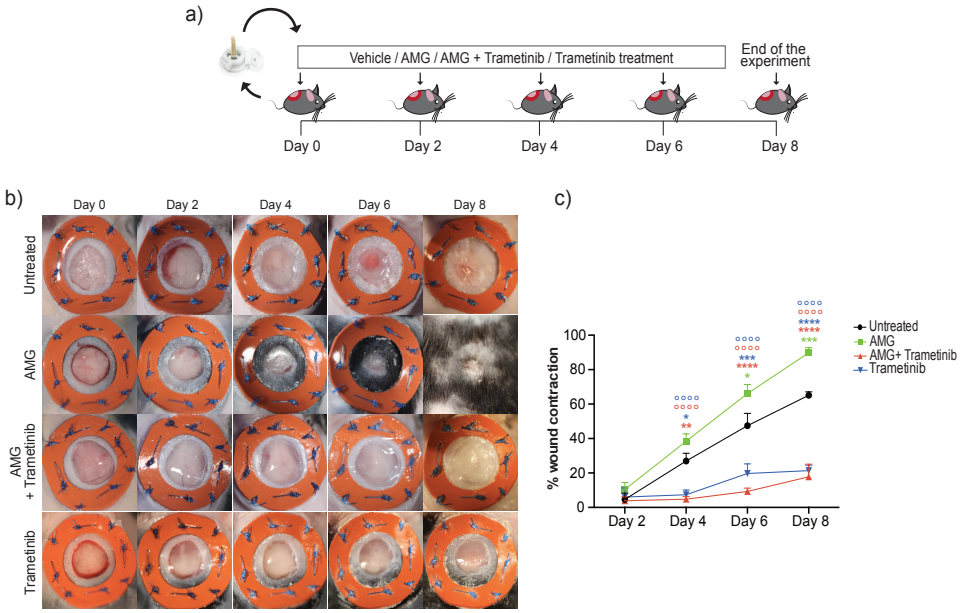


Figure 20: AMG-based treatment accelerates and ERK signalling pathway inhibition suppress wound healing. (a) Representation of the wound healing study performed in C57BL/6 mice (females, 12 weeks old). Autologous micro grafts were obtained crumbling 0,5 cm of skin biopsy, obtained during the creation of the wound, using the provided tissue disruptor rigeneracons®. **(b)** Representative images of the wound healing study. Animals were topically treated with vehicle (DMSO, 1:3 in PBS), AMG (DMSO, 1:3) + MEK inhibitor - trametinib (0.2 mg) and trametinib (0.2 mg) (PBS, 1:3) alone on days 2, 4 and 6. The 8th day the experiment was completed and animals were sacrificed. Wound skin samples were collected for further analysis. Differences *vs* untreated animals were calculated with two-way ANOVA and indicated as ** P < 0.01; *** P < 0.005; ****P < 0.001. Differences *vs* the AMG condition were calculated with two-way ANOVA and indicated as °°°°P < 0.001.

Chapter 5

General Discussion

As the most important protective barrier of the body from the external environment, the skin is regularly exposed to potential injuries. In this frame, the wound healing is recognized as an essential and vital process. When an injury occurs the physiological barrier surface of the skin is disrupted and many cell types migrate towards the wound in an effort to enhance the healing. Both acute and chronic wounds hinder patient quality life and are life-threatening. The healing process involves several biological and physiological processes, such as inflammation, cell adhesion, migration, proliferation, angiogenesis and extracellular matrix remodelling [90]. The healing process becomes more difficult in larger wounds and is impaired in aged people or patients suffering of metabolic disease, such as diabetes, and exposed to cancer therapy, making the need for simple, effective and scarless treatments highly requested. However, traumatic injuries and impaired wound conditions affect million of people worldwide leading to an ample health and economical problem [7,67]. Despite the innovations in technological techniques, surgical advancement and research, the incomplete understanding of the fundamental molecular basis of the wound healing, lead to a lack of suitable therapeutic approaches able to improve the endogenous regenerative capacity. Aiming at the total restoration of the tissue functionality and reducing the aesthetic impact on the patient with scarless wound healing represents the main goal of the clinical wound care.

AMG treatment and its potential effects in tissue regeneration and wound healing

Studies have attributed a stem cells-mediated effect to the new autologous micro graft (AMG)-based technique and their positive outcome. In this frame, the presence of mesenchymal stem cells (MSCs) within the AMG solution, assessed by expression of surface markers including CD90, CD34, CD73 and CD105, led speculate on their immunomodulatory and secretory capacity to promote the healing process [72,91]. In accordance with the positive paracrine functions of MSCs, in this project, we focused on unveiling the molecular mechanism behind

the AMG-treatment, revealing the growth factors-mediated effect and the signalling pathways involved in its favourable outcome.

Interestingly, our results showed that AMG exposition was able to significantly accelerate closure in both *in vitro* and *in vivo* wound healing models, without affecting cell cycle, discarding a proliferation-mediated effect on the accelerated wound closure. The therapeutic effect of AMG-based treatments in skin regeneration, induced an increase in cell migration rate due to activation of MMPs enzymatic activity through growth factors-dependent ERK signalling pathway activation. *In vitro* inhibition of both ERK phosphorylation and MMPs enzymatic activity significantly reduced the migration rate, leading to a delay in the closure of our artificial wounds, demonstrating that both ERK signalling pathway and matrix MMPs enzymatic activity are involved in AMG-dependent accelerated wound closure (figure 18a and 18b) (figure 15c and 15d).

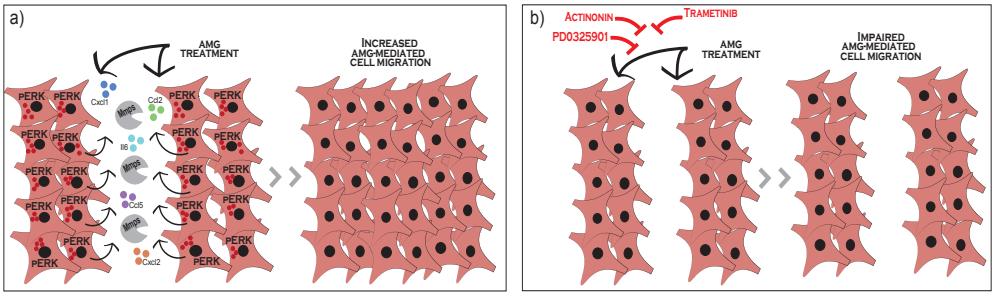


Figure 1: Schematic representation of AMG-based treatment molecular mechanism and its involvement in the closure of in vitro "artificial" wounds. a) Activation of ERK phosphorylation, increasing in chemokines and MMPs gene expression and enzymatic activity upon AMG treatment lead to an acceleration of the closure of our *in vitro* "artificial" wounds. **b)** The use of specific MEK/ERK and MMPs inhibitors, PD0325901, Trametinib and Actinonin respectively lead to *in vitro* scratch closure impairment and to *in vivo* inhibition of the healing process restraining both wound contraction capacity and reepithelialisation.

Moreover, *in vivo* inhibition of ERK phosphorylation, using the commercially available MEK inhibitor Trametinib, blocked significantly the AMG-mediated beneficial effect, demonstrating that the activation of the MAPK signalling pathway is a key point of the AMG molecular mechanism (figure 20). MAPK signalling pathway, via ERK activation, is associated with positive regulation of cell migration and cell motility both *in vitro* [40] and *in vivo* [87]. Moreover, we shown that soluble AMG fraction is enriched by a myriad of pro-motility growth factors such as epidermal growth factor (EGF), fibroblast like growth factor (bFGF) and transforming growth factor beta (TGF-β) (figure 6a). The presence of several cytokines and growth factors, including EGF and b-FGF [29] are known to trigger many cell signalling pathways which play essential roles during the healing processes.

Signalling pathways underlying the molecular mechanism of AMG treatment and its relation with the wound healing process

In our study, we showed that AMG-based treatment lead to a significant increase in MMPs expression and enzymatic activity, including Mmp1a, Mmp1b, Mmp9, Mmp10 and Mmp12 (figure 10a and 10b). Interestingly, combination of scratch assays, *in vitro* inhibition of the ERK signalling pathway and gene expression analyses showed that inhibition of MEK/ERK pathway was able to significantly revert increased MMPs expression exerted by AMG-cell treatment (Figure 19a), including Mmp1a, Mmp1b, Mmp9 and Mmp10. This result indicates that the ERK signalling pathway is essential for the AMG-induced MMPs gene expression. Surprisingly, Mmp12 expression, which was highly up-regulated upon AMG treatment, showed no changes at the mRNA expression level following the MEK/ERK pathway inhibition, suggesting that AMG treatment stimulates other signalling pathways which, in turn, play a role in the AMG-mediated Mmp12 expression. It has been previously shown that MMPs expression is largely controlled both at the transcriptional level by several trans-

activators transcription factors and signalling pathways, including NF-κB, AP-I and β-catenin/Tcf-4 [50], Smad pathways, focal adhesion kinase (FAK) and, as well as at the post-transcriptional level due to epigenetic modifications [29]. Moreover, their expression and enzymatic activity require specific structural modifications leading catalytically active MMPs [29]. Among the transcription factors involved in the MMPs activation, AP-1 has been shown to be one of the most important, playing pivotal roles during the wound healing process. Involvement of AP-I transcription factor in wound healing is demonstrated by the fact that specific growth factors, such as EGF, FGF, TGFβ, TNF-α and interleukin proteins stimulate AP-I activity through MAPK signalling pathway activation [52]. Moreover, increased MMPs trans-activation through AP-1 is generally achieved through mitogen-activated protein kinase (MAPK) signalling pathway through the activation of c-Fos and c-Jun, downstream members of ERK1/2 and JNK1/2 signalling pathways [88] (Yan et al 2006). Our working hypothesis is focused on the fact that MMPs expression might be determined through a growth factors-dependent ERK signalling pathway induction via AP-1 transcription factor activation upon AMG treatment, leading to an improvement in skin regeneration capacity, induced by increasing cell migration rate. However, in our study, not all the MMPs holding an AP-1 binding site in their promoter region were up-regulated upon AMG-treatment. which could suggest that other important pathways and transcription factors may be activated upon AMG treatment and that they may play pivotal roles in the molecular mechanism of the this treatment.

Moreover, a qualitative profiling analysis of the catalytically active form of MMPs was performed establishing their involvement in the closure of our *in vitro* artificial wounds. By using an MMP-inhibitor in association with a highly specific MMPs activity assay, we were able to show high levels of MMPs activities upon AMG treatment compared to untreated cells in an *in vitro* wound healing model, which was reverted by the presence of the MMP-inhibitor (Figure 15a, 15b, 15c and 15d). In conclusion, we established the contributions of both MMPs gene expression and enzymatic activity in the AMG-mediated effect and, in particular,

the link between matrix metalloproteinases expression and MAPK signalling pathway activation. MMPs are known to be present both in acute and chronic wounds, playing a pivotal role in the ECM turnover and synthesis of new ECM. However, further experiments may be interesting to verify our working hypothesis and assessing the favourable involvement of AP-1 transcription factor in inducing MMPs gene regulation and protein activity during wound healing process. Silencing of AP-1 may provide a better understanding of the role of this growth factor in the regulating the gene expression and in turn enzymatic activity of specific wound healing-associated MMPs.

Classified in different groups depending on their substrate specificity, MMPs include collagenases, gelatinases, stromelysins, metalloelastases, matrylysins and membrane-type MMP [48]. Our results pointed out the involvement of MMPs specifically belonging to the collagenases (Mmp1a, Mmp1b and Mmp13), gelatinases (Mmp9), stromelysins (Mmp3, Mmp10) and metalloelastases (Mmp12) families. Altogether, these enzymes play pivotal roles in the cleavage of structural proteins allowing reepithelialisation and wound contraction [29]. MMPs hold abilities that make them appropriated for enhancing cell migration during the healing process. However, MMPs functions are not only involved in ECM turnover. Indeed, MMPs are known to regulate the immune system [47], cell migration, angiogenesis, production of bio-active fragments with independent activity, including growth factors, cytokines and chemokynes, which lead to activation/deactivation of specific signalling pathways [49]. Interestingly, MMP-deficient mice models failed the wound healing [92]; These evidences show the essential role of MMPs activities during the wound healing process. In this frame, the wound healing process points up the several roles – mainly positive, but some either detrimental - that MMPs play during the sequential healing phases, through their activity of converting structural protein in bio-active signalling molecules [8]. Especially, MMPs have been tight linked to the inflammatory [47], reepithelialisation phase of the wound healing process, proving to be crucial for the wound contraction [92-94] as well as the remodelling phase. Indeed, if a proper wound healing has to be achieved, the extra cellular matrix

(ECM) has to be remodelled correctly and MMPs are key regulators of this phase. Despite the fundamental role of the MMPs in skin wound healing, the uncontrolled expression and aberrantly enzymatic activity of MMPs can lead to wound pathogenesis, characterized by increased proteolysis, critical loss of newly synthesized ECM and disruption of cell migration [35]. The imbalance in the MMPs activity represent the main problem of diabetic patients, where the increased proteolytic environment is caused by an alteration in MMPs/TIMPs activity, leading to a impaired wound conditions [95]. The MMPs are generally expressed at basal level in a wild type conditions, becoming increased during normal wound healing and being extremely up-regulated in impaired wound conditions. Therefore, a better understanding of the critical relationship between MMPs proteolytic activities, with their beneficial or detrimental effects and wound healing process needs to be elucidated in order to establish new treatments able to improve the tissue regeneration capacity. In conclusion, the expression of these double-edge sword enzymes during the healing process has to be thigh regulated in a timely manner in order to allow the accomplishment of the wound healing.

MAPK-dependent AMG beneficial effect in wound healing and skin regeneration

As previously discussed, our results showed upon AMG treatment a significant improvement of the wound healing process in both *in vitro* and *in vivo* models. The increasing in migration rate as well as the *in vivo* skin wound contraction was tightly dependent on the activation of the ERK-MAPK signalling sub-pathway. Extracellular signal-regulated kinase - ERK - belongs to the big family of the Mitogen-activated protein kinase (MAPK) signalling pathway, and it's known to play essential roles in signal transduction stimulating transcription of several important genes, such as Elk-1, c-fos, AP-1, ATF and NF-κB [44]. In our study, activation of MAPK signalling pathway have led to an acceleration of *in vitro* cell migration and *in vivo* wound healing, encouraging other studies in this

field. However, the enhancement in skin wound healing related to the MAPK cascade activation seems to be generally linked with its capacity to stimulate the proliferative stage of the healing process [44,87]. Indeed, the mitogen-activated protein kinase signalling pathway (MAPK), with its sub-groups – ERK, JNK and p38 – is known to respond and transduce signals from different kind of stimuli, evoking physiological responses inducing mainly cell proliferation, differentiation, development, inflammation responses and programmed cell death [96]. However, the MAPK signalling pathways is also known to play a role in the tumour environment, regulating both tumour suppression and pro-oncogenic signals. Mutations can arise in all the mediators involved in cascade, including the membrane receptors, RAS protein signal transducers and downstream effectors, leading to an over-activity of the signalling pathway. Several mutations in the MAPK have been already identified in human cancers, including melanoma, ovarian cancer and colorectal cancer [97]. The unclear role of the MAPK signalling pathway depends on the tumour environment, playing pivotal roles in physiological and malignant migration. Despite the double-edge sword role of the MAPK cascade in cancer, recent evidences are showing the involvement of the JNK- and ERK-MAPK sub-groups in the enhancement of cell migration and cell shape changes, angiogenesis [98] and, most importantly, in regulating tissue repair functions, including cell migration, collagen synthesis and ECM contraction in fibroblast cells [99]. In this frame, our study supported the literature in demonstrating that EGF- and IGF-dependent ERK activation leads to stimulation of migrating fibroblasts [100]. Moreover, in our results, increasing in p-ERK level upon AMG treatment has been identified, displaying a normal intermittent activation of the signalling pathway and, in turn, not showing any over-activation of the respective cascade (figure 17a and 17b). This activation lasts between minutes up to hours for a sustained activation and both the duration of the signal and its downregulation are important in the regulation of the signalling [101]. On the other end, no changes in the cell cycle upon AMG-treatment and ERK activation were found (Figure 4a and 4b). This result has been sustained through gene expression analysis of specific immediate early

genes regulated by the ERK signalling pathway, including Elk-1 and c-fos, which are essential for the progression of the proliferation and differentiation. In our *in vitro* wound healing system, both Elk-1 and c-fos have been not detected, supporting our assumption that no proliferation-mediated effect are linked with the molecular mechanism of the AMG-based treatment. The positive effect of the AMG treatment in promoting ERK-dependent cell migration was drastically suppressed by using the specific MEK inhibitors - PD0325901 and Trametinib -, resulting in a significant delay in the *in vitro* scratch-closure and in a complete suppression of the wound contraction capacity in the *in vivo* wound healing model (figure 18a and 18b) (figure 20b and 20c). Here, we speculated on the differences between the *in vitro* and *in vivo* environment and its outcome in the healing process. The *in vivo* use of the MEK inhibitor may interfere with all the wound healing phases, restraining both cell migration and cell proliferation of many cell types present at the wound site, including epithelial cells, immune cells and fibroblasts, leading to a stop of the progression of the healing process.

Another important aspect of our study that needs to be pointed out is the cytokines/chemokines differential expression upon AMG treatment. These signalling proteins play essential roles in the wound healing process, stimulating cell migration of several cell types in the wound site [23]. Specific CXC and CC chemokine families up-regulation has been identified upon treatment, including CXCL1, CXCL2 and CCL2, which play essential roles in immune cells chemotaxis and during the reepithelialisation phase of the wound repair process (figure 11d). Lack of these signalling molecules lead to *in vivo* wound healing delay with detrimental effects on both reepithelialisation and angiogenesis phases [102]. These findings allow speculating on the ability of the AMG treatment in accelerating the inflammatory response, well-known stage of the wound healing process, leading to an earlier up-regulation of important chemokines families, which play crucial roles in the process.

Future perspectives

Nowadays, knowing the number of patient yearly exposed to traumatic injuries and impaired wound healing condition, a strong and immediate need of effective therapeutic approaches is highly required. As the external barrier of the body, the skin is the most exposed organ to stress factors, leading to cell/tissue damages. The peculiarity of skin has developed during evolution a complex process allowing to restore large tissue losses. However, the presence of several limitations, including its multifactorial aetiology, the lack of funding for supporting the research fields and the absence of proper preclinical models [7], leads to an incomplete understanding of this vital process. Biomedical and bioengineering researches are constantly working towards the development of the best therapeutic treatment able to hold all the aims of the tissue remodelling. The innovative AMG-based treatment showed favourable outcome in both *in vitro* and *in vivo* healing process, through an ERK-dependent MMPs up-regulation, upstream regulated by a pool of growth factors. In this frame and for the first time, our results shed light on the molecular mechanism behind the AMG-based treatment, demonstrating their potential efficacy in triggering the whole wound healing process. This is possible by stimulating earlier signalling responses and accelerating the regeneration capacity in the treatment of acute wound healing conditions. In a future perspective, it would be important to assess whether the AMG molecular mechanism is conserved in other mammalian models, including human cells and chronic disease models. To evaluate this, *in vitro* cell scratch assays and migration studies combined with functional gene and protein inhibitions could be performed on human epithelial cells or human dermal fibroblasts. Moreover, *in vivo* wound healing assays on chronic wound models, including murine models which resembles the type 2 diabetes could be used to assess the potential of the AMG-based treatment in impaired wound conditions and if also in these cases the molecular mechanism is maintained.

Appendix

Table 2. DEGs associated to AMG treatment exposure

GeneID	log2FoldChange	padj
Hmox1	3,306931355	2,15E-16
Slc7a11	5,491300291	5,86E-15
Nfkbiz	3,050796105	1,96E-09
Hcar2	5,156317254	2,83E-09
Micall2	2,272516359	1,75E-08
Dio3os	-2,895155597	2,99E-08
Dusp10	2,234225223	5,63E-08
Rgs16	2,333795272	6,58E-07
Nos2	8,703141124	1,11E-06
Lphn2	-2,110417692	2,76E-06
Col5a3	1,938595683	3,04E-06
Ifi205	3,638767775	6,19E-06
Gfpt2	1,937041483	6,32E-06
Slpi	3,341930466	8,15E-06
Ccl2	4,89933496	8,21E-06
Hoxc12	-2,322171324	8,84E-06
Rhbdf2	2,031676699	1,12E-05
Atoh8	-2,870703818	1,12E-05
Zc3h12a	3,632511475	1,19E-05
Magi3	-1,959902185	2,12E-05
Smad9	-3,187979764	2,43E-05
Tnrc18	-1,957664829	2,68E-05
Fam46b	-2,03971319	2,68E-05
Cables1	-2,807735969	3,10E-05
Dhrs3	-2,658565392	4,12E-05
Has1	3,137736873	4,87E-05
Abhd17c	1,769777353	5,66E-05
Lif	6,870260515	7,70E-05
Zfp521	-2,032513341	7,70E-05

Mum1l1	-2,189247074	7,70E-05
Flrt1	-2,936930672	7,70E-05
Cxcl1	7,762473226	8,00E-05
Icam1	2,758981589	8,25E-05
Id2	-2,103201784	8,25E-05
Casp4	2,19937069	9,49E-05
Sema7a	2,308616683	9,87E-05
Dio3	-2,30063604	0,000107142
Cacna1h	-2,317392374	0,000140088
Kprp	4,202885064	0,000164727
Ptgs2os2	1,810014248	0,000164727
Gsdmd	1,749318846	0,000164727
Mrgprf	-2,037807531	0,000164727
Nqo1	1,765342187	0,000188001
Gpr68	5,695973524	0,000268328
RP24-422C24.2	-2,413152358	0,00032058
Mmp3	4,442384887	0,000321107
Ereg	3,159821232	0,000326638
Pawr	-1,711107649	0,000330646
Gsap	2,541344327	0,000356488
Maf	-2,368823382	0,000460986
Ptgs2	1,610010527	0,000526589
Arg2	3,586250016	0,000543989
Rbfox1	2,291387359	0,000543989
Stac	2,689818559	0,000625309
Rgl1	-1,73074714	0,000635493
Ccl20	9,575174962	0,000645679
Smox	2,336201263	0,000706801
Il11	3,188060862	0,000972209
Cxcl2	9,558202105	0,001018875
Cxcl5	4,787233251	0,001121112
Smad6	-2,017238657	0,001130349
Il1rl1	1,522338409	0,001152168
Vegfa	1,539547471	0,001227886

4632428N05Rik	-1,955154371	0,001227886
Fign	-3,098402097	0,001227886
Tppp	-2,927865077	0,00160299
Cep72	-2,002789632	0,001680267
Lcn2	1,865327784	0,001734072
Klhl24	-1,640003345	0,001734072
Mmp1b	4,653703884	0,002658845
Sertad4	-1,659408011	0,002658845
Gm26682	2,219708285	0,002710325
Foxn3	-2,051904067	0,002710325
Ccl7	2,435981145	0,002746958
Bcl3	2,248857338	0,002746958
Blvrb	1,810404316	0,002746958
Txnrd1	2,311426294	0,00304603
Ptx3	3,008485233	0,003107665
Pdpn	1,389458792	0,003638266
Plet1	2,457985447	0,004087664
Gm16685	8,607352759	0,004290178
Il6	6,122781635	0,004290178
Fgfr2	-2,309745086	0,004921396
Sorbs1	-1,715620971	0,005385168
H2-T10	3,090221311	0,00563326
Ets1	1,430939145	0,005778784
Ctnnd2	-2,031798803	0,005818891
Esam	1,700127111	0,006762369
Vcam1	1,754859044	0,00682153
Ttc28	-1,595799336	0,007387308
Fosl1	1,375359258	0,007920835
Stx6	1,422122464	0,00795899
Nfkb1	1,850655123	0,008488529
Ptges	2,813618902	0,008839054
Slc22a4	1,777270432	0,008839054
Fzd7	-1,4458205	0,008839054
Peli2	-2,318651476	0,008839054

Slc40a1	3,401740856	0,008845504
Adora2b	1,589365821	0,008845504
Sphk1	1,541871801	0,008845504
Kif13b	-1,596895337	0,008845504
Cxcl16	4,786979264	0,008942617
Tgm1	3,406901725	0,008942617
Gm15242	4,672117612	0,00914161
Thbs1	-1,26021243	0,00914161
Masp1	-1,892289385	0,00914161
Cyp7b1	2,912852872	0,00981823
Cd40	4,370249532	0,00997147
Sele	4,217007479	0,009977622
Ikzf2	-1,857030825	0,010574305
Snai2	-1,398107725	0,010917786
Denr	1,561199498	0,01127015
Ier5	1,552819296	0,011374915
Slc8a1	-2,123901837	0,011422018
Mecom	-2,038880282	0,011565344
Map4k3	-1,346125842	0,012352811
Gsr	1,400391068	0,012387917
Gm9687	2,864703538	0,012439469
Hivep2	1,281716647	0,012439469
Bcor	-1,437667947	0,012768066
Adtrp	3,136921748	0,012816458
Tfec	3,895195412	0,013217787
Pcdh18	-1,769583748	0,013471573
Bdkrb2	2,105455807	0,013865339
Arhgef28	-1,615818634	0,013865339
Dtl	-1,716109119	0,014988976
Nfkbib	1,39977226	0,015567645
Dnmt3l	3,579546796	0,015573423
Igsf10	-1,21126166	0,016089023
Tox	-2,081514236	0,016089023
Gareml	1,498228819	0,016744018

Map3k8	1,873516961	0,0170154
Dtx4	1,384770298	0,017602024
Rab20	1,464621024	0,018068625
Greb1l	-1,753289874	0,018567348
Kctd12b	-1,921519598	0,018979297
Gpr84	8,762536798	0,020124977
Zfp808	-2,503710346	0,02023188
Slc25a25	1,258521511	0,020712092
Hr	2,243290351	0,020771438
Ubash3b	1,28671217	0,020814806
Akr1b8	1,277299791	0,02086937
Flt1	2,350275805	0,021830212
Crebrf	-1,399635949	0,021830212
Adra1d	-2,593197046	0,023175476
Adamts5	-1,932131829	0,023950726
Shroom3	-1,907210174	0,024402286
Spsb1	1,153813726	0,025058403
Aim1	-2,109306783	0,025058403
3010026O09Rik	-2,121765544	0,025058403
Gca	-1,611025247	0,025344542
Mmp13	2,254016751	0,025557099
Cog5	-1,399285414	0,025557099
Lrp6	-1,168421017	0,025964677
Slc2a6	1,758852146	0,02606179
Neurl3	4,776320111	0,026272989
Il16	-2,05208889	0,026411673
Ankrd44	-1,406476156	0,026714394
Add3	-1,897589476	0,026714394
Tmem132e	4,906158806	0,027486712
Birc3	1,669126253	0,027838768
Bcl2l15	2,573328255	0,030431109
Nfkbia	3,989162148	0,031474163
Hip1	-1,318579506	0,032042882
Psmb8	1,599509227	0,033023626

Mafg	1,280505494	0,033023626
Oacyl	2,181849559	0,033281714
Ptgs2os	1,421389088	0,033281714
Trib1	1,232755254	0,033439937
Rab32	1,347430819	0,035587524
Zfpm2	1,284313677	0,035587524
Stk10	1,243727944	0,035587524
Tlr5	-1,899326116	0,035587524
Plscr1	2,91055459	0,03577995
Srxn1	2,58451008	0,038836032
Fnip2	1,375813365	0,038904654
Tbx3	1,958993748	0,039717804
Icosl	3,752029358	0,040240484
Sema6d	1,430744344	0,040240484
Ston1	-1,465906665	0,040695779
Gatad2b	-1,397816796	0,042799338
Spns2	-2,084453248	0,043367649
Cxcl3	5,019026007	0,043812708
Lrig1	2,201404	0,043831883
Lfng	-1,612690286	0,044193448
Sprr1a	4,033623982	0,044248114
Ccl5	7,102919172	0,044468823
Unc5c	-1,292733363	0,045025469
Slitrk6	-1,677243978	0,045321367
Tnfrsf8	4,628836774	0,046789019
Saa3	1,90720953	0,046789019
Sqstm1	1,670682735	0,046789019
Klhl13	-1,104176085	0,046789019
Pik3r3	-1,325626014	0,046789019
Lurap1l	-1,371059325	0,046789019
Dlk2	-1,913446104	0,046789019
Mina	1,23808251	0,047145399
5830432E09Rik	2,029994917	0,047247704
Mef2c	-1,809896644	0,047900069

Clspn	-1,34246039	0,048019691
Fam26e	-1,399685296	0,048019691
Ppp1r3c	-1,679543737	0,048019691
Ppard	1,249593597	0,049944536

Table 3. Hub nodes related to the input genelist and associated to AMG treatment

i	GeneID	DEGs	Hub
10090.ENSMUSP00000137353	Ccl19	-	hub
10090.ENSMUSP00000136791	NoMapping	-	hub
10090.ENSMUSP00000136780	Ccl21a	-	hub
10090.ENSMUSP00000135967	NoMapping	-	hub
10090.ENSMUSP00000133957	Grm7	-	hub
10090.ENSMUSP00000130874	Chrm2	-	hub
10090.ENSMUSP00000129767	Psma2	-	hub
10090.ENSMUSP00000126758	Ccr9	-	hub
10090.ENSMUSP00000125548	Psma3	-	hub
10090.ENSMUSP00000114180	Ubc	-	hub
10090.ENSMUSP00000110978	Grm8	-	hub
10090.ENSMUSP00000109064	Ccl20	up	hub
10090.ENSMUSP00000108716	Cxcl9	-	hub
10090.ENSMUSP00000107069	Ccr5	-	hub
10090.ENSMUSP00000103671	Ccl27a	-	hub
10090.ENSMUSP00000103378	Gabbr2	-	hub
10090.ENSMUSP00000102857	Psmd4	-	hub
10090.ENSMUSP00000101801	Npb	-	hub
10090.ENSMUSP00000101236	Oprm1	-	hub
10090.ENSMUSP00000099794	Gcg	-	hub
10090.ENSMUSP00000099436	Psmb3	-	hub
10090.ENSMUSP00000099423	Ccr7	-	hub
10090.ENSMUSP00000097623	Kng2	-	hub
10090.ENSMUSP00000096847	Ccl28	-	hub
10090.ENSMUSP00000096595	Npy2r	-	hub
10090.ENSMUSP00000095597	Nps	-	hub

10090.ENSMUSP00000095029	Ccr6	-	hub
10090.ENSMUSP00000093316	Fpr-s1	-	hub
10090.ENSMUSP00000093311	Fpr-rs4	-	hub
10090.ENSMUSP00000093297	Fpr-rs7	-	hub
10090.ENSMUSP00000093296	Fpr-rs6	-	hub
10090.ENSMUSP00000093200	Npw	-	hub
10090.ENSMUSP00000089519	Gm4950	-	hub
10090.ENSMUSP00000088057	Psma5	-	hub
10090.ENSMUSP00000086592	Agtr2	-	hub
10090.ENSMUSP00000086052	Htr1d	-	hub
10090.ENSMUSP00000085346	Nms	-	hub
10090.ENSMUSP00000085293	S1pr3	-	hub
10090.ENSMUSP00000080543	Gm5239	-	hub
10090.ENSMUSP00000080370	Gper1	-	hub
10090.ENSMUSP00000078625	NoMapping	-	hub
10090.ENSMUSP00000075170	Drd2	-	hub
10090.ENSMUSP00000074885	Cxcl2	up	hub
10090.ENSMUSP00000074259	Gnai1	-	hub
10090.ENSMUSP00000072800	Cxcl12	-	hub
10090.ENSMUSP00000071513	Oprl1	-	hub
10090.ENSMUSP00000071353	Ccr1l1	-	hub
10090.ENSMUSP00000071179	Fpr-rs3	-	hub
10090.ENSMUSP00000071054	Psmc3	-	hub
10090.ENSMUSP00000070728	Btrc	-	hub
10090.ENSMUSP00000069872	Mtnr1a	-	hub
10090.ENSMUSP00000069080	Casr	-	hub
10090.ENSMUSP00000068578	Sstr2	-	hub
10090.ENSMUSP00000066822	Penk	-	hub
10090.ENSMUSP00000066381	Galr1	-	hub
10090.ENSMUSP00000065799	Fpr2	-	hub
10090.ENSMUSP00000065157	Npy5r	-	hub
10090.ENSMUSP00000063670	Gpr17	-	hub
10090.ENSMUSP00000063136	Htr1f	-	hub
10090.ENSMUSP00000062741	Rxfp3	-	hub
10090.ENSMUSP00000062677	Ccr4	-	hub
10090.ENSMUSP00000062588	Ccr10	-	hub
10090.ENSMUSP00000060776	Cxcr6	-	hub
10090.ENSMUSP00000060003	C5ar1	-	hub
10090.ENSMUSP00000059705	Adra2c	-	hub

10090.ENSMUSP00000058732	Rxfp4	-	hub
10090.ENSMUSP00000058040	Sstr3	-	hub
10090.ENSMUSP00000057543	Gnai2	-	hub
10090.ENSMUSP00000056774	Pik3r1	-	hub
10090.ENSMUSP00000056576	Npy4r	-	hub
10090.ENSMUSP00000056432	Npsr1	-	hub
10090.ENSMUSP00000055797	Cnr1	-	hub
10090.ENSMUSP00000055256	Gng2	-	hub
10090.ENSMUSP00000054210	Pnoc	-	hub
10090.ENSMUSP00000054104	Hcar2	up	hub
10090.ENSMUSP00000054062	Galr2	-	hub
10090.ENSMUSP00000053638	Aplnr	-	hub
10090.ENSMUSP00000053394	S1pr2	-	hub
10090.ENSMUSP00000052894	Fpr1	-	hub
10090.ENSMUSP00000052581	Lpar1	-	hub
10090.ENSMUSP00000052444	Cxcr3	-	hub
10090.ENSMUSP00000051657	Psmd8	-	hub
10090.ENSMUSP00000051392	Rln3	-	hub
10090.ENSMUSP00000051085	Sstr5	-	hub
10090.ENSMUSP00000050898	Htr1b	-	hub
10090.ENSMUSP00000050444	Cxcr5	-	hub
10090.ENSMUSP00000050077	Oprd1	-	hub
10090.ENSMUSP00000049909	Ccr2	-	hub
10090.ENSMUSP00000049714	Cxcr1	-	hub
10090.ENSMUSP00000048092	C3ar1	-	hub
10090.ENSMUSP00000047646	Cxcl10	-	hub
10090.ENSMUSP00000046233	Npbwr1	-	hub
10090.ENSMUSP00000046012	Apln	-	hub
10090.ENSMUSP00000045530	Npy1r	-	hub
10090.ENSMUSP00000045335	Bdkrb1	-	hub
10090.ENSMUSP00000044718	Nmur2	-	hub
10090.ENSMUSP00000044573	Sstr4	-	hub
10090.ENSMUSP00000044352	Pmch	-	hub
10090.ENSMUSP00000043522	Adora1	-	hub
10090.ENSMUSP00000041968	Psmd7	-	hub
10090.ENSMUSP00000040808	Chrm4	-	hub
10090.ENSMUSP00000039600	Ccl5	up	hub
10090.ENSMUSP00000039107	Ccr3	-	hub
10090.ENSMUSP00000038884	Htr5a	-	hub

10090.ENSMUSP00000038744	Skp1	-	hub
10090.ENSMUSP00000038473	Ccr8	-	hub
10090.ENSMUSP00000037712	Lpar3	-	hub
10090.ENSMUSP00000037045	Sstr1	-	hub
10090.ENSMUSP00000035551	Avp	-	hub
10090.ENSMUSP00000035037	Pik3cb	-	hub
10090.ENSMUSP00000034848	Psma4	-	hub
10090.ENSMUSP00000034369	Psmb10	-	hub
10090.ENSMUSP00000034325	Lpar2	-	hub
10090.ENSMUSP00000034296	Pik3r2	-	hub
10090.ENSMUSP00000033805	Psmd10	-	hub
10090.ENSMUSP00000033765	Avpr2	-	hub
10090.ENSMUSP00000033154	Plk1	-	hub
10090.ENSMUSP00000033008	Psma1	-	hub
10090.ENSMUSP00000032824	Psmc4	-	hub
10090.ENSMUSP00000031843	Npy	-	hub
10090.ENSMUSP00000031697	Cul1	-	hub
10090.ENSMUSP00000031327	Cxcl1	up	hub
10090.ENSMUSP00000031326	Cxcl3	up	hub
10090.ENSMUSP00000031320	Pf4	-	hub
10090.ENSMUSP00000031319	Ppbp	-	hub
10090.ENSMUSP00000031318	Cxcl5	up	hub
10090.ENSMUSP00000031146	Nmu	-	hub
10090.ENSMUSP00000030940	Gnb1	-	hub
10090.ENSMUSP00000030815	Cort	-	hub
10090.ENSMUSP00000030642	Psmb2	-	hub
10090.ENSMUSP00000030561	Gnat3	-	hub
10090.ENSMUSP00000030464	Pik3r3	down	hub
10090.ENSMUSP00000029653	Egf	-	hub
10090.ENSMUSP00000029326	Sucnr1	-	hub
10090.ENSMUSP00000029201	Pik3ca	-	hub
10090.ENSMUSP00000029082	Psma7	-	hub
10090.ENSMUSP00000028278	Psmd14	-	hub
10090.ENSMUSP00000028233	C5	-	hub
10090.ENSMUSP00000028083	Psmb7	-	hub
10090.ENSMUSP00000027440	Nmur1	-	hub
10090.ENSMUSP00000027432	Psmd1	-	hub
10090.ENSMUSP00000027372	Cxcr2	-	hub
10090.ENSMUSP00000027038	Oprk1	-	hub

10090.ENSMUSP00000026911	Ccr1	-	hub
10090.ENSMUSP00000026569	Drd4	-	hub
10090.ENSMUSP00000026560	Psmd13	-	hub
10090.ENSMUSP00000026119	Gcgr	-	hub
10090.ENSMUSP00000025842	Gal	-	hub
10090.ENSMUSP00000025561	Anxa1	-	hub
10090.ENSMUSP00000025541	Gnaq	-	hub
10090.ENSMUSP00000025338	Gabbr1	-	hub
10090.ENSMUSP00000025196	Psmb8	up	hub
10090.ENSMUSP00000024988	C3	-	hub
10090.ENSMUSP00000024004	Ccl25	-	hub
10090.ENSMUSP00000023959	Grm2	-	hub
10090.ENSMUSP00000023840	Cxcl13	-	hub
10090.ENSMUSP00000023589	Kng1	-	hub
10090.ENSMUSP00000023390	Drd3	-	hub
10090.ENSMUSP00000023036	Rbx1	-	hub
10090.ENSMUSP00000022803	Psmb5	-	hub
10090.ENSMUSP00000022380	Psmc6	-	hub
10090.ENSMUSP00000022256	Psmd6	-	hub
10090.ENSMUSP00000022235	Htr1a	-	hub
10090.ENSMUSP00000021595	Psmc1	-	hub
10090.ENSMUSP00000021412	Psma6	-	hub
10090.ENSMUSP00000021283	Pik3r5	-	hub
10090.ENSMUSP00000021090	Grb2	-	hub
10090.ENSMUSP00000021063	Psmd12	-	hub
10090.ENSMUSP00000021049	Psmc5	-	hub
10090.ENSMUSP00000020990	Pomc	-	hub
10090.ENSMUSP00000020329	Egfr	-	hub
10090.ENSMUSP00000020099	Cdk1	-	hub
10090.ENSMUSP00000019266	Ccl9	-	hub
10090.ENSMUSP00000019071	Ccl6	-	hub
10090.ENSMUSP00000019064	Cxcl16	up	hub
10090.ENSMUSP00000018430	Psmb6	-	hub
10090.ENSMUSP00000017572	Psmd11	-	hub
10090.ENSMUSP00000017460	Ppy	-	hub
10090.ENSMUSP00000017455	Pyy	-	hub
10090.ENSMUSP00000017365	Psmd3	-	hub
10090.ENSMUSP00000014913	Psmb1	-	hub
10090.ENSMUSP00000007708	Ppp2r1a	-	hub

10090.ENSMUSP00000007212	Psmd2	-	hub
10090.ENSMUSP00000005923	Psmb4	-	hub
10090.ENSMUSP00000005606	Prkaca	-	hub
10090.ENSMUSP00000005406	App	-	hub
10090.ENSMUSP00000004480	Sst	-	hub
10090.ENSMUSP00000004076	Grm3	-	hub
10090.ENSMUSP00000001652	Bdkrb2	up	hub
10090.ENSMUSP00000000631	Grm6	-	hub
10090.ENSMUSP00000000001	Gnai3	-	hub
10090.ENSMUSP00000137726	Usp35	-	no
10090.ENSMUSP00000137658	Tnfsf12	-	no
10090.ENSMUSP00000137596	NoMapping	-	no
10090.ENSMUSP00000137582	NoMapping	-	no
10090.ENSMUSP00000137400	Oaz1	-	no
10090.ENSMUSP00000137393	Il11ra2	-	no
10090.ENSMUSP00000137380	NoMapping	-	no
10090.ENSMUSP00000137349	Gm5225	-	no
10090.ENSMUSP00000137193	Il18	-	no
10090.ENSMUSP00000137031	Igkv4-62	-	no
10090.ENSMUSP00000136950	Epn2	-	no
10090.ENSMUSP00000136914	Oaz2	-	no
10090.ENSMUSP00000136734	NoMapping	-	no
10090.ENSMUSP00000136655	Gm5741	-	no
10090.ENSMUSP00000136588	Hsd3b4	-	no
10090.ENSMUSP00000136581	Gm21972	-	no
10090.ENSMUSP00000136564	Gm9125	-	no
10090.ENSMUSP00000136458	Gm4858	-	no
10090.ENSMUSP00000136371	NoMapping	-	no
10090.ENSMUSP00000136116	Ttc28	down	no
10090.ENSMUSP00000136035	Gyg1	-	no
10090.ENSMUSP00000135993	NoMapping	-	no
10090.ENSMUSP00000135960	Gm21897	-	no
10090.ENSMUSP00000135427	Hist2h2bb	-	no
10090.ENSMUSP00000134894	Ppp1r3e	-	no
10090.ENSMUSP00000134735	Psme1	-	no
10090.ENSMUSP00000134672	Pla2g6	-	no
10090.ENSMUSP00000134591	Cyp2j8	-	no
10090.ENSMUSP00000134303	Mecom	down	no
10090.ENSMUSP00000134112	Gm20441	-	no

10090.ENSMUSP00000133811	Cyp2j12	-	no
10090.ENSMUSP00000133564	Dnm2	-	no
10090.ENSMUSP00000133523	Cct4	-	no
10090.ENSMUSP00000133499	Psmb9	-	no
10090.ENSMUSP00000133377	Mpig6b	-	no
10090.ENSMUSP00000133117	Fga	-	no
10090.ENSMUSP00000133064	Fgfr3	-	no
10090.ENSMUSP00000132906	Dbf4	-	no
10090.ENSMUSP00000132838	Nedd4l	-	no
10090.ENSMUSP00000132735	Hnrnpd	-	no
10090.ENSMUSP00000132547	Mef2c	down	no
10090.ENSMUSP00000132180	Cyp2j11	-	no
10090.ENSMUSP00000132140	Psmb11	-	no
10090.ENSMUSP00000132130	NoMapping	-	no
10090.ENSMUSP00000131991	Tnnc1	-	no
10090.ENSMUSP00000131401	Sspo	-	no
10090.ENSMUSP00000131373	Rnf19b	-	no
10090.ENSMUSP00000131355	Glg1	-	no
10090.ENSMUSP00000131316	Hspg2	-	no
10090.ENSMUSP00000131206	Ube2d2	-	no
10090.ENSMUSP00000131010	Sphk1	up	no
10090.ENSMUSP00000130738	Cul3	-	no
10090.ENSMUSP00000130668	Ncam1	-	no
10090.ENSMUSP00000130604	Plce1	-	no
10090.ENSMUSP00000130359	Aph1c	-	no
10090.ENSMUSP00000130294	Ctbp2	-	no
10090.ENSMUSP00000130225	C130060K24Rik	-	no
10090.ENSMUSP00000130194	Slc3a2	-	no
10090.ENSMUSP00000130167	Mpl	-	no
10090.ENSMUSP00000129872	NoMapping	-	no
10090.ENSMUSP00000129800	Sh3glb1	-	no
10090.ENSMUSP00000129781	Il5ra	-	no
10090.ENSMUSP00000129739	Eps15l1	-	no
10090.ENSMUSP00000129584	Bcar1	-	no
10090.ENSMUSP00000129565	Gstp1	-	no
10090.ENSMUSP00000129491	Shc2	-	no
10090.ENSMUSP00000129463	Cables1	down	no
10090.ENSMUSP00000129181	Grm5	-	no
10090.ENSMUSP00000129163	Rab11a	-	no

10090.ENSMUSP00000129001	Nfatc1	-	no
10090.ENSMUSP00000128926	Slc8a2	-	no
10090.ENSMUSP00000128803	Myl6	-	no
10090.ENSMUSP00000128759	Gtse1	-	no
10090.ENSMUSP00000128729	Sct	-	no
10090.ENSMUSP00000128661	Odc1	-	no
10090.ENSMUSP00000128652	Fbxw25	-	no
10090.ENSMUSP00000128388	Pdgfd	-	no
10090.ENSMUSP00000128387	Hectd2	-	no
10090.ENSMUSP00000127997	Gm5819	-	no
10090.ENSMUSP00000127995	Blm	-	no
10090.ENSMUSP00000127941	Inpp5d	-	no
10090.ENSMUSP00000127885	NoMapping	-	no
10090.ENSMUSP00000127842	Ap2a1	-	no
10090.ENSMUSP00000127808	Gm20425	-	no
10090.ENSMUSP00000127709	Fam3c	-	no
10090.ENSMUSP00000127374	Mgll	-	no
10090.ENSMUSP00000126847	Htr7	-	no
10090.ENSMUSP00000126796	Lcp2	-	no
10090.ENSMUSP00000126762	Gm2564	-	no
10090.ENSMUSP00000126597	Micu1	-	no
10090.ENSMUSP00000126219	Il7	-	no
10090.ENSMUSP00000126169	Cldn20	-	no
10090.ENSMUSP00000126108	Acvr2b	-	no
10090.ENSMUSP00000126092	Pik3c2a	-	no
10090.ENSMUSP00000125977	Rps24	-	no
10090.ENSMUSP00000125752	Pdcd10	-	no
10090.ENSMUSP00000125267	Gm5286	-	no
10090.ENSMUSP00000125255	Cabp2	-	no
10090.ENSMUSP00000125217	Cyp2c40	-	no
10090.ENSMUSP00000125142	Kcnip2	-	no
10090.ENSMUSP00000125063	Cacna1i	-	no
10090.ENSMUSP00000124963	Prkg2	-	no
10090.ENSMUSP00000124942	Gm10696	-	no
10090.ENSMUSP00000124782	Pip4p1	-	no
10090.ENSMUSP00000124524	Fbxo41	-	no
10090.ENSMUSP00000124376	Ctnna2	-	no
10090.ENSMUSP00000123799	Asl	-	no
10090.ENSMUSP00000123566	Gm21974	-	no

10090.ENSMUSP00000123238	Reps1	-	no
10090.ENSMUSP00000122552	Dhrs3	down	no
10090.ENSMUSP00000122420	Cdc23	-	no
10090.ENSMUSP00000122219	Prlr	-	no
10090.ENSMUSP00000122080	Ptgir	-	no
10090.ENSMUSP00000122072	Ramp2	-	no
10090.ENSMUSP00000121390	Epn3	-	no
10090.ENSMUSP00000121203	Ctsd	-	no
10090.ENSMUSP00000121111	Map2k2	-	no
10090.ENSMUSP00000120904	Tmed7	-	no
10090.ENSMUSP00000120840	Fbxo7	-	no
10090.ENSMUSP00000120803	Pkd1l1	-	no
10090.ENSMUSP00000120632	Ppat	-	no
10090.ENSMUSP00000120598	Cers1	-	no
10090.ENSMUSP00000120421	Nos1	-	no
10090.ENSMUSP00000120152	Stat3	-	no
10090.ENSMUSP00000119891	Cdk5rap2	-	no
10090.ENSMUSP00000119745	Mpnd	-	no
10090.ENSMUSP00000119564	Gk	-	no
10090.ENSMUSP00000119557	Il9r	-	no
10090.ENSMUSP00000119485	Inpp5e	-	no
10090.ENSMUSP00000119465	Aim2	-	no
10090.ENSMUSP00000119369	Becn1	-	no
10090.ENSMUSP00000119303	Numb	-	no
10090.ENSMUSP00000118491	Abi1	-	no
10090.ENSMUSP00000118458	Pla2g4b	-	no
10090.ENSMUSP00000118179	Copa	-	no
10090.ENSMUSP00000117872	Fbxw10	-	no
10090.ENSMUSP00000117496	Mef2a	-	no
10090.ENSMUSP00000117299	Haus2	-	no
10090.ENSMUSP00000117153	Itgb3bp	-	no
10090.ENSMUSP00000117082	Dcaf10	-	no
10090.ENSMUSP00000116271	Lcp1	-	no
10090.ENSMUSP00000116108	Tcp1	-	no
10090.ENSMUSP00000116040	Gm11639	-	no
10090.ENSMUSP00000115974	NoMapping	-	no
10090.ENSMUSP00000115883	Vegfa	up	no
10090.ENSMUSP00000115750	Dna2	-	no
10090.ENSMUSP00000115325	Fzd3	-	no

10090.ENSMUSP00000115247	Nrg4	-	no
10090.ENSMUSP00000114909	Efcab6	-	no
10090.ENSMUSP00000114839	Arpc4	-	no
10090.ENSMUSP00000114203	Fzr1	-	no
10090.ENSMUSP00000114123	Erbb4	-	no
10090.ENSMUSP00000114114	Fzd10	-	no
10090.ENSMUSP00000114076	Igf2	-	no
10090.ENSMUSP00000113891	Gata4	-	no
10090.ENSMUSP00000113851	Bcl3	up	no
10090.ENSMUSP00000113843	S1pr5	-	no
10090.ENSMUSP00000113778	Rapgef2	-	no
10090.ENSMUSP00000113672	Cth	-	no
10090.ENSMUSP00000113571	Ank1	-	no
10090.ENSMUSP00000113488	Pde4d	-	no
10090.ENSMUSP00000113388	Atm	-	no
10090.ENSMUSP00000113342	Il23r	-	no
10090.ENSMUSP00000113341	Csnk1e	-	no
10090.ENSMUSP00000113308	Synj1	-	no
10090.ENSMUSP00000113188	Wnt5b	-	no
10090.ENSMUSP00000113071	Msn	-	no
10090.ENSMUSP00000112934	Magi3	down	no
10090.ENSMUSP00000112905	Gm20489	-	no
10090.ENSMUSP00000112765	Btc	-	no
10090.ENSMUSP00000112665	Ecm1	-	no
10090.ENSMUSP00000112481	Ctsf	-	no
10090.ENSMUSP00000112436	Cacna1a	-	no
10090.ENSMUSP00000112430	Fgfr2	down	no
10090.ENSMUSP00000112221	Nck1	-	no
10090.ENSMUSP00000112138	Snap23	-	no
10090.ENSMUSP00000112006	Ctss	-	no
10090.ENSMUSP00000111942	Arl1	-	no
10090.ENSMUSP00000111568	NoMapping	-	no
10090.ENSMUSP00000111479	Pik3c3	-	no
10090.ENSMUSP00000111457	Synj2	-	no
10090.ENSMUSP00000111393	Tmem173	-	no
10090.ENSMUSP00000111391	Cacna1f	-	no
10090.ENSMUSP00000111297	Diaph1	-	no
10090.ENSMUSP00000111269	Txnrd2	-	no
10090.ENSMUSP00000111175	Bcor	down	no

10090.ENSMUSP00000111048	Ccnf	-	no
10090.ENSMUSP00000110957	Cldn16	-	no
10090.ENSMUSP00000110804	Ubxn7	-	no
10090.ENSMUSP00000110760	Gng13	-	no
10090.ENSMUSP00000110611	Kalrn	-	no
10090.ENSMUSP00000110593	Dcc	-	no
10090.ENSMUSP00000110563	Adcy5	-	no
10090.ENSMUSP00000110409	Gpr45	-	no
10090.ENSMUSP00000110371	Cacnb2	-	no
10090.ENSMUSP00000110221	Glp1r	-	no
10090.ENSMUSP00000110198	Cetn2	-	no
10090.ENSMUSP00000110158	Gls	-	no
10090.ENSMUSP00000110115	Cblb	-	no
10090.ENSMUSP00000110006	Aox2	-	no
10090.ENSMUSP00000109979	Add1	-	no
10090.ENSMUSP00000109881	Gm973	-	no
10090.ENSMUSP00000109761	Stx18	-	no
10090.ENSMUSP00000109688	Cldn34d	-	no
10090.ENSMUSP00000109635	Itsn1	-	no
10090.ENSMUSP00000109552	Dctn1	-	no
10090.ENSMUSP00000109502	Amer1	-	no
10090.ENSMUSP00000109388	Odf2	-	no
10090.ENSMUSP00000109348	Sptan1	-	no
10090.ENSMUSP00000109288	Gfpt1	-	no
10090.ENSMUSP00000109271	Kat5	-	no
10090.ENSMUSP00000109237	Copg1	-	no
10090.ENSMUSP00000109234	Txk	-	no
10090.ENSMUSP00000109190	Fnbp1	-	no
10090.ENSMUSP00000109144	Kdr	-	no
10090.ENSMUSP00000109010	Flrt1	down	no
10090.ENSMUSP00000108961	Ubr2	-	no
10090.ENSMUSP00000108771	Mtmr14	-	no
10090.ENSMUSP00000108767	Ugt1a10	-	no
10090.ENSMUSP00000108762	Ugt1a6b	-	no
10090.ENSMUSP00000108742	Brpf1	-	no
10090.ENSMUSP00000108683	Adamts7	-	no
10090.ENSMUSP00000108678	Shroom3	down	no
10090.ENSMUSP00000108660	Cntrl	-	no
10090.ENSMUSP00000108603	Catsperd	-	no

10090.ENSMUSP00000108468	Mapk10	-	no
10090.ENSMUSP00000108131	Golga3	-	no
10090.ENSMUSP00000108075	Sh3kbp1	-	no
10090.ENSMUSP00000108008	Map4k3	down	no
10090.ENSMUSP00000107869	Cacna1d	-	no
10090.ENSMUSP00000107851	Klhl12	-	no
10090.ENSMUSP00000107827	Prkcd	-	no
10090.ENSMUSP00000107795	Tmsb4x	-	no
10090.ENSMUSP00000107695	Cacna1s	-	no
10090.ENSMUSP00000107670	Fbxw28	-	no
10090.ENSMUSP00000107576	Mapk8	-	no
10090.ENSMUSP00000107499	Pik3c2g	-	no
10090.ENSMUSP00000107498	Sufu	-	no
10090.ENSMUSP00000107367	Tctn1	-	no
10090.ENSMUSP00000107214	Diablo	-	no
10090.ENSMUSP00000106906	Ncf1	-	no
10090.ENSMUSP00000106789	Akt3	-	no
10090.ENSMUSP00000106772	Dtx2	-	no
10090.ENSMUSP00000106724	Gnrh1	-	no
10090.ENSMUSP00000106693	Ntsr2	-	no
10090.ENSMUSP00000106625	Tlr5	down	no
10090.ENSMUSP00000106481	Dld	-	no
10090.ENSMUSP00000106180	Sord	-	no
10090.ENSMUSP00000106145	Hecw1	-	no
10090.ENSMUSP00000106137	Gli3	-	no
10090.ENSMUSP00000106102	Hist1h2bm	-	no
10090.ENSMUSP00000106099	Hist1h2bp	-	no
10090.ENSMUSP00000106085	Hist1h2bk	-	no
10090.ENSMUSP00000105743	Plcb1	-	no
10090.ENSMUSP00000105709	NoMapping	-	no
10090.ENSMUSP00000105663	Ptk2	-	no
10090.ENSMUSP00000105584	Serpina3i	-	no
10090.ENSMUSP00000105583	Serpina3j	-	no
10090.ENSMUSP00000105531	Tmed9	-	no
10090.ENSMUSP00000105522	Ninl	-	no
10090.ENSMUSP00000105359	H2afv	-	no
10090.ENSMUSP00000105348	Mta1	-	no
10090.ENSMUSP00000105248	Cep250	-	no
10090.ENSMUSP00000105179	Rasa1	-	no

10090.ENSMUSP00000105051	Wnt7b	-	no
10090.ENSMUSP00000104992	Slpi	up	no
10090.ENSMUSP00000104977	Tubgcp6	-	no
10090.ENSMUSP00000104964	Kcnip1	-	no
10090.ENSMUSP00000104931	Nfatc3	-	no
10090.ENSMUSP00000104890	Map3k1	-	no
10090.ENSMUSP00000104830	Ube2v1	-	no
10090.ENSMUSP00000104445	Hist3h2a	-	no
10090.ENSMUSP00000104436	Arfrp1	-	no
10090.ENSMUSP00000104411	Wnt9a	-	no
10090.ENSMUSP00000104301	Chd3	-	no
10090.ENSMUSP00000104298	Tp53	-	no
10090.ENSMUSP00000104168	Pla2g4c	-	no
10090.ENSMUSP00000104158	Nlrp1a	-	no
10090.ENSMUSP00000104154	Nlrp1b	-	no
10090.ENSMUSP00000104040	B9d2	-	no
10090.ENSMUSP00000103965	Cp	-	no
10090.ENSMUSP00000103960	Ccne2	-	no
10090.ENSMUSP00000103916	Fbxo27	-	no
10090.ENSMUSP00000103884	Prkci	-	no
10090.ENSMUSP00000103869	Gnb4	-	no
10090.ENSMUSP00000103786	Zbtb32	-	no
10090.ENSMUSP00000103690	Kif24	-	no
10090.ENSMUSP00000103658	Ccne1	-	no
10090.ENSMUSP00000103571	Shank1	-	no
10090.ENSMUSP00000103483	Clta	-	no
10090.ENSMUSP00000103350	Spop	-	no
10090.ENSMUSP00000103305	Fbxw7	-	no
10090.ENSMUSP00000103207	Sh2d2a	-	no
10090.ENSMUSP00000103169	Med1	-	no
10090.ENSMUSP00000102855	Pip5k1a	-	no
10090.ENSMUSP00000102796	Adamtsl1	-	no
10090.ENSMUSP00000102635	Hsd3b2	-	no
10090.ENSMUSP00000102630	Hsd3b1	-	no
10090.ENSMUSP00000102591	Anapc15	-	no
10090.ENSMUSP00000102546	Dnajc6	-	no
10090.ENSMUSP00000102538	Ngf	-	no
10090.ENSMUSP00000102296	Gstm6	-	no
10090.ENSMUSP00000102078	Prdx1	-	no

10090.ENSMUSP00000101944	Cyp2u1	-	no
10090.ENSMUSP00000101913	Itgal	-	no
10090.ENSMUSP00000101898	Ube2d3	-	no
10090.ENSMUSP00000101849	Itgam	-	no
10090.ENSMUSP00000101843	Unc5c	down	no
10090.ENSMUSP00000101834	Cep131	-	no
10090.ENSMUSP00000101734	Adgrl2	down	no
10090.ENSMUSP00000101518	Fgf3	-	no
10090.ENSMUSP00000101514	Rps6ka1	-	no
10090.ENSMUSP00000101315	Pik3cd	-	no
10090.ENSMUSP00000101060	Adora2a	-	no
10090.ENSMUSP00000101049	Col18a1	-	no
10090.ENSMUSP00000101032	Icoslg	up	no
10090.ENSMUSP00000100979	Tcf3	-	no
10090.ENSMUSP00000100964	Pip5k1c	-	no
10090.ENSMUSP00000100962	Tbxa2r	-	no
10090.ENSMUSP00000100920	Kitlg	-	no
10090.ENSMUSP00000100869	Rnf41	-	no
10090.ENSMUSP00000100581	Hist2h2aa1,Hist2h2aa2	-	no
10090.ENSMUSP00000100534	Mcts2	-	no
10090.ENSMUSP00000100041	Gata3	-	no
10090.ENSMUSP00000100026	Cntfr	-	no
10090.ENSMUSP00000100020	Cetn4	-	no
10090.ENSMUSP00000100002	Ehmt1	-	no
10090.ENSMUSP00000099991	Pdpk1	-	no
10090.ENSMUSP00000099986	Pold2	-	no
10090.ENSMUSP00000099985	Myl7	-	no
10090.ENSMUSP00000099984	Gck	-	no
10090.ENSMUSP00000099981	Col15a1	-	no
10090.ENSMUSP00000099955	Adamts13	-	no
10090.ENSMUSP00000099944	Ppp3r1	-	no
10090.ENSMUSP00000099928	Rel	-	no
10090.ENSMUSP00000099916	Ptges	up	no
10090.ENSMUSP00000099904	Ass1	-	no
10090.ENSMUSP00000099891	Icos	-	no
10090.ENSMUSP00000099865	Tenm2	-	no
10090.ENSMUSP00000099862	Tek	-	no
10090.ENSMUSP00000099860	Il12b	-	no

10090.ENSMUSP00000099859	Ublcp1	-	no
10090.ENSMUSP00000099853	NoMapping	-	no
10090.ENSMUSP00000099842	Jak1	-	no
10090.ENSMUSP00000099835	Sqstm1	up	no
10090.ENSMUSP00000099819	Vdac1	-	no
10090.ENSMUSP00000099805	Orc1	-	no
10090.ENSMUSP00000099804	Rapgef6	-	no
10090.ENSMUSP00000099790	Eps15	-	no
10090.ENSMUSP00000099718	Itga4	-	no
10090.ENSMUSP00000099717	B9d1	-	no
10090.ENSMUSP00000099658	Rbbp4	-	no
10090.ENSMUSP00000099657	Hdac1	-	no
10090.ENSMUSP00000099652	Tjp1	-	no
10090.ENSMUSP00000099645	Fgf11	-	no
10090.ENSMUSP00000099623	Arrb2	-	no
10090.ENSMUSP00000099605	Il22ra1	-	no
10090.ENSMUSP00000099593	Rasgrp1	-	no
10090.ENSMUSP00000099587	Ppp1cc	-	no
10090.ENSMUSP00000099584	Arpc3	-	no
10090.ENSMUSP00000099583	Plcb2	-	no
10090.ENSMUSP00000099529	Sema6d	up	no
10090.ENSMUSP00000099510	Mtor	-	no
10090.ENSMUSP00000099504	Kcnip3	-	no
10090.ENSMUSP00000099475	Cltc	-	no
10090.ENSMUSP00000099473	Adra1d	-	no
10090.ENSMUSP00000099468	Mtmr4	-	no
10090.ENSMUSP00000099445	Gip	-	no
10090.ENSMUSP00000099432	Fbxl20	-	no
10090.ENSMUSP00000099428	Thra	-	no
10090.ENSMUSP00000099404	Plcg1	-	no
10090.ENSMUSP00000099384	Tnnc2	-	no
10090.ENSMUSP00000099375	Itga2b	-	no
10090.ENSMUSP00000099368	Cttn	-	no
10090.ENSMUSP00000099366	Plcd3	-	no
10090.ENSMUSP00000099364	Nsf	-	no
10090.ENSMUSP00000099320	Fbf1	-	no
10090.ENSMUSP00000098927	Plb1	-	no
10090.ENSMUSP00000098897	Mad2l1	-	no
10090.ENSMUSP00000098680	Gpr27	-	no

10090.ENSMUSP00000098641	Serpina3f	-	no
10090.ENSMUSP00000098639	Serpina3m	-	no
10090.ENSMUSP00000098436	Selplg	-	no
10090.ENSMUSP00000098295	Psmd9	-	no
10090.ENSMUSP00000098127	Cacna1g	-	no
10090.ENSMUSP00000098066	Actb	-	no
10090.ENSMUSP00000098056	Eif2ak1	-	no
10090.ENSMUSP00000097972	B3glct	-	no
10090.ENSMUSP00000097910	Lmo7	-	no
10090.ENSMUSP00000097889	Cldn10	-	no
10090.ENSMUSP00000097885	Mycb	-	no
10090.ENSMUSP00000097874	Prkcg	-	no
10090.ENSMUSP00000097809	Ttf1	-	no
10090.ENSMUSP00000097738	Copz1	-	no
10090.ENSMUSP00000097605	Dync1i2	-	no
10090.ENSMUSP00000097601	Fgf12	-	no
10090.ENSMUSP00000097547	Fyn	-	no
10090.ENSMUSP00000097294	Hist1h2bb	-	no
10090.ENSMUSP00000097185	Chrm5	-	no
10090.ENSMUSP00000097071	Cyp2c68	-	no
10090.ENSMUSP00000096939	Plxnc1	-	no
10090.ENSMUSP00000096932	Ube2n	-	no
10090.ENSMUSP00000096930	Rasgrf2	-	no
10090.ENSMUSP00000096830	Srxn1	up	no
10090.ENSMUSP00000096829	Csnk2a1	-	no
10090.ENSMUSP00000096712	Itga7	-	no
10090.ENSMUSP00000096705	Mgst2	-	no
10090.ENSMUSP00000096477	Gm4778	-	no
10090.ENSMUSP00000096231	Cib3	-	no
10090.ENSMUSP00000096139	Gsta1	-	no
10090.ENSMUSP00000096122	Adcy7	-	no
10090.ENSMUSP00000096119	Cyld	-	no
10090.ENSMUSP00000096057	Il20rb	-	no
10090.ENSMUSP00000095962	Fbxw18	-	no
10090.ENSMUSP00000095929	Mc1r	-	no
10090.ENSMUSP00000095866	Arrb1	-	no
10090.ENSMUSP00000095792	Rragd	-	no
10090.ENSMUSP00000095736	Il11ra1	-	no
10090.ENSMUSP00000095572	Efcab7	-	no

10090.ENSMUSP00000095263	Ugt1a5	-	no
10090.ENSMUSP00000095253	Ramp1	-	no
10090.ENSMUSP00000095149	Cep76	-	no
10090.ENSMUSP00000095030	Fgfr1op	-	no
10090.ENSMUSP00000094873	Prkce	-	no
10090.ENSMUSP00000094863	NoMapping	-	no
10090.ENSMUSP00000094778	Tuba1a	-	no
10090.ENSMUSP00000094225	Skp2	-	no
10090.ENSMUSP00000094151	A1bg	-	no
10090.ENSMUSP00000094084	Ncf4	-	no
10090.ENSMUSP00000094083	Csf2rb2	-	no
10090.ENSMUSP00000094082	Csf2rb	-	no
10090.ENSMUSP00000094076	Maff	-	no
10090.ENSMUSP00000093978	Gng3	-	no
10090.ENSMUSP00000093959	Mta2	-	no
10090.ENSMUSP00000093830	Asah2	-	no
10090.ENSMUSP00000093702	Prss3	-	no
10090.ENSMUSP00000093698	Gm10334	-	no
10090.ENSMUSP00000093653	Ptgdr	-	no
10090.ENSMUSP00000093644	Vti1a	-	no
10090.ENSMUSP00000093470	Tbpl1	-	no
10090.ENSMUSP00000093325	Tmf1	-	no
10090.ENSMUSP00000093236	Cldn9	-	no
10090.ENSMUSP00000093185	Fgf14	-	no
10090.ENSMUSP00000093044	Tas2r13	-	no
10090.ENSMUSP00000093043	Tas2r115	-	no
10090.ENSMUSP00000093040	Tas2r140	-	no
10090.ENSMUSP00000092901	Jund	-	no
10090.ENSMUSP00000092845	Fbxw9	-	no
10090.ENSMUSP00000092828	Rasgrp3	-	no
10090.ENSMUSP00000092799	Znrf1	-	no
10090.ENSMUSP00000092602	Klhl9	-	no
10090.ENSMUSP00000092492	Il11	up	no
10090.ENSMUSP00000092487	Cyp4a12b	-	no
10090.ENSMUSP00000092384	Gipr	-	no
10090.ENSMUSP00000092375	Inpp5b	-	no
10090.ENSMUSP00000092355	Relb	-	no
10090.ENSMUSP00000092252	Pla2g4d	-	no
10090.ENSMUSP00000092233	Ugt2b36	-	no

10090.ENSMUSP00000092200	Rasgrp4	-	no
10090.ENSMUSP00000092163	Ffar3	-	no
10090.ENSMUSP00000092136	Golt1a	-	no
10090.ENSMUSP00000092019	Id1	-	no
10090.ENSMUSP00000091940	Shc1	-	no
10090.ENSMUSP00000091882	Cdc25a	-	no
10090.ENSMUSP00000091799	Cldn3	-	no
10090.ENSMUSP00000091696	Flcn	-	no
10090.ENSMUSP00000091495	Ccnd1	-	no
10090.ENSMUSP00000091469	Cdc6	-	no
10090.ENSMUSP00000091463	Fzd2	-	no
10090.ENSMUSP00000091455	Crhr1	-	no
10090.ENSMUSP00000091452	Cdc27	-	no
10090.ENSMUSP00000091429	Rnf213	-	no
10090.ENSMUSP00000091422	Birc2	-	no
10090.ENSMUSP00000091319	Cep162	-	no
10090.ENSMUSP00000091312	Cep70	-	no
10090.ENSMUSP00000091306	Cep63	-	no
10090.ENSMUSP00000091238	Casp3	-	no
10090.ENSMUSP00000091151	Fcho1	-	no
10090.ENSMUSP00000091015	NoMapping	-	no
10090.ENSMUSP00000090853	Cyfip2	-	no
10090.ENSMUSP00000090789	Taf1c	-	no
10090.ENSMUSP00000090277	Pcgf1	-	no
10090.ENSMUSP00000090237	Src	-	no
10090.ENSMUSP00000090177	Smurf2	-	no
10090.ENSMUSP00000090155	Sgpl1	-	no
10090.ENSMUSP00000090090	Ank3	-	no
10090.ENSMUSP00000089948	Mbd3	-	no
10090.ENSMUSP00000089936	Gng7	-	no
10090.ENSMUSP00000089728	Usp14	-	no
10090.ENSMUSP00000089703	Lama3	-	no
10090.ENSMUSP00000089336	Hist1h2ah	-	no
10090.ENSMUSP00000089198	NoMapping	-	no
10090.ENSMUSP00000088837	Insr	-	no
10090.ENSMUSP00000088801	Mfn1	-	no
10090.ENSMUSP00000088491	Bcan	-	no
10090.ENSMUSP00000088366	Tdpoz2	-	no
10090.ENSMUSP00000088288	Hist2h2ac	-	no

10090.ENSMUSP00000088287	Hist2h2be	-	no
10090.ENSMUSP00000088175	Tac1	-	no
10090.ENSMUSP00000088174	Rap1a	-	no
10090.ENSMUSP00000088079	Il3ra	-	no
10090.ENSMUSP00000087912	Cd59b	-	no
10090.ENSMUSP00000087744	Efcab1	-	no
10090.ENSMUSP00000087714	Trio	-	no
10090.ENSMUSP00000087611	Ncald	-	no
10090.ENSMUSP00000087525	Pla2g4e	-	no
10090.ENSMUSP00000087457	Itgb1	-	no
10090.ENSMUSP00000087327	Masp1	down	no
10090.ENSMUSP00000087208	Cep152	-	no
10090.ENSMUSP00000087119	Mmp14	-	no
10090.ENSMUSP00000087073	Htra2	-	no
10090.ENSMUSP00000086948	Aak1	-	no
10090.ENSMUSP00000086852	Uba52	-	no
10090.ENSMUSP00000086820	Il2rb	-	no
10090.ENSMUSP00000086731	Gpr15	-	no
10090.ENSMUSP00000086730	Magi1	-	no
10090.ENSMUSP00000086701	Uba3	-	no
10090.ENSMUSP00000086564	Tnfrsf13c	-	no
10090.ENSMUSP00000086383	Hrh1	-	no
10090.ENSMUSP00000086207	Mapk12	-	no
10090.ENSMUSP00000086204	Mapk11	-	no
10090.ENSMUSP00000085913	Myl9	-	no
10090.ENSMUSP00000085872	Magi2	-	no
10090.ENSMUSP00000085581	Ube2c	-	no
10090.ENSMUSP00000085218	Stx16	-	no
10090.ENSMUSP00000085030	Tnip2	-	no
10090.ENSMUSP00000085016	Notch3	-	no
10090.ENSMUSP00000084918	Aldh1a1	-	no
10090.ENSMUSP00000084846	Aldoa	-	no
10090.ENSMUSP00000084701	Bmpr2	-	no
10090.ENSMUSP00000084656	Kcnip4	-	no
10090.ENSMUSP00000084578	Ppp1r3c	down	no
10090.ENSMUSP00000084489	Cyp2c65	-	no
10090.ENSMUSP00000084487	Cyp2c66	-	no
10090.ENSMUSP00000084196	Gpr55	-	no
10090.ENSMUSP00000083725	Slc8a1	down	no

10090.ENSMUSP00000083709	Pxn	-	no
10090.ENSMUSP00000083652	Rfc5	-	no
10090.ENSMUSP00000083650	Fbxl12	-	no
10090.ENSMUSP00000083611	Nck2	-	no
10090.ENSMUSP00000083587	Icam1	up	no
10090.ENSMUSP00000083583	Gpr25	-	no
10090.ENSMUSP00000083393	Anapc5	-	no
10090.ENSMUSP00000083375	Glul	-	no
10090.ENSMUSP00000083281	Ap2s1	-	no
10090.ENSMUSP00000083204	F5	-	no
10090.ENSMUSP00000083193	Caln1	-	no
10090.ENSMUSP00000082952	Lefty2	-	no
10090.ENSMUSP00000082941	Card11	-	no
10090.ENSMUSP00000082862	Mark4	-	no
10090.ENSMUSP00000082827	Smurf1	-	no
10090.ENSMUSP00000082816	Pml	-	no
10090.ENSMUSP00000082754	Usp12	-	no
10090.ENSMUSP00000082710	Traf5	-	no
10090.ENSMUSP00000082682	Hmgb1	-	no
10090.ENSMUSP00000082173	Cacna2d2	-	no
10090.ENSMUSP00000082127	Serpina3b	-	no
10090.ENSMUSP00000082125	Serpina3c	-	no
10090.ENSMUSP00000082053	Ppp2r5c	-	no
10090.ENSMUSP00000082051	Fbxw16	-	no
10090.ENSMUSP00000081880	Golga4	-	no
10090.ENSMUSP00000081867	Dnah11	-	no
10090.ENSMUSP00000081573	Cdc26	-	no
10090.ENSMUSP00000081547	Bub3	-	no
10090.ENSMUSP00000081544	Oat	-	no
10090.ENSMUSP00000081531	Dock1	-	no
10090.ENSMUSP00000081416	Insl5	-	no
10090.ENSMUSP00000081370	Cyp4a12a	-	no
10090.ENSMUSP00000081369	Cyp4a32	-	no
10090.ENSMUSP00000081334	Cldn19	-	no
10090.ENSMUSP00000081263	Wasf2	-	no
10090.ENSMUSP00000081041	Fgfr1	-	no
10090.ENSMUSP00000081012	Gpx2	-	no
10090.ENSMUSP00000081011	Gpx3	-	no
10090.ENSMUSP00000081010	Gpx1	-	no

10090.ENSMUSP00000081009	Sephs2	-	no
10090.ENSMUSP00000081004	Selenop	-	no
10090.ENSMUSP00000080974	Cd36	-	no
10090.ENSMUSP00000080846	Cyp2b9	-	no
10090.ENSMUSP00000080736	Tas2r131	-	no
10090.ENSMUSP00000080716	Erbb3	-	no
10090.ENSMUSP00000080694	Rps6ka6	-	no
10090.ENSMUSP00000080674	Tas2r110	-	no
10090.ENSMUSP00000080650	Rnf217	-	no
10090.ENSMUSP00000080608	NoMapping	-	no
10090.ENSMUSP00000080601	Dtx3l	-	no
10090.ENSMUSP00000080548	Tor4a	-	no
10090.ENSMUSP00000080472	Tdpoz3	-	no
10090.ENSMUSP00000080325	Sh3pxd2a	-	no
10090.ENSMUSP00000080162	Adrb3	-	no
10090.ENSMUSP00000080066	Sfi1	-	no
10090.ENSMUSP00000079991	Plcg2	-	no
10090.ENSMUSP00000079926	Pikfyve	-	no
10090.ENSMUSP00000079752	Lrp2	-	no
10090.ENSMUSP00000079628	Rps17	-	no
10090.ENSMUSP00000079553	Sgip1	-	no
10090.ENSMUSP00000079460	Fbxw22	-	no
10090.ENSMUSP00000079453	Tas2r114	-	no
10090.ENSMUSP00000079380	Rac1	-	no
10090.ENSMUSP00000079341	Gnas	-	no
10090.ENSMUSP00000079324	Met	-	no
10090.ENSMUSP00000079309	Tbpl2	-	no
10090.ENSMUSP00000079306	Hspa2	-	no
10090.ENSMUSP00000079022	Aldoart2	-	no
10090.ENSMUSP00000078945	Htt	-	no
10090.ENSMUSP00000078875	Fcer1g	-	no
10090.ENSMUSP00000078795	Znrf2	-	no
10090.ENSMUSP00000078753	Gpr84	up	no
10090.ENSMUSP00000078741	Notch2	-	no
10090.ENSMUSP00000078740	Ugt2a2	-	no
10090.ENSMUSP00000078723	Pth	-	no
10090.ENSMUSP00000078715	Myl3	-	no
10090.ENSMUSP00000078682	Ctbp1	-	no
10090.ENSMUSP00000078630	Gss	-	no

10090.ENSMUSP00000078584	Cldn24	-	no
10090.ENSMUSP00000078503	Fbxw20	-	no
10090.ENSMUSP00000078440	Nlrp3	-	no
10090.ENSMUSP00000078429	Tuba4a	-	no
10090.ENSMUSP00000078383	Cep89	-	no
10090.ENSMUSP00000078339	Gm10093	-	no
10090.ENSMUSP00000078044	Tas2r113	-	no
10090.ENSMUSP00000077899	Kl	-	no
10090.ENSMUSP00000077878	Il15ra	-	no
10090.ENSMUSP00000077813	Xcr1	-	no
10090.ENSMUSP00000077716	Rab43	-	no
10090.ENSMUSP00000077687	Aldoart1	-	no
10090.ENSMUSP00000077611	Rxfp1	-	no
10090.ENSMUSP00000077586	Cacna1h	down	no
10090.ENSMUSP00000077553	Memo1	-	no
10090.ENSMUSP00000077438	Cacnb4	-	no
10090.ENSMUSP00000077314	Gng8	-	no
10090.ENSMUSP00000077290	Hist1h2bh	-	no
10090.ENSMUSP00000077197	Rnf114	-	no
10090.ENSMUSP00000077168	Glmn	-	no
10090.ENSMUSP00000077135	Gpbar1	-	no
10090.ENSMUSP00000077132	Itga1	-	no
10090.ENSMUSP00000077021	Cyp2b19	-	no
10090.ENSMUSP00000076933	Arpc5	-	no
10090.ENSMUSP00000076911	Pik3c2b	-	no
10090.ENSMUSP00000076880	Calml3	-	no
10090.ENSMUSP00000076578	Cyp2b23	-	no
10090.ENSMUSP00000076576	Klk1b4	-	no
10090.ENSMUSP00000076491	Rxra	-	no
10090.ENSMUSP00000076397	Hist3h2ba	-	no
10090.ENSMUSP00000076383	Sftpd	-	no
10090.ENSMUSP00000076162	Cks1brt	-	no
10090.ENSMUSP00000076160	Cop1	-	no
10090.ENSMUSP00000076155	Gnb5	-	no
10090.ENSMUSP00000076115	Efna5	-	no
10090.ENSMUSP00000076043	Tas2r106	-	no
10090.ENSMUSP00000075918	Fbxw19	-	no
10090.ENSMUSP00000075876	Tas2r38	-	no
10090.ENSMUSP00000075794	Nlrp4e	-	no

10090.ENSMUSP00000075773	Ggt6	-	no
10090.ENSMUSP00000075721	Fbxw11	-	no
10090.ENSMUSP00000075509	Tas2r124	-	no
10090.ENSMUSP00000075497	Fnip2	up	no
10090.ENSMUSP00000075483	Tas2r125	-	no
10090.ENSMUSP00000075463	Pdgfa	-	no
10090.ENSMUSP00000075423	Csf2ra	-	no
10090.ENSMUSP00000075339	Taf1b	-	no
10090.ENSMUSP00000075338	Tdpoz4	-	no
10090.ENSMUSP00000075269	Mysm1	-	no
10090.ENSMUSP00000075266	Fbxo40	-	no
10090.ENSMUSP00000075255	Ugt2b37	-	no
10090.ENSMUSP00000075167	Abl1	-	no
10090.ENSMUSP00000075070	Calcr	-	no
10090.ENSMUSP00000075005	Sult2b1	-	no
10090.ENSMUSP00000074810	Orm2	-	no
10090.ENSMUSP00000074733	Cyp4f13	-	no
10090.ENSMUSP00000074708	Osm	-	no
10090.ENSMUSP00000074684	Nfe2	-	no
10090.ENSMUSP00000074581	Gpr65	-	no
10090.ENSMUSP00000074573	Hcst	-	no
10090.ENSMUSP00000074359	Glipr1	-	no
10090.ENSMUSP00000074310	Hist1h2ak	-	no
10090.ENSMUSP00000074198	Nfatc2	-	no
10090.ENSMUSP00000074142	H2afj	-	no
10090.ENSMUSP00000074009	Ifnlr1	-	no
10090.ENSMUSP00000073974	Axin1	-	no
10090.ENSMUSP00000073875	Calcrl	-	no
10090.ENSMUSP00000073778	Dcaf8	-	no
10090.ENSMUSP00000073764	Aldh3a2	-	no
10090.ENSMUSP00000073617	Fbxw24	-	no
10090.ENSMUSP00000073601	Vkorc1l1	-	no
10090.ENSMUSP00000073546	Nrg1	-	no
10090.ENSMUSP00000073444	Ugt1a9	-	no
10090.ENSMUSP00000073268	NoMapping	-	no
10090.ENSMUSP00000073190	Lct	-	no
10090.ENSMUSP00000073164	Syt9	-	no
10090.ENSMUSP00000073136	Stx5	-	no
10090.ENSMUSP00000072989	Hist1h2af	-	no

10090.ENSMUSP00000072859	Nfkb2	-	no
10090.ENSMUSP00000072858	Hist2h2ab	-	no
10090.ENSMUSP00000072803	Ugt1a1	-	no
10090.ENSMUSP00000072660	Sctr	-	no
10090.ENSMUSP00000072615	Sphk2	-	no
10090.ENSMUSP00000072598	Ugt2b38	-	no
10090.ENSMUSP00000072387	Ube2d2b	-	no
10090.ENSMUSP00000072344	Dcaf11	-	no
10090.ENSMUSP00000072334	Elmo1	-	no
10090.ENSMUSP00000072330	Myod1	-	no
10090.ENSMUSP00000072264	Cyp2b10	-	no
10090.ENSMUSP00000072237	Tas2r104	-	no
10090.ENSMUSP00000072197	Tpm3-rs7	-	no
10090.ENSMUSP00000072195	Hk1	-	no
10090.ENSMUSP00000072145	Vsnl1	-	no
10090.ENSMUSP00000072134	Pi4kb	-	no
10090.ENSMUSP00000072074	Ggt5	-	no
10090.ENSMUSP00000071976	Try10	-	no
10090.ENSMUSP00000071811	Fbxw26	-	no
10090.ENSMUSP00000071756	Hpcal1	-	no
10090.ENSMUSP00000071626	Tas2r120	-	no
10090.ENSMUSP00000071619	Elmo2	-	no
10090.ENSMUSP00000071615	Tas2r123	-	no
10090.ENSMUSP00000071486	Actg1	-	no
10090.ENSMUSP00000071370	Nhlrc2	-	no
10090.ENSMUSP00000071289	Nf1	-	no
10090.ENSMUSP00000071214	Eif2s1	-	no
10090.ENSMUSP00000071135	Tubb4a	-	no
10090.ENSMUSP00000071078	Cope	-	no
10090.ENSMUSP00000071035	Smad1	-	no
10090.ENSMUSP00000071017	Rnf144b	-	no
10090.ENSMUSP00000070993	Ywhae	-	no
10090.ENSMUSP00000070958	Agtr1a	-	no
10090.ENSMUSP00000070925	Ptafr	-	no
10090.ENSMUSP00000070901	Cib1	-	no
10090.ENSMUSP00000070868	Pla2g4a	-	no
10090.ENSMUSP00000070840	Uts2b	-	no
10090.ENSMUSP00000070827	Naip2	-	no
10090.ENSMUSP00000070791	Tas2r136	-	no

10090.ENSMUSP00000070751	Bsg	-	no
10090.ENSMUSP00000070726	Ppp2r5a	-	no
10090.ENSMUSP00000070662	Rlim	-	no
10090.ENSMUSP00000070554	Usp46	-	no
10090.ENSMUSP00000070504	Haus6	-	no
10090.ENSMUSP00000070250	Agfg1	-	no
10090.ENSMUSP00000070109	Ggcx	-	no
10090.ENSMUSP00000070019	Prkcb	-	no
10090.ENSMUSP00000069957	Cnr2	-	no
10090.ENSMUSP00000069850	Cebpb	-	no
10090.ENSMUSP00000069768	Tas2r117	-	no
10090.ENSMUSP00000069752	Rras2	-	no
10090.ENSMUSP00000069681	Fgf7	-	no
10090.ENSMUSP00000069670	Plpp2	-	no
10090.ENSMUSP00000069631	Dhrs9	-	no
10090.ENSMUSP00000069567	Ghrl	-	no
10090.ENSMUSP00000069549	Rock1	-	no
10090.ENSMUSP00000069529	Stx3	-	no
10090.ENSMUSP00000069457	Ghr	-	no
10090.ENSMUSP00000069418	C4b	-	no
10090.ENSMUSP00000069416	Itgb5	-	no
10090.ENSMUSP00000069300	Tas2r109	-	no
10090.ENSMUSP00000069284	Pi4k2a	-	no
10090.ENSMUSP00000069238	Cers3	-	no
10090.ENSMUSP00000069114	Ackr3	-	no
10090.ENSMUSP00000069081	Gnpda1	-	no
10090.ENSMUSP00000068931	Mta3	-	no
10090.ENSMUSP00000068834	Trib1	up	no
10090.ENSMUSP00000068699	Pla2g3	-	no
10090.ENSMUSP00000068568	Retsat	-	no
10090.ENSMUSP00000068487	Tgoln1	-	no
10090.ENSMUSP00000068333	Htr6	-	no
10090.ENSMUSP00000068298	Agtr1b	-	no
10090.ENSMUSP00000068282	Ugt2b17	-	no
10090.ENSMUSP00000068230	Fbxo30	-	no
10090.ENSMUSP00000068120	Ghrhr	-	no
10090.ENSMUSP00000068087	Stx17	-	no
10090.ENSMUSP00000067964	Gpsm1	-	no
10090.ENSMUSP00000067897	Rxfp2	-	no

10090.ENSMUSP00000067786	Sos1	-	no
10090.ENSMUSP00000067783	Fzd5	-	no
10090.ENSMUSP00000067734	Tas2r40	-	no
10090.ENSMUSP00000067708	Actn2	-	no
10090.ENSMUSP00000067640	Tas2r129	-	no
10090.ENSMUSP00000067496	Siah2	-	no
10090.ENSMUSP00000067400	Pik3r4	-	no
10090.ENSMUSP00000067395	Gcc1	-	no
10090.ENSMUSP00000067305	Acvr2a	-	no
10090.ENSMUSP00000067085	Irs4	-	no
10090.ENSMUSP00000067082	Tas2r107	-	no
10090.ENSMUSP00000067066	Lif	up	no
10090.ENSMUSP00000067057	Adcyap1	-	no
10090.ENSMUSP00000066842	Mcm8	-	no
10090.ENSMUSP00000066841	Nlrp4a	-	no
10090.ENSMUSP00000066789	Ep300	-	no
10090.ENSMUSP00000066669	P2ry14	-	no
10090.ENSMUSP00000066613	Fbxw14	-	no
10090.ENSMUSP00000066427	Cldn17	-	no
10090.ENSMUSP00000066403	Lonrf1	-	no
10090.ENSMUSP00000066359	Fam49b	-	no
10090.ENSMUSP00000066256	Ercc6	-	no
10090.ENSMUSP00000066238	Rap1b	-	no
10090.ENSMUSP00000066222	Cib4	-	no
10090.ENSMUSP00000066068	Actn4	-	no
10090.ENSMUSP00000066050	Epm2a	-	no
10090.ENSMUSP00000065949	Cenpj	-	no
10090.ENSMUSP00000065798	Smad5	-	no
10090.ENSMUSP00000065719	Plpp3	-	no
10090.ENSMUSP00000065679	Ppp1r3b	-	no
10090.ENSMUSP00000065624	Dcaf17	-	no
10090.ENSMUSP00000065393	Prss2	-	no
10090.ENSMUSP00000065089	Aldh7a1	-	no
10090.ENSMUSP00000064878	Wnt5a	-	no
10090.ENSMUSP00000064865	Hbb-bh1	-	no
10090.ENSMUSP00000064761	Adm2	-	no
10090.ENSMUSP00000064694	Pld1	-	no
10090.ENSMUSP00000064680	Junb	-	no
10090.ENSMUSP00000064551	Lifr	-	no

10090.ENSMUSP00000064498	Try5	-	no
10090.ENSMUSP00000064333	Wnt11	-	no
10090.ENSMUSP00000064276	G6pc3	-	no
10090.ENSMUSP00000064205	Il6st	-	no
10090.ENSMUSP00000064132	Tescl	-	no
10090.ENSMUSP00000063986	Cx3cr1	-	no
10090.ENSMUSP00000063954	Tas2r7	-	no
10090.ENSMUSP00000063910	Gpr20	-	no
10090.ENSMUSP00000063804	Rab39a	-	no
10090.ENSMUSP00000063795	Irs1	-	no
10090.ENSMUSP00000063784	Adcyap1r1	-	no
10090.ENSMUSP00000063743	Tas2r3	-	no
10090.ENSMUSP00000063734	Ezr	-	no
10090.ENSMUSP00000063644	Prkn	-	no
10090.ENSMUSP00000063562	Pgr	-	no
10090.ENSMUSP00000063520	Cysltr1	-	no
10090.ENSMUSP00000063293	Syt1	-	no
10090.ENSMUSP00000063258	Slc8a3	-	no
10090.ENSMUSP00000063066	Plxna1	-	no
10090.ENSMUSP00000063054	Rab33b	-	no
10090.ENSMUSP00000062920	Tpm3	-	no
10090.ENSMUSP00000062919	Tas2r39	-	no
10090.ENSMUSP00000062864	Pik3cg	-	no
10090.ENSMUSP00000062782	Vav2	-	no
10090.ENSMUSP00000062637	C2cd3	-	no
10090.ENSMUSP00000062607	Pla2g4f	-	no
10090.ENSMUSP00000062601	Cldn34c4	-	no
10090.ENSMUSP00000062467	Keap1	-	no
10090.ENSMUSP00000062392	Prkca	-	no
10090.ENSMUSP00000062256	Adrb2	-	no
10090.ENSMUSP00000062045	Cldn14	-	no
10090.ENSMUSP00000062037	Acer1	-	no
10090.ENSMUSP00000061991	Phka1	-	no
10090.ENSMUSP00000061923	Mcm2	-	no
10090.ENSMUSP00000061754	F2r	-	no
10090.ENSMUSP00000061604	Crbn	-	no
10090.ENSMUSP00000061560	Glp2r	-	no
10090.ENSMUSP00000061410	Gpr18	-	no
10090.ENSMUSP00000061402	Ppp1r3d	-	no

10090.ENSMUSP00000061317	Vps53	-	no
10090.ENSMUSP00000061305	Fbxl7	-	no
10090.ENSMUSP00000061296	P2ry10	-	no
10090.ENSMUSP00000061243	Gpr4	-	no
10090.ENSMUSP00000061185	Crh	-	no
10090.ENSMUSP00000061153	Ghsr	-	no
10090.ENSMUSP00000061126	Cyp4a10	-	no
10090.ENSMUSP00000060844	Irs3	-	no
10090.ENSMUSP00000060828	Syk	-	no
10090.ENSMUSP00000060617	Prok1	-	no
10090.ENSMUSP00000060584	Cyp2c70	-	no
10090.ENSMUSP00000060433	Shb	-	no
10090.ENSMUSP00000060421	Cdc37l1	-	no
10090.ENSMUSP00000060205	Efcab9	-	no
10090.ENSMUSP00000060137	Fbxl22	-	no
10090.ENSMUSP00000060073	Jak3	-	no
10090.ENSMUSP00000060054	Chd4	-	no
10090.ENSMUSP00000060027	Guca1a	-	no
10090.ENSMUSP00000059977	Ptgs1	-	no
10090.ENSMUSP00000059637	Nlrc4	-	no
10090.ENSMUSP00000059501	Vamp8	-	no
10090.ENSMUSP00000059276	Cul4b	-	no
10090.ENSMUSP00000059270	Gp1bb	-	no
10090.ENSMUSP00000059211	Ercc8	-	no
10090.ENSMUSP00000059192	Mcm3	-	no
10090.ENSMUSP00000059129	Socs3	-	no
10090.ENSMUSP00000059034	Prokr1	-	no
10090.ENSMUSP00000059033	Hip1	down	no
10090.ENSMUSP00000058990	Cog7	-	no
10090.ENSMUSP00000058846	Aph1a	-	no
10090.ENSMUSP00000058757	Ptpn11	-	no
10090.ENSMUSP00000058723	Tmed3	-	no
10090.ENSMUSP00000058691	Mc2r	-	no
10090.ENSMUSP00000058683	Ugt1a7c	-	no
10090.ENSMUSP00000058629	Fzd1	-	no
10090.ENSMUSP00000058611	Naip5	-	no
10090.ENSMUSP00000058320	Pacsin2	-	no
10090.ENSMUSP00000058233	Fbxo10	-	no
10090.ENSMUSP00000058230	Hcrtr2	-	no

10090.ENSMUSP00000058175	Fbxw15	-	no
10090.ENSMUSP00000058168	Dcaf7	-	no
10090.ENSMUSP00000058021	Timeless	-	no
10090.ENSMUSP00000058006	Tas2r105	-	no
10090.ENSMUSP00000057956	Erbin	-	no
10090.ENSMUSP00000057896	Kif9	-	no
10090.ENSMUSP00000057578	Hcrt	-	no
10090.ENSMUSP00000057573	Fbxo31	-	no
10090.ENSMUSP00000057563	Gp1ba	-	no
10090.ENSMUSP00000057510	Gpr68	up	no
10090.ENSMUSP00000057462	Vti1b	-	no
10090.ENSMUSP00000057392	Cetn1	-	no
10090.ENSMUSP00000057182	Mtm1	-	no
10090.ENSMUSP00000056977	Ajuba	-	no
10090.ENSMUSP00000056836	Cfd	-	no
10090.ENSMUSP00000056784	Acvr1	-	no
10090.ENSMUSP00000056752	Fgf4	-	no
10090.ENSMUSP00000056668	Igf1	-	no
10090.ENSMUSP00000056659	Prokr2	-	no
10090.ENSMUSP00000056604	Hist1h2ba	-	no
10090.ENSMUSP00000056581	Tas2r41	-	no
10090.ENSMUSP00000056358	Fbxw21	-	no
10090.ENSMUSP00000056152	Otc	-	no
10090.ENSMUSP00000055919	Csnk2a2	-	no
10090.ENSMUSP00000055869	P2ry4	-	no
10090.ENSMUSP00000055803	Glb1	-	no
10090.ENSMUSP00000055746	Qrfp	-	no
10090.ENSMUSP00000055697	P2ry6	-	no
10090.ENSMUSP00000055579	Chrm3	-	no
10090.ENSMUSP00000055564	Ffar1	-	no
10090.ENSMUSP00000055137	Oxgr1	-	no
10090.ENSMUSP00000054990	Nhlrc1	-	no
10090.ENSMUSP00000054914	Il1rl1	up	no
10090.ENSMUSP00000054837	Gli2	-	no
10090.ENSMUSP00000054834	Tmed2	-	no
10090.ENSMUSP00000054776	Mc4r	-	no
10090.ENSMUSP00000054499	Fn1	-	no
10090.ENSMUSP00000054426	F2rl3	-	no
10090.ENSMUSP00000054270	Jun	-	no

10090.ENSMUSP00000054219	Cldn2	-	no
10090.ENSMUSP00000053986	Lpar4	-	no
10090.ENSMUSP00000053962	Lcn2	up	no
10090.ENSMUSP00000053908	Ston2	-	no
10090.ENSMUSP00000053899	Mafg	up	no
10090.ENSMUSP00000053897	Erbb2	-	no
10090.ENSMUSP00000053891	Itga2	-	no
10090.ENSMUSP00000053786	Fbxw13	-	no
10090.ENSMUSP00000053703	Adra1a	-	no
10090.ENSMUSP00000053700	Tas2r16	-	no
10090.ENSMUSP00000053551	Fzd9	-	no
10090.ENSMUSP00000053543	Meaf6	-	no
10090.ENSMUSP00000053489	Cxcr4	-	no
10090.ENSMUSP00000053420	Cldn4	-	no
10090.ENSMUSP00000053080	Spata21	-	no
10090.ENSMUSP00000053046	Subh2bv	-	no
10090.ENSMUSP00000052777	Pik3ap1	-	no
10090.ENSMUSP00000052755	Dcaf5	-	no
10090.ENSMUSP00000052716	Fbxl13	-	no
10090.ENSMUSP00000052600	Ffar2	-	no
10090.ENSMUSP00000052592	Gsto2	-	no
10090.ENSMUSP00000052584	Lrrk2	-	no
10090.ENSMUSP00000052522	Pik3r6	-	no
10090.ENSMUSP00000052285	Catsperg2	-	no
10090.ENSMUSP00000052262	Vamp7	-	no
10090.ENSMUSP00000052226	Gk2	-	no
10090.ENSMUSP00000052103	Akt2	-	no
10090.ENSMUSP00000052089	Catsperb	-	no
10090.ENSMUSP00000051895	Gp5	-	no
10090.ENSMUSP00000051887	Cldn8	-	no
10090.ENSMUSP00000051830	Dnmt3b	-	no
10090.ENSMUSP00000051694	Catsper4	-	no
10090.ENSMUSP00000051619	Mapk3	-	no
10090.ENSMUSP00000051544	Vamp4	-	no
10090.ENSMUSP00000051487	Hpcal4	-	no
10090.ENSMUSP00000051432	H2afx	-	no
10090.ENSMUSP00000051368	Ltb4r	-	no
10090.ENSMUSP00000051353	P2ry12	-	no
10090.ENSMUSP00000051335	Zfpm2	up	no

10090.ENSMUSP00000051331	Axin2	-	no
10090.ENSMUSP00000051223	Ywhag	-	no
10090.ENSMUSP00000051215	Hk3	-	no
10090.ENSMUSP00000051132	Oxtr	-	no
10090.ENSMUSP00000051092	Picalm	-	no
10090.ENSMUSP00000050897	S1pr1	-	no
10090.ENSMUSP00000050788	Phkb	-	no
10090.ENSMUSP00000050478	Cyp4f14	-	no
10090.ENSMUSP00000050464	Cyp2j9	-	no
10090.ENSMUSP00000050412	S1pr4	-	no
10090.ENSMUSP00000050119	Ackr2	-	no
10090.ENSMUSP00000050076	Adrm1	-	no
10090.ENSMUSP00000049973	Haus3	-	no
10090.ENSMUSP00000049963	Hrh3	-	no
10090.ENSMUSP00000049920	Nphp4	-	no
10090.ENSMUSP00000049852	Fzd4	-	no
10090.ENSMUSP00000049729	Masp2	-	no
10090.ENSMUSP00000049725	Cldn23	-	no
10090.ENSMUSP00000049683	Ch25h	-	no
10090.ENSMUSP00000049676	NoMapping	-	no
10090.ENSMUSP00000049592	Gpr150	-	no
10090.ENSMUSP00000049528	Rbbp6	-	no
10090.ENSMUSP00000049527	Taar1	-	no
10090.ENSMUSP00000049457	Cacna2d1	-	no
10090.ENSMUSP00000049394	Cbr1	-	no
10090.ENSMUSP00000049391	Aox3	-	no
10090.ENSMUSP00000049228	Cftr	-	no
10090.ENSMUSP00000049204	Prickle1	-	no
10090.ENSMUSP00000049175	Gna15	-	no
10090.ENSMUSP00000049161	Ctf1	-	no
10090.ENSMUSP00000049095	Ins1	-	no
10090.ENSMUSP00000049079	Mtmr3	-	no
10090.ENSMUSP00000049063	Trpc5	-	no
10090.ENSMUSP00000049054	Ppp1r3a	-	no
10090.ENSMUSP00000049026	Fnip1	-	no
10090.ENSMUSP00000049007	Ctnna1	-	no
10090.ENSMUSP00000048997	Golim4	-	no
10090.ENSMUSP00000048969	Spsb1	up	no
10090.ENSMUSP00000048929	Aox4	-	no

10090.ENSMUSP00000048857	NoMapping	-	no
10090.ENSMUSP00000048765	Mbl1	-	no
10090.ENSMUSP00000048736	Ptger4	-	no
10090.ENSMUSP00000048704	Serpinf2	-	no
10090.ENSMUSP00000048667	F13a1	-	no
10090.ENSMUSP00000048603	Cog6	-	no
10090.ENSMUSP00000048562	Fbxl16	-	no
10090.ENSMUSP00000048376	Malt1	-	no
10090.ENSMUSP00000048363	Psen1	-	no
10090.ENSMUSP00000048358	Ltb4r2	-	no
10090.ENSMUSP00000048320	Cc2d2a	-	no
10090.ENSMUSP00000048319	Orc3	-	no
10090.ENSMUSP00000048284	Cyp2c54	-	no
10090.ENSMUSP00000048244	Anapc10	-	no
10090.ENSMUSP00000048062	Shank3	-	no
10090.ENSMUSP00000048057	Inppl1	-	no
10090.ENSMUSP00000048041	Cd59a	-	no
10090.ENSMUSP00000048036	Tubg1	-	no
10090.ENSMUSP00000047968	S100b	-	no
10090.ENSMUSP00000047950	Cdc16	-	no
10090.ENSMUSP00000047774	Htr2a	-	no
10090.ENSMUSP00000047712	Cbr3	-	no
10090.ENSMUSP00000047627	Trim69	-	no
10090.ENSMUSP00000047586	Gngt2	-	no
10090.ENSMUSP00000047529	Myf6	-	no
10090.ENSMUSP00000047518	Ramp3	-	no
10090.ENSMUSP00000047467	Usp28	-	no
10090.ENSMUSP00000047403	Mylip	-	no
10090.ENSMUSP00000047376	Gls2	-	no
10090.ENSMUSP00000047358	Mc3r	-	no
10090.ENSMUSP00000047261	Mmp1b	up	no
10090.ENSMUSP00000047012	Fbxw8	-	no
10090.ENSMUSP00000046920	Uts2r	-	no
10090.ENSMUSP00000046837	Ptpa	-	no
10090.ENSMUSP00000046557	Gng12	-	no
10090.ENSMUSP00000046503	Nlrp4c	-	no
10090.ENSMUSP00000046324	Gstt2	-	no
10090.ENSMUSP00000046255	Rbbp8	-	no
10090.ENSMUSP00000045901	Tubg2	-	no

10090.ENSMUSP00000045838	Dusp10	up	no
10090.ENSMUSP00000045792	Fbxl5	-	no
10090.ENSMUSP00000045770	Tlr4	-	no
10090.ENSMUSP00000045710	Fgf1	-	no
10090.ENSMUSP00000045675	Pkd2l1	-	no
10090.ENSMUSP00000045547	Cdon	-	no
10090.ENSMUSP00000045487	4930544G11Rik	-	no
10090.ENSMUSP00000045460	Psme4	-	no
10090.ENSMUSP00000045430	Catsper1	-	no
10090.ENSMUSP00000045409	Ogt	-	no
10090.ENSMUSP00000045402	Ppp1r3f	-	no
10090.ENSMUSP00000045362	Cyp2c37	-	no
10090.ENSMUSP00000045344	Clspn	down	no
10090.ENSMUSP00000045239	Golgb1	-	no
10090.ENSMUSP00000045142	Islr	-	no
10090.ENSMUSP00000045065	Gm9774	-	no
10090.ENSMUSP00000045016	Cog3	-	no
10090.ENSMUSP00000044903	Thbs1	down	no
10090.ENSMUSP00000044877	Bet1	-	no
10090.ENSMUSP00000044866	Sos2	-	no
10090.ENSMUSP00000044831	Atrip	-	no
10090.ENSMUSP00000044808	Efcab11	-	no
10090.ENSMUSP00000044797	Cog5	down	no
10090.ENSMUSP00000044769	Atg5	-	no
10090.ENSMUSP00000044730	P2yr13	-	no
10090.ENSMUSP00000044722	Cyp2c38	-	no
10090.ENSMUSP00000044682	Psenen	-	no
10090.ENSMUSP00000044660	Cacna2d4	-	no
10090.ENSMUSP00000044654	Tex264	-	no
10090.ENSMUSP00000044466	Inpp4b	-	no
10090.ENSMUSP00000044276	Sh3pxd2b	-	no
10090.ENSMUSP00000044227	Itga9	-	no
10090.ENSMUSP00000044123	Siah1a	-	no
10090.ENSMUSP00000044089	Tas2r4	-	no
10090.ENSMUSP00000044049	Tubgcp4	-	no
10090.ENSMUSP00000043957	Lama1	-	no
10090.ENSMUSP00000043956	Iapp	-	no
10090.ENSMUSP00000043936	Htr2c	-	no
10090.ENSMUSP00000043881	Nlrp4b	-	no

10090.ENSMUSP00000043851	Mtmr7	-	no
10090.ENSMUSP00000043849	Tgfb2	-	no
10090.ENSMUSP00000043790	Mks1	-	no
10090.ENSMUSP00000043467	Dhrs11	-	no
10090.ENSMUSP00000043437	Ric1	-	no
10090.ENSMUSP00000043340	Epn1	-	no
10090.ENSMUSP00000043190	Gna11	-	no
10090.ENSMUSP00000043146	Shc4	-	no
10090.ENSMUSP00000043108	Brip1	-	no
10090.ENSMUSP00000043092	Blvrb	up	no
10090.ENSMUSP00000042987	Rps6ka5	-	no
10090.ENSMUSP00000042959	Fcho2	-	no
10090.ENSMUSP00000042927	Dner	-	no
10090.ENSMUSP00000042867	Wnt8b	-	no
10090.ENSMUSP00000042860	Gnpnat1	-	no
10090.ENSMUSP00000042705	Gng10	-	no
10090.ENSMUSP00000042702	Rpgrip1l	-	no
10090.ENSMUSP00000042676	Rmi2	-	no
10090.ENSMUSP00000042642	Il22ra2	-	no
10090.ENSMUSP00000042632	Chrm1	-	no
10090.ENSMUSP00000042590	Psma8	-	no
10090.ENSMUSP00000042364	Myl12b	-	no
10090.ENSMUSP00000042342	Tubb4b	-	no
10090.ENSMUSP00000042327	Lpar6	-	no
10090.ENSMUSP00000042271	Spag9	-	no
10090.ENSMUSP00000042232	Hebp1	-	no
10090.ENSMUSP00000042219	Fbxl4	-	no
10090.ENSMUSP00000042211	Sema7a	up	no
10090.ENSMUSP00000042181	Cldn11	-	no
10090.ENSMUSP00000042150	Rras	-	no
10090.ENSMUSP00000042095	Serpina3k	-	no
10090.ENSMUSP00000041925	Cldn5	-	no
10090.ENSMUSP00000041908	Nlrp4f	-	no
10090.ENSMUSP00000041902	Cbl	-	no
10090.ENSMUSP00000041825	Fzd7	down	no
10090.ENSMUSP00000041774	Gata6	-	no
10090.ENSMUSP00000041766	Naip6	-	no
10090.ENSMUSP00000041700	Fbxl18	-	no
10090.ENSMUSP00000041676	Cldn22	-	no

10090.ENSMUSP00000041675	Kyat3	-	no
10090.ENSMUSP00000041644	Brk1	-	no
10090.ENSMUSP00000041636	Calm4	-	no
10090.ENSMUSP00000041627	Wwp1	-	no
10090.ENSMUSP00000041442	Hsd3b5	-	no
10090.ENSMUSP00000041427	Lefty1	-	no
10090.ENSMUSP00000041370	Gatad2b	down	no
10090.ENSMUSP00000041282	Map2k4	-	no
10090.ENSMUSP00000041260	Aldh1b1	-	no
10090.ENSMUSP00000041190	Klhl13	down	no
10090.ENSMUSP00000041184	Psmf1	-	no
10090.ENSMUSP00000041173	Nfkbiz	up	no
10090.ENSMUSP00000041157	Spon1	-	no
10090.ENSMUSP00000041135	Rasgrp2	-	no
10090.ENSMUSP00000041061	Hrh4	-	no
10090.ENSMUSP00000041047	Pth2	-	no
10090.ENSMUSP00000041035	Rmi1	-	no
10090.ENSMUSP00000040956	Sccpdh	-	no
10090.ENSMUSP00000040847	Adrb1	-	no
10090.ENSMUSP00000040802	Haus8	-	no
10090.ENSMUSP00000040741	Sem1	-	no
10090.ENSMUSP00000040715	Cysltr2	-	no
10090.ENSMUSP00000040580	Galm	-	no
10090.ENSMUSP00000040516	Kiss1r	-	no
10090.ENSMUSP00000040477	Fshr	-	no
10090.ENSMUSP00000040321	Ppp2r2d	-	no
10090.ENSMUSP00000040315	Mapk6	-	no
10090.ENSMUSP00000040307	Map3k7	-	no
10090.ENSMUSP00000040244	Akr1b8	up	no
10090.ENSMUSP00000040229	Dtx4	up	no
10090.ENSMUSP00000040048	Acer2	-	no
10090.ENSMUSP00000040033	Npffr2	-	no
10090.ENSMUSP00000039955	Cblc	-	no
10090.ENSMUSP00000039943	Usp38	-	no
10090.ENSMUSP00000039844	Actr1a	-	no
10090.ENSMUSP00000039776	Pold1	-	no
10090.ENSMUSP00000039709	Pcm1	-	no
10090.ENSMUSP00000039691	Drd5	-	no
10090.ENSMUSP00000039684	Gm5771	-	no

10090.ENSMUSP00000039670	Unkl	-	no
10090.ENSMUSP00000039660	Fzd8	-	no
10090.ENSMUSP00000039621	Rfc3	-	no
10090.ENSMUSP00000039472	Fgb	-	no
10090.ENSMUSP00000039376	Exo1	-	no
10090.ENSMUSP00000039109	Ppp1ca	-	no
10090.ENSMUSP00000039047	Atg14	-	no
10090.ENSMUSP00000039041	Flt3	-	no
10090.ENSMUSP00000038931	Gstp2	-	no
10090.ENSMUSP00000038925	Elane	-	no
10090.ENSMUSP00000038881	Ccp110	-	no
10090.ENSMUSP00000038838	Lyn	-	no
10090.ENSMUSP00000038833	Ripk2	-	no
10090.ENSMUSP00000038674	Cep135	-	no
10090.ENSMUSP00000038638	Fbxl8	-	no
10090.ENSMUSP00000038612	Kyat1	-	no
10090.ENSMUSP00000038527	Cib2	-	no
10090.ENSMUSP00000038514	Irs2	-	no
10090.ENSMUSP00000038502	Cplx1	-	no
10090.ENSMUSP00000038489	Atg12	-	no
10090.ENSMUSP00000038483	Ptger2	-	no
10090.ENSMUSP00000038409	Plcb4	-	no
10090.ENSMUSP00000038368	Copg2	-	no
10090.ENSMUSP00000038170	Hrh2	-	no
10090.ENSMUSP00000037978	Trim36	-	no
10090.ENSMUSP00000037858	Fermt3	-	no
10090.ENSMUSP00000037788	Cep72	down	no
10090.ENSMUSP00000037735	Golga1	-	no
10090.ENSMUSP00000037694	Fgf2	-	no
10090.ENSMUSP00000037596	Cep78	-	no
10090.ENSMUSP00000037586	Gpr176	-	no
10090.ENSMUSP00000037583	Tmed10	-	no
10090.ENSMUSP00000037574	Trpc4ap	-	no
10090.ENSMUSP00000037487	Cyp7b1	up	no
10090.ENSMUSP00000037416	Cacna1b	-	no
10090.ENSMUSP00000037385	Lepr	-	no
10090.ENSMUSP00000037377	Fbxo2	-	no
10090.ENSMUSP00000037258	Ugt1a2	-	no
10090.ENSMUSP00000037255	Grm1	-	no

10090.ENSMUSP00000037224	Rnf146	-	no
10090.ENSMUSP00000037222	Catsper2	-	no
10090.ENSMUSP00000037180	Prex1	-	no
10090.ENSMUSP00000037126	Bub1b	-	no
10090.ENSMUSP00000037018	Fgg	-	no
10090.ENSMUSP00000036907	H2afz	-	no
10090.ENSMUSP00000036765	P2ry2	-	no
10090.ENSMUSP00000036749	Ldlrap1	-	no
10090.ENSMUSP00000036705	Gak	-	no
10090.ENSMUSP00000036656	Sgpp2	-	no
10090.ENSMUSP00000036585	Rxrb	-	no
10090.ENSMUSP00000036580	Wnt4	-	no
10090.ENSMUSP00000036505	Fbxw4	-	no
10090.ENSMUSP00000036384	Rac2	-	no
10090.ENSMUSP00000036326	Crlf2	-	no
10090.ENSMUSP00000036320	Trhr	-	no
10090.ENSMUSP00000036288	Cct2	-	no
10090.ENSMUSP00000036285	Smad6	down	no
10090.ENSMUSP00000036270	Vav3	-	no
10090.ENSMUSP00000036245	Hsd3b7	-	no
10090.ENSMUSP00000036177	Rad9b	-	no
10090.ENSMUSP00000036162	Pi4ka	-	no
10090.ENSMUSP00000036159	Ptgdr2	-	no
10090.ENSMUSP00000036141	Amdhd2	-	no
10090.ENSMUSP00000036044	Apob	-	no
10090.ENSMUSP00000035900	Bmpr1a	-	no
10090.ENSMUSP00000035826	Haus1	-	no
10090.ENSMUSP00000035658	Qsox1	-	no
10090.ENSMUSP00000035579	Lgals3bp	-	no
10090.ENSMUSP00000035506	Fbxo21	-	no
10090.ENSMUSP00000035400	Nckap1l	-	no
10090.ENSMUSP00000035328	Uba6	-	no
10090.ENSMUSP00000035272	Tln2	-	no
10090.ENSMUSP00000035250	Alox12b	-	no
10090.ENSMUSP00000035216	Uba7	-	no
10090.ENSMUSP00000035166	Uba5	-	no
10090.ENSMUSP00000035164	Topbp1	-	no
10090.ENSMUSP00000035158	Tf	-	no
10090.ENSMUSP00000035120	Cck	-	no

10090.ENSMUSP00000035115	Vipr1	-	no
10090.ENSMUSP00000035099	Gorasp1	-	no
10090.ENSMUSP00000035092	Myd88	-	no
10090.ENSMUSP00000035065	Ptgs2	up	no
10090.ENSMUSP00000035048	Cldn18	-	no
10090.ENSMUSP00000035045	Mras	-	no
10090.ENSMUSP00000035033	Copb2	-	no
10090.ENSMUSP00000035029	Rbp2	-	no
10090.ENSMUSP00000034973	Smad3	-	no
10090.ENSMUSP00000034964	Tipin	-	no
10090.ENSMUSP00000034934	Aph1b	-	no
10090.ENSMUSP00000034915	Ctsh	-	no
10090.ENSMUSP00000034903	Gsta4	-	no
10090.ENSMUSP00000034902	Gsta2	-	no
10090.ENSMUSP00000034874	Cyp11a1	-	no
10090.ENSMUSP00000034859	Fbxo22	-	no
10090.ENSMUSP00000034856	Mpi	-	no
10090.ENSMUSP00000034777	Calml4	-	no
10090.ENSMUSP00000034774	Itga11	-	no
10090.ENSMUSP00000034754	Bnip2	-	no
10090.ENSMUSP00000034740	Nedd4	-	no
10090.ENSMUSP00000034723	Aldh1a2	-	no
10090.ENSMUSP00000034713	Ldlr	-	no
10090.ENSMUSP00000034625	Chek1	-	no
10090.ENSMUSP00000034607	Arcn1	-	no
10090.ENSMUSP00000034602	Cd3d	-	no
10090.ENSMUSP00000034594	Il10ra	-	no
10090.ENSMUSP00000034567	Dlat	-	no
10090.ENSMUSP00000034560	Ppp2r1b	-	no
10090.ENSMUSP00000034534	Ets1	up	no
10090.ENSMUSP00000034497	Mmp3	up	no
10090.ENSMUSP00000034492	Mmp1a	-	no
10090.ENSMUSP00000034460	Cog2	-	no
10090.ENSMUSP00000034443	Cdh15	-	no
10090.ENSMUSP00000034415	Taf1d	-	no
10090.ENSMUSP00000034408	Gpr83	-	no
10090.ENSMUSP00000034405	Mre11	-	no
10090.ENSMUSP00000034398	Cep57	-	no
10090.ENSMUSP00000034396	Mtmr2	-	no

10090.ENSMUSP00000034391	Cog8	-	no
10090.ENSMUSP00000034308	Bco1	-	no
10090.ENSMUSP00000034203	Cog4	-	no
10090.ENSMUSP00000034198	Gnao1	-	no
10090.ENSMUSP00000034187	Mmp2	-	no
10090.ENSMUSP00000034150	Gab1	-	no
10090.ENSMUSP00000034093	Eif2ak3	-	no
10090.ENSMUSP00000034085	Brd7	-	no
10090.ENSMUSP00000034029	Ednra	-	no
10090.ENSMUSP00000034014	Fgf20	-	no
10090.ENSMUSP00000034000	Asah1	-	no
10090.ENSMUSP00000033992	Gsr	up	no
10090.ENSMUSP00000033990	Wrn	-	no
10090.ENSMUSP00000033952	Sfrp1	-	no
10090.ENSMUSP00000033939	Ikbkb	-	no
10090.ENSMUSP00000033936	Dkk4	-	no
10090.ENSMUSP00000033929	Tnks	-	no
10090.ENSMUSP00000033919	Vegfc	-	no
10090.ENSMUSP00000033900	Rab20	up	no
10090.ENSMUSP00000033892	Tnfsf13b	-	no
10090.ENSMUSP00000033846	Angpt2	-	no
10090.ENSMUSP00000033828	Gas6	-	no
10090.ENSMUSP00000033751	Vegfd	-	no
10090.ENSMUSP00000033737	Haus7	-	no
10090.ENSMUSP00000033730	Grpr	-	no
10090.ENSMUSP00000033720	Rbbp7	-	no
10090.ENSMUSP00000033671	Rps6ka3	-	no
10090.ENSMUSP00000033664	Il2rg	-	no
10090.ENSMUSP00000033662	Pdha1	-	no
10090.ENSMUSP00000033652	Phka2	-	no
10090.ENSMUSP00000033646	Il13ra2	-	no
10090.ENSMUSP00000033621	Gla	-	no
10090.ENSMUSP00000033617	Btk	-	no
10090.ENSMUSP00000033610	Nox1	-	no
10090.ENSMUSP00000033581	Fgf16	-	no
10090.ENSMUSP00000033567	Awat2	-	no
10090.ENSMUSP00000033553	Heph	-	no
10090.ENSMUSP00000033544	Brcc3	-	no
10090.ENSMUSP00000033539	F8	-	no

10090.ENSMUSP00000033502	Gata1	-	no
10090.ENSMUSP00000033473	Fgf13	-	no
10090.ENSMUSP00000033466	Cd40lg	-	no
10090.ENSMUSP00000033418	Il13ra1	-	no
10090.ENSMUSP00000033389	Fgf15	-	no
10090.ENSMUSP00000033383	Usp11	-	no
10090.ENSMUSP00000033326	Wee1	-	no
10090.ENSMUSP00000033189	Cckbr	-	no
10090.ENSMUSP00000033182	Ilk	-	no
10090.ENSMUSP00000033158	Ubfd1	-	no
10090.ENSMUSP00000033152	Chp2	-	no
10090.ENSMUSP00000033099	Fgf21	-	no
10090.ENSMUSP00000033086	Phkg2	-	no
10090.ENSMUSP00000033081	Fbxl19	-	no
10090.ENSMUSP00000033075	Stx4	-	no
10090.ENSMUSP00000033056	Pycard	-	no
10090.ENSMUSP00000033054	Adm	-	no
10090.ENSMUSP00000033020	Acer3	-	no
10090.ENSMUSP00000033012	Copb1	-	no
10090.ENSMUSP00000033004	Il4r	-	no
10090.ENSMUSP00000033000	Il21r	-	no
10090.ENSMUSP00000032997	Lat	-	no
10090.ENSMUSP00000032992	Eif3c	-	no
10090.ENSMUSP00000032968	Cd19	-	no
10090.ENSMUSP00000032946	Rab6a	-	no
10090.ENSMUSP00000032920	Cdipt	-	no
10090.ENSMUSP00000032910	Mylpf	-	no
10090.ENSMUSP00000032907	Calca	-	no
10090.ENSMUSP00000032879	Rab30	-	no
10090.ENSMUSP00000032874	Sh3gl3	-	no
10090.ENSMUSP00000032818	Fbxo17	-	no
10090.ENSMUSP00000032815	Nfkbib	up	no
10090.ENSMUSP00000032800	Tyrobp	-	no
10090.ENSMUSP00000032779	Ctsc	-	no
10090.ENSMUSP00000032629	Cyfip1	-	no
10090.ENSMUSP00000032627	Tubgcp5	-	no
10090.ENSMUSP00000032489	Ltbr	-	no
10090.ENSMUSP00000032477	Necap1	-	no
10090.ENSMUSP00000032457	Atg7	-	no

10090.ENSMUSP00000032399	Kras	-	no
10090.ENSMUSP00000032371	Gys2	-	no
10090.ENSMUSP00000032356	Plcz1	-	no
10090.ENSMUSP00000032322	Lrp6	down	no
10090.ENSMUSP00000032317	Tas2r103	-	no
10090.ENSMUSP00000032315	Tas2r116	-	no
10090.ENSMUSP00000032262	Clec1b	-	no
10090.ENSMUSP00000032203	A2m	-	no
10090.ENSMUSP00000032180	Wnt7a	-	no
10090.ENSMUSP00000032152	Prok2	-	no
10090.ENSMUSP00000032133	Gp9	-	no
10090.ENSMUSP00000032122	Tacr1	-	no
10090.ENSMUSP00000032105	Lrig1	up	no
10090.ENSMUSP00000032094	Fbxl14	-	no
10090.ENSMUSP00000032078	Cct7	-	no
10090.ENSMUSP00000032066	Tgfa	-	no
10090.ENSMUSP00000031982	Hpgds	-	no
10090.ENSMUSP00000031913	Try4	-	no
10090.ENSMUSP00000031910	Prss1	-	no
10090.ENSMUSP00000031897	Gstk1	-	no
10090.ENSMUSP00000031817	Herc6	-	no
10090.ENSMUSP00000031810	Cep41	-	no
10090.ENSMUSP00000031726	Gnb2	-	no
10090.ENSMUSP00000031695	Wasl	-	no
10090.ENSMUSP00000031681	Wnt16	-	no
10090.ENSMUSP00000031673	Gngt1	-	no
10090.ENSMUSP00000031670	Gng11	-	no
10090.ENSMUSP00000031654	Pomp	-	no
10090.ENSMUSP00000031653	Flt1	up	no
10090.ENSMUSP00000031625	Arpc1a	-	no
10090.ENSMUSP00000031622	Ocm	-	no
10090.ENSMUSP00000031607	Dtx1	-	no
10090.ENSMUSP00000031583	Acacb	-	no
10090.ENSMUSP00000031565	Fscn1	-	no
10090.ENSMUSP00000031555	Lfng	down	no
10090.ENSMUSP00000031519	Cabp1	-	no
10090.ENSMUSP00000031495	Pla2g1b	-	no
10090.ENSMUSP00000031422	Anapc7	-	no
10090.ENSMUSP00000031411	Aldh2	-	no

10090.ENSMUSP00000031402	NoMapping	-	no
10090.ENSMUSP00000031377	Scarb2	-	no
10090.ENSMUSP00000031355	Uso1	-	no
10090.ENSMUSP00000031324	Ereg	up	no
10090.ENSMUSP00000031314	Alb	-	no
10090.ENSMUSP00000031304	Tesc	-	no
10090.ENSMUSP00000031280	Fgf5	-	no
10090.ENSMUSP00000031221	Cdc7	-	no
10090.ENSMUSP00000031195	Ugt2a3	-	no
10090.ENSMUSP00000031186	Ugt2b35	-	no
10090.ENSMUSP00000031183	Ugt2b1	-	no
10090.ENSMUSP00000031181	Ugt2b34	-	no
10090.ENSMUSP00000031172	Gnrhr	-	no
10090.ENSMUSP00000031117	Gnpda2	-	no
10090.ENSMUSP00000031093	Cckar	-	no
10090.ENSMUSP00000031081	Pi4k2b	-	no
10090.ENSMUSP00000031072	Anapc4	-	no
10090.ENSMUSP00000031017	Fosl2	-	no
10090.ENSMUSP00000031003	Ppp2r2c	-	no
10090.ENSMUSP00000030948	Dvl1	-	no
10090.ENSMUSP00000030935	Fam213b	-	no
10090.ENSMUSP00000030922	Prkcz	-	no
10090.ENSMUSP00000030884	Mfn2	-	no
10090.ENSMUSP00000030872	Orc5	-	no
10090.ENSMUSP00000030858	Fbxo6	-	no
10090.ENSMUSP00000030834	Nos3	-	no
10090.ENSMUSP00000030814	Cdk5	-	no
10090.ENSMUSP00000030803	Uts2	-	no
10090.ENSMUSP00000030797	Vamp3	-	no
10090.ENSMUSP00000030769	Psmc2	-	no
10090.ENSMUSP00000030747	Casp9	-	no
10090.ENSMUSP00000030698	Stx12	-	no
10090.ENSMUSP00000030693	Fgr	-	no
10090.ENSMUSP00000030683	Hgf	-	no
10090.ENSMUSP00000030673	Csf3r	-	no
10090.ENSMUSP00000030581	Azin2	-	no
10090.ENSMUSP00000030572	Hpca	-	no
10090.ENSMUSP00000030562	Hcrtr1	-	no
10090.ENSMUSP00000030556	Ptpn12	-	no

10090.ENSMUSP00000030536	Pink1	-	no
10090.ENSMUSP00000030531	Pla2g2e	-	no
10090.ENSMUSP00000030530	Pla2g2c	-	no
10090.ENSMUSP00000030528	Pla2g2d	-	no
10090.ENSMUSP00000030526	Pla2g2f	-	no
10090.ENSMUSP00000030524	Pla2g5	-	no
10090.ENSMUSP00000030487	Cyp4a14	-	no
10090.ENSMUSP00000030417	Cdc42	-	no
10090.ENSMUSP00000030399	Rragc	-	no
10090.ENSMUSP00000030384	Edn2	-	no
10090.ENSMUSP00000030339	Tnfrsf8	up	no
10090.ENSMUSP00000030336	Tnfrsf1b	-	no
10090.ENSMUSP00000030332	Gpx7	-	no
10090.ENSMUSP00000030317	Pdpn	up	no
10090.ENSMUSP00000030305	Cyp2j13	-	no
10090.ENSMUSP00000030303	Cyp2j6	-	no
10090.ENSMUSP00000030299	Cyp2j5	-	no
10090.ENSMUSP00000030289	Usp1	-	no
10090.ENSMUSP00000030212	Sh3gl2	-	no
10090.ENSMUSP00000030190	Rgp1	-	no
10090.ENSMUSP00000030187	Tln1	-	no
10090.ENSMUSP00000030158	Dctn3	-	no
10090.ENSMUSP00000030145	Dcaf12	-	no
10090.ENSMUSP00000030051	Txn	-	no
10090.ENSMUSP00000030047	Tnfsf8	-	no
10090.ENSMUSP00000030044	Orm1	-	no
10090.ENSMUSP00000029991	Ppp3r2	-	no
10090.ENSMUSP00000029975	Cga	-	no
10090.ENSMUSP00000029948	Bmpr1b	-	no
10090.ENSMUSP00000029879	Nbn	-	no
10090.ENSMUSP00000029876	Calb1	-	no
10090.ENSMUSP00000029875	Pip4p2	-	no
10090.ENSMUSP00000029842	Bcl10	-	no
10090.ENSMUSP00000029822	Tacr3	-	no
10090.ENSMUSP00000029812	Nfkb1	up	no
10090.ENSMUSP00000029744	Itga10	-	no
10090.ENSMUSP00000029740	Rnf115	-	no
10090.ENSMUSP00000029712	Ntrk1	-	no
10090.ENSMUSP00000029711	Insrr	-	no

10090.ENSMUSP00000029674	Efna4	-	no
10090.ENSMUSP00000029673	Efna3	-	no
10090.ENSMUSP00000029670	Ptgfr	-	no
10090.ENSMUSP00000029665	Dkk2	-	no
10090.ENSMUSP00000029652	Pdgfc	-	no
10090.ENSMUSP00000029649	Ctso	-	no
10090.ENSMUSP00000029632	Lrat	-	no
10090.ENSMUSP00000029629	Pla2g12a	-	no
10090.ENSMUSP00000029625	Sfrp2	-	no
10090.ENSMUSP00000029624	Mcub	-	no
10090.ENSMUSP00000029623	Tlr2	-	no
10090.ENSMUSP00000029574	Vcam1	up	no
10090.ENSMUSP00000029566	Efna1	-	no
10090.ENSMUSP00000029559	Il6ra	-	no
10090.ENSMUSP00000029489	Gstm4	-	no
10090.ENSMUSP00000029463	Hsd3b6	-	no
10090.ENSMUSP00000029445	Nras	-	no
10090.ENSMUSP00000029429	Wnt2b	-	no
10090.ENSMUSP00000029371	Smad9	down	no
10090.ENSMUSP00000029368	Ccna1	-	no
10090.ENSMUSP00000029345	Il12a	-	no
10090.ENSMUSP00000029331	P2ry1	-	no
10090.ENSMUSP00000029311	Trpc4	-	no
10090.ENSMUSP00000029297	Slc7a11	up	no
10090.ENSMUSP00000029270	Ccna2	-	no
10090.ENSMUSP00000029172	Ghrh	-	no
10090.ENSMUSP00000029131	Ggt7	-	no
10090.ENSMUSP00000029128	Map1lc3a	-	no
10090.ENSMUSP00000029126	Itch	-	no
10090.ENSMUSP00000029084	Ntsr1	-	no
10090.ENSMUSP00000029046	Fabp5	-	no
10090.ENSMUSP00000029030	Edn3	-	no
10090.ENSMUSP00000029018	Zbp1	-	no
10090.ENSMUSP00000028997	Aurka	-	no
10090.ENSMUSP00000028981	Mapre1	-	no
10090.ENSMUSP00000028969	Tpx2	-	no
10090.ENSMUSP00000028964	Rbck1	-	no
10090.ENSMUSP00000028955	Angpt4	-	no
10090.ENSMUSP00000028926	Napb	-	no

10090.ENSMUSP00000028881	Il1b	-	no
10090.ENSMUSP00000028836	Bmp2	-	no
10090.ENSMUSP00000028829	Spred1	-	no
10090.ENSMUSP00000028817	Pcna	-	no
10090.ENSMUSP00000028764	Oxt	-	no
10090.ENSMUSP00000028740	Ttbk2	-	no
10090.ENSMUSP00000028727	Snap25	-	no
10090.ENSMUSP00000028696	Ddb2	-	no
10090.ENSMUSP00000028681	F2	-	no
10090.ENSMUSP00000028635	Cops2	-	no
10090.ENSMUSP00000028624	Gatm	-	no
10090.ENSMUSP00000028533	Fshb	-	no
10090.ENSMUSP00000028522	Itga6	-	no
10090.ENSMUSP00000028517	Ola1	-	no
10090.ENSMUSP00000028499	Itgav	-	no
10090.ENSMUSP00000028426	Cers6	-	no
10090.ENSMUSP00000028386	Nckap1	-	no
10090.ENSMUSP00000028348	Itgb6	-	no
10090.ENSMUSP00000028342	Ssna1	-	no
10090.ENSMUSP00000028341	Anapc2	-	no
10090.ENSMUSP00000028311	Traf2	-	no
10090.ENSMUSP00000028288	Notch1	-	no
10090.ENSMUSP00000028239	Gsn	-	no
10090.ENSMUSP00000028234	Traf1	-	no
10090.ENSMUSP00000028225	Psmd5	-	no
10090.ENSMUSP00000028224	Gapvd1	-	no
10090.ENSMUSP00000028214	Sh3glb2	-	no
10090.ENSMUSP00000028162	Ptges2	-	no
10090.ENSMUSP00000028129	Slc2a8	-	no
10090.ENSMUSP00000028111	Il2ra	-	no
10090.ENSMUSP00000028106	Itga8	-	no
10090.ENSMUSP00000028098	Orc4	-	no
10090.ENSMUSP00000028005	Mgst3	-	no
10090.ENSMUSP00000028004	Aldh9a1	-	no
10090.ENSMUSP00000027986	Optn	-	no
10090.ENSMUSP00000027980	Mcm10	-	no
10090.ENSMUSP00000027973	Sephs1	-	no
10090.ENSMUSP00000027933	Dtl	down	no
10090.ENSMUSP00000027931	Nek2	-	no

10090.ENSMUSP00000027874	Sele	up	no
10090.ENSMUSP00000027860	Xcl1	-	no
10090.ENSMUSP00000027856	Dcaf6	-	no
10090.ENSMUSP00000027817	Spta1	-	no
10090.ENSMUSP00000027785	Sdccag8	-	no
10090.ENSMUSP00000027775	Efcab2	-	no
10090.ENSMUSP00000027760	Rgl1	down	no
10090.ENSMUSP00000027754	Ncf2	-	no
10090.ENSMUSP00000027753	Lamc2	-	no
10090.ENSMUSP00000027752	Lamc1	-	no
10090.ENSMUSP00000027748	Rgs16	up	no
10090.ENSMUSP00000027743	Stx6	up	no
10090.ENSMUSP00000027730	Myog	-	no
10090.ENSMUSP00000027690	Avpr1b	-	no
10090.ENSMUSP00000027650	Cd55	-	no
10090.ENSMUSP00000027601	Mcm6	-	no
10090.ENSMUSP00000027579	Actr3	-	no
10090.ENSMUSP00000027560	Htr4	-	no
10090.ENSMUSP00000027559	Tnfrsf11a	-	no
10090.ENSMUSP00000027532	Scly	-	no
10090.ENSMUSP00000027518	Spp2	-	no
10090.ENSMUSP00000027505	Ing5	-	no
10090.ENSMUSP00000027495	02-set	-	no
10090.ENSMUSP00000027431	Htr2b	-	no
10090.ENSMUSP00000027421	Trip12	-	no
10090.ENSMUSP00000027393	Bard1	-	no
10090.ENSMUSP00000027362	Plcd4	-	no
10090.ENSMUSP00000027356	Cyp27a1	-	no
10090.ENSMUSP00000027287	Inpp4a	-	no
10090.ENSMUSP00000027198	Orc2	-	no
10090.ENSMUSP00000027165	Cd28	-	no
10090.ENSMUSP00000027164	Ctla4	-	no
10090.ENSMUSP00000027151	Myl1	-	no
10090.ENSMUSP00000027144	Cps1	-	no
10090.ENSMUSP00000027137	Slc40a1	up	no
10090.ENSMUSP00000027083	Pth2r	-	no
10090.ENSMUSP00000027067	Gsta3	-	no
10090.ENSMUSP00000027015	Casp1	-	no
10090.ENSMUSP00000027012	Casp4	up	no

10090.ENSMUSP00000026999	Smad7	-	no
10090.ENSMUSP00000026978	Xiap	-	no
10090.ENSMUSP00000026866	Sclt1	-	no
10090.ENSMUSP00000026858	Plk4	-	no
10090.ENSMUSP00000026845	Il6	up	no
10090.ENSMUSP00000026817	Nmb	-	no
10090.ENSMUSP00000026795	Alox5	-	no
10090.ENSMUSP00000026704	Cct8	-	no
10090.ENSMUSP00000026617	Phkg1	-	no
10090.ENSMUSP00000026599	Apool	-	no
10090.ENSMUSP00000026572	Hras	-	no
10090.ENSMUSP00000026557	Bet1l	-	no
10090.ENSMUSP00000026552	Cyp2e1	-	no
10090.ENSMUSP00000026547	Tubgcp2	-	no
10090.ENSMUSP00000026479	Dctn2	-	no
10090.ENSMUSP00000026474	Gli1	-	no
10090.ENSMUSP00000026466	Tac3	-	no
10090.ENSMUSP00000026436	Baiap2	-	no
10090.ENSMUSP00000026428	Myl6b	-	no
10090.ENSMUSP00000026416	Cdk2	-	no
10090.ENSMUSP00000026390	Rabgef1	-	no
10090.ENSMUSP00000026360	Itgb8	-	no
10090.ENSMUSP00000026328	Prdx4	-	no
10090.ENSMUSP00000026302	Maged2	-	no
10090.ENSMUSP00000026292	Huwe1	-	no
10090.ENSMUSP00000026256	Fbxl15	-	no
10090.ENSMUSP00000026241	Fgf8	-	no
10090.ENSMUSP00000026227	Twnk	-	no
10090.ENSMUSP00000026217	Chuk	-	no
10090.ENSMUSP00000026211	Cyp2c23	-	no
10090.ENSMUSP00000026156	Rfng	-	no
10090.ENSMUSP00000026148	Cbr2	-	no
10090.ENSMUSP00000026144	Dcxr	-	no
10090.ENSMUSP00000026128	Anapc11	-	no
10090.ENSMUSP00000026062	Casp7	-	no
10090.ENSMUSP00000026050	Gsto1	-	no
10090.ENSMUSP00000026012	Cyp17a1	-	no
10090.ENSMUSP00000025999	Add3	down	no
10090.ENSMUSP00000025981	Tctn3	-	no

10090.ENSMUSP00000025968	Cyp2c39	-	no
10090.ENSMUSP00000025966	Cyp2c55	-	no
10090.ENSMUSP00000025961	Prdx3	-	no
10090.ENSMUSP00000025946	Cyp26a1	-	no
10090.ENSMUSP00000025925	Pla2g16	-	no
10090.ENSMUSP00000025914	Vegfb	-	no
10090.ENSMUSP00000025912	Plcb3	-	no
10090.ENSMUSP00000025867	Rela	-	no
10090.ENSMUSP00000025856	Lrp5	-	no
10090.ENSMUSP00000025850	Fosl1	up	no
10090.ENSMUSP00000025844	Ctsw	-	no
10090.ENSMUSP00000025804	Rab1b	-	no
10090.ENSMUSP00000025803	Dkk1	-	no
10090.ENSMUSP00000025800	Pip5k1b	-	no
10090.ENSMUSP00000025797	Mbl2	-	no
10090.ENSMUSP00000025791	Grk2	-	no
10090.ENSMUSP00000025773	Pold4	-	no
10090.ENSMUSP00000025761	Cabp4	-	no
10090.ENSMUSP00000025740	Rad9a	-	no
10090.ENSMUSP00000025729	Tnks2	-	no
10090.ENSMUSP00000025724	Il33	-	no
10090.ENSMUSP00000025711	Vps51	-	no
10090.ENSMUSP00000025705	Jak2	-	no
10090.ENSMUSP00000025695	Ppp2r5b	-	no
10090.ENSMUSP00000025656	Aldh1a7	-	no
10090.ENSMUSP00000025649	Ddb1	-	no
10090.ENSMUSP00000025617	Rfk	-	no
10090.ENSMUSP00000025602	Gna14	-	no
10090.ENSMUSP00000025601	Lpxn	-	no
10090.ENSMUSP00000025569	Tmem216	-	no
10090.ENSMUSP00000025523	Csf1r	-	no
10090.ENSMUSP00000025522	Pdgfrb	-	no
10090.ENSMUSP00000025472	Pcyox1l	-	no
10090.ENSMUSP00000025453	Smad2	-	no
10090.ENSMUSP00000025425	Cep192	-	no
10090.ENSMUSP00000025418	Psmg2	-	no
10090.ENSMUSP00000025402	Gnal	-	no
10090.ENSMUSP00000025395	Grp	-	no
10090.ENSMUSP00000025393	Smad4	-	no

10090.ENSMUSP00000025377	Ppp2r2b	-	no
10090.ENSMUSP00000025363	Hbegf	-	no
10090.ENSMUSP00000025266	Lta	-	no
10090.ENSMUSP00000025263	Tnf	-	no
10090.ENSMUSP00000025262	Ltb	-	no
10090.ENSMUSP00000025246	Csnk2b	-	no
10090.ENSMUSP00000025239	Bin1	-	no
10090.ENSMUSP00000025230	C2	-	no
10090.ENSMUSP00000025223	Cyp21	-	no
10090.ENSMUSP00000025178	Vps52	-	no
10090.ENSMUSP00000025166	Cdh2	-	no
10090.ENSMUSP00000025078	Map3k8	up	no
10090.ENSMUSP00000025075	Bambi	-	no
10090.ENSMUSP00000024916	Lhcgr	-	no
10090.ENSMUSP00000024884	Eif2ak2	-	no
10090.ENSMUSP00000024846	Myl12a	-	no
10090.ENSMUSP00000024791	Trem2	-	no
10090.ENSMUSP00000024774	Guca1b	-	no
10090.ENSMUSP00000024748	Gtpbp2	-	no
10090.ENSMUSP00000024742	Nfkbie	-	no
10090.ENSMUSP00000024739	Hsp90ab1	-	no
10090.ENSMUSP00000024699	Cldn6	-	no
10090.ENSMUSP00000024698	Tnfrsf12a	-	no
10090.ENSMUSP00000024599	Igf2r	-	no
10090.ENSMUSP00000024575	Rps6ka2	-	no
10090.ENSMUSP00000024565	Nox3	-	no
10090.ENSMUSP00000024206	Gnb3	-	no
10090.ENSMUSP00000024179	Nfatc4	-	no
10090.ENSMUSP00000024044	Cd4	-	no
10090.ENSMUSP00000024031	Acy1	-	no
10090.ENSMUSP00000023994	Serping1	-	no
10090.ENSMUSP00000023884	Gm853	-	no
10090.ENSMUSP00000023869	Denr	up	no
10090.ENSMUSP00000023867	Rfc2	-	no
10090.ENSMUSP00000023829	Cdkn1a	-	no
10090.ENSMUSP00000023814	Npff	-	no
10090.ENSMUSP00000023762	Cers5	-	no
10090.ENSMUSP00000023734	Wnt1	-	no
10090.ENSMUSP00000023732	Wnt10b	-	no

10090.ENSMUSP00000023693	Ifnar2	-	no
10090.ENSMUSP00000023691	Il10rb	-	no
10090.ENSMUSP00000023689	Ifnar1	-	no
10090.ENSMUSP00000023687	Ifngr2	-	no
10090.ENSMUSP00000023684	Gart	-	no
10090.ENSMUSP00000023673	Runx1	-	no
10090.ENSMUSP00000023629	Pros1	-	no
10090.ENSMUSP00000023612	Ets2	-	no
10090.ENSMUSP00000023611	Adamts5	down	no
10090.ENSMUSP00000023598	Rfc4	-	no
10090.ENSMUSP00000023590	Hrg	-	no
10090.ENSMUSP00000023583	Ahsg	-	no
10090.ENSMUSP00000023535	Iqcb1	-	no
10090.ENSMUSP00000023534	Golgb1	-	no
10090.ENSMUSP00000023507	Gsk3b	-	no
10090.ENSMUSP00000023502	Snx4	-	no
10090.ENSMUSP00000023486	Tfrc	-	no
10090.ENSMUSP00000023467	Pak2	-	no
10090.ENSMUSP00000023462	Mapk1	-	no
10090.ENSMUSP00000023449	Snap29	-	no
10090.ENSMUSP00000023364	Pla2g10	-	no
10090.ENSMUSP00000023359	Nde1	-	no
10090.ENSMUSP00000023356	Snai2	down	no
10090.ENSMUSP00000023353	Mcm4	-	no
10090.ENSMUSP00000023270	Cep97	-	no
10090.ENSMUSP00000023238	Gsdmdc1	up	no
10090.ENSMUSP00000023214	Dgat1	-	no
10090.ENSMUSP00000023154	Cldn1	-	no
10090.ENSMUSP00000023151	Bcl6	-	no
10090.ENSMUSP00000023128	Itga5	-	no
10090.ENSMUSP00000023086	Smdt1	-	no
10090.ENSMUSP00000023007	Adcy8	-	no
10090.ENSMUSP00000022986	Fbxo32	-	no
10090.ENSMUSP00000022921	Angpt1	-	no
10090.ENSMUSP00000022909	Dcaf13	-	no
10090.ENSMUSP00000022906	Fzd6	-	no
10090.ENSMUSP00000022890	Rnf19a	-	no
10090.ENSMUSP00000022856	Rad1	-	no
10090.ENSMUSP00000022842	Cct5	-	no

10090.ENSMUSP00000022821	Dhrs4	-	no
10090.ENSMUSP00000022791	Fbxo4	-	no
10090.ENSMUSP00000022784	Haus4	-	no
10090.ENSMUSP00000022746	Osmr	-	no
10090.ENSMUSP00000022720	Fbxl3	-	no
10090.ENSMUSP00000022718	Ednrb	-	no
10090.ENSMUSP00000022697	Fgf17	-	no
10090.ENSMUSP00000022691	Hr	up	no
10090.ENSMUSP00000022665	Rhobtb2	-	no
10090.ENSMUSP00000022656	Bora	-	no
10090.ENSMUSP00000022622	Ptk2b	-	no
10090.ENSMUSP00000022616	Clu	-	no
10090.ENSMUSP00000022592	Tnfsf11	-	no
10090.ENSMUSP00000022563	Mtmr6	-	no
10090.ENSMUSP00000022545	Fgf9	-	no
10090.ENSMUSP00000022543	Micu2	-	no
10090.ENSMUSP00000022458	Bap1	-	no
10090.ENSMUSP00000022331	Opn4	-	no
10090.ENSMUSP00000022304	Thrb	-	no
10090.ENSMUSP00000022296	Ube2e1	-	no
10090.ENSMUSP00000022282	Gpx8	-	no
10090.ENSMUSP00000022268	Pdhb	-	no
10090.ENSMUSP00000022246	Fgf10	-	no
10090.ENSMUSP00000022217	Zfyve16	-	no
10090.ENSMUSP00000022185	F2rl1	-	no
10090.ENSMUSP00000022182	F2rl2	-	no
10090.ENSMUSP00000022140	Ocln	-	no
10090.ENSMUSP00000022136	Rad17	-	no
10090.ENSMUSP00000022009	Cetn3	-	no
10090.ENSMUSP00000021991	Mterf3	-	no
10090.ENSMUSP00000021961	Catsper3	-	no
10090.ENSMUSP00000021933	Ctsl	-	no
10090.ENSMUSP00000021932	Drd1	-	no
10090.ENSMUSP00000021898	Shc3	-	no
10090.ENSMUSP00000021844	Ripk1	-	no
10090.ENSMUSP00000021796	Edn1	-	no
10090.ENSMUSP00000021770	Scgn	-	no
10090.ENSMUSP00000021750	Ryr2	-	no
10090.ENSMUSP00000021734	Gng4	-	no

10090.ENSMUSP00000021729	Gpr132	-	no
10090.ENSMUSP00000021706	Traf3	-	no
10090.ENSMUSP00000021698	Hsp90aa1	-	no
10090.ENSMUSP00000021674	Fos	-	no
10090.ENSMUSP00000021609	Golga5	-	no
10090.ENSMUSP00000021554	Actn1	-	no
10090.ENSMUSP00000021550	Arg2	up	no
10090.ENSMUSP00000021496	Serpina3a	-	no
10090.ENSMUSP00000021450	Sgpp1	-	no
10090.ENSMUSP00000021447	Ppp2r5e	-	no
10090.ENSMUSP00000021413	Nfkbia	up	no
10090.ENSMUSP00000021346	Tshr	-	no
10090.ENSMUSP00000021335	Scfd1	-	no
10090.ENSMUSP00000021329	Gosr2	-	no
10090.ENSMUSP00000021324	Map3k14	-	no
10090.ENSMUSP00000021323	1700023F06Rik	-	no
10090.ENSMUSP00000021290	Rcvrn	-	no
10090.ENSMUSP00000021284	Ntn1	-	no
10090.ENSMUSP00000021277	Aurkb	-	no
10090.ENSMUSP00000021273	Vamp2	-	no
10090.ENSMUSP00000021262	Alox8	-	no
10090.ENSMUSP00000021116	Unk	-	no
10090.ENSMUSP00000021107	Itgb4	-	no
10090.ENSMUSP00000021091	Pafah1b1	-	no
10090.ENSMUSP00000021040	Cct6b	-	no
10090.ENSMUSP00000021029	Efcab3	-	no
10090.ENSMUSP00000021028	Itgb3	-	no
10090.ENSMUSP00000021011	Ccl7	up	no
10090.ENSMUSP00000020991	Dnmt3a	-	no
10090.ENSMUSP00000020984	Adcy3	-	no
10090.ENSMUSP00000020964	Fkbp1b	-	no
10090.ENSMUSP00000020911	Sdc1	-	no
10090.ENSMUSP00000020904	Rock2	-	no
10090.ENSMUSP00000020843	Acaca	-	no
10090.ENSMUSP00000020769	Dbnl	-	no
10090.ENSMUSP00000020706	Adcy1	-	no
10090.ENSMUSP00000020687	Pttg1	-	no
10090.ENSMUSP00000020683	Hus1	-	no
10090.ENSMUSP00000020664	Itk	-	no

10090.ENSMUSP00000020657	Ube2b	-	no
10090.ENSMUSP00000020634	Mapk9	-	no
10090.ENSMUSP00000020629	Gfpt2	up	no
10090.ENSMUSP00000020617	Flt4	-	no
10090.ENSMUSP00000020608	Ppp2ca	-	no
10090.ENSMUSP00000020579	Hmmr	-	no
10090.ENSMUSP00000020577	Fgf22	-	no
10090.ENSMUSP00000020507	Fgf18	-	no
10090.ENSMUSP00000020493	Pofut2	-	no
10090.ENSMUSP00000020484	Txnrd1	up	no
10090.ENSMUSP00000020408	Mdm2	-	no
10090.ENSMUSP00000020391	Rab36	-	no
10090.ENSMUSP00000020323	Avpr1a	-	no
10090.ENSMUSP00000020316	Tbk1	-	no
10090.ENSMUSP00000020312	Mcu	-	no
10090.ENSMUSP00000020307	Anapc16	-	no
10090.ENSMUSP00000020287	Npffr1	-	no
10090.ENSMUSP00000020283	H2afy2	-	no
10090.ENSMUSP00000020278	Tacr2	-	no
10090.ENSMUSP00000020277	Hkdc1	-	no
10090.ENSMUSP00000020271	Srgn	-	no
10090.ENSMUSP00000020257	Sirt1	-	no
10090.ENSMUSP00000020238	Hsp90b1	-	no
10090.ENSMUSP00000020234	Timp3	-	no
10090.ENSMUSP00000020212	Cep83	-	no
10090.ENSMUSP00000020188	Ifngr1	-	no
10090.ENSMUSP00000020185	Il20ra	-	no
10090.ENSMUSP00000020174	Stx7	-	no
10090.ENSMUSP00000020163	Nedd1	-	no
10090.ENSMUSP00000020161	Arg1	-	no
10090.ENSMUSP00000020157	Apaf1	-	no
10090.ENSMUSP00000020101	Rhobtb1	-	no
10090.ENSMUSP00000020085	Ube2d1	-	no
10090.ENSMUSP00000020062	Gprc6a	-	no
10090.ENSMUSP00000020040	Nts	-	no
10090.ENSMUSP00000020015	Nmbr	-	no
10090.ENSMUSP00000019911	Hdac2	-	no
10090.ENSMUSP00000019907	Fbxo5	-	no
10090.ENSMUSP00000019906	Vip	-	no

10090.ENSMUSP00000019697	Haus5	-	no
10090.ENSMUSP00000019615	Cdc37	-	no
10090.ENSMUSP00000019608	Ptger1	-	no
10090.ENSMUSP00000019514	NoMapping	-	no
10090.ENSMUSP00000019470	Psme3	-	no
10090.ENSMUSP00000019469	G6pc	-	no
10090.ENSMUSP00000019443	Rnf31	-	no
10090.ENSMUSP00000019362	Dvl2	-	no
10090.ENSMUSP00000019074	Ccl4	-	no
10090.ENSMUSP00000019068	Alox15	-	no
10090.ENSMUSP00000019051	Alox12e	-	no
10090.ENSMUSP00000018966	Sfrp5	-	no
10090.ENSMUSP00000018875	Ap2b1	-	no
10090.ENSMUSP00000018851	Dync1h1	-	no
10090.ENSMUSP00000018816	Copz2	-	no
10090.ENSMUSP00000018805	Cog1	-	no
10090.ENSMUSP00000018800	Myl4	-	no
10090.ENSMUSP00000018748	Tbx3	up	no
10090.ENSMUSP00000018737	Sparc	-	no
10090.ENSMUSP00000018713	Cldn7	-	no
10090.ENSMUSP00000018691	Pip4k2b	-	no
10090.ENSMUSP00000018645	Ncor1	-	no
10090.ENSMUSP00000018644	Adora2b	up	no
10090.ENSMUSP00000018630	Wnt9b	-	no
10090.ENSMUSP00000018610	Nos2	up	no
10090.ENSMUSP00000018544	04-set	-	no
10090.ENSMUSP00000018429	Pld2	-	no
10090.ENSMUSP00000018333	Uchl5	-	no
10090.ENSMUSP00000018313	Mfng	-	no
10090.ENSMUSP00000018287	Mafk	-	no
10090.ENSMUSP00000018274	Csnk1d	-	no
10090.ENSMUSP00000018156	Rac3	-	no
10090.ENSMUSP00000018113	Ptgis	-	no
10090.ENSMUSP00000017975	Rab5a	-	no
10090.ENSMUSP00000017920	Crk	-	no
10090.ENSMUSP00000017881	Mmp9	-	no
10090.ENSMUSP00000017821	Wsb1	-	no
10090.ENSMUSP00000017799	Cd40	up	no
10090.ENSMUSP00000017604	Cyba	-	no

10090.ENSMUSP00000017552	Cacnb1	-	no
10090.ENSMUSP00000017309	Gast	-	no
10090.ENSMUSP00000017290	Brca1	-	no
10090.ENSMUSP00000017153	Sdc4	-	no
10090.ENSMUSP00000016680	Cul4a	-	no
10090.ENSMUSP00000016511	Ptk6	-	no
10090.ENSMUSP00000016452	Ube2a	-	no
10090.ENSMUSP00000016400	Ctsz	-	no
10090.ENSMUSP00000016315	Lamb3	-	no
10090.ENSMUSP00000016144	NoMapping	-	no
10090.ENSMUSP00000016081	H2afy	-	no
10090.ENSMUSP00000015994	Adamtsl4	-	no
10090.ENSMUSP00000015987	Rxrg	-	no
10090.ENSMUSP00000015891	Vps45	-	no
10090.ENSMUSP00000015858	Cers2	-	no
10090.ENSMUSP00000015800	Hspa8	-	no
10090.ENSMUSP00000015771	Gata5	-	no
10090.ENSMUSP00000015749	Srf	-	no
10090.ENSMUSP00000015664	Ctsk	-	no
10090.ENSMUSP00000015612	Notch4	-	no
10090.ENSMUSP00000015596	Ager	-	no
10090.ENSMUSP00000015484	Cybb	-	no
10090.ENSMUSP00000015394	Mmp13	up	no
10090.ENSMUSP00000015358	Mtmr1	-	no
10090.ENSMUSP00000015239	Fbxw5	-	no
10090.ENSMUSP00000015234	Ptgds	-	no
10090.ENSMUSP00000015197	Gata2	-	no
10090.ENSMUSP00000015100	Ppp1cb	-	no
10090.ENSMUSP00000014911	Tbp	-	no
10090.ENSMUSP00000014743	Csf1	-	no
10090.ENSMUSP00000014578	Plg	-	no
10090.ENSMUSP00000014499	Anapc1	-	no
10090.ENSMUSP00000014263	Ugt1a6	-	no
10090.ENSMUSP00000014221	Chp1	-	no
10090.ENSMUSP00000014080	Myl2	-	no
10090.ENSMUSP00000013970	Pip4k2c	-	no
10090.ENSMUSP00000013949	Birc3	up	no
10090.ENSMUSP00000013931	Ehmt2	-	no
10090.ENSMUSP00000013807	Pten	-	no

10090.ENSMUSP00000013773	Cad	-	no
10090.ENSMUSP00000012627	Rpa3	-	no
10090.ENSMUSP00000012426	Wnt8a	-	no
10090.ENSMUSP00000012348	Gstm2	-	no
10090.ENSMUSP00000011895	Sptbn4	-	no
10090.ENSMUSP00000011526	Dhdh	-	no
10090.ENSMUSP00000011315	Vipr2	-	no
10090.ENSMUSP00000011058	Pdhx	-	no
10090.ENSMUSP00000010941	Wnt2	-	no
10090.ENSMUSP00000010804	Plcd1	-	no
10090.ENSMUSP00000010753	Psen2	-	no
10090.ENSMUSP00000010605	Il12rb2	-	no
10090.ENSMUSP00000010536	Gosr1	-	no
10090.ENSMUSP00000010189	Tmem115	-	no
10090.ENSMUSP00000010049	Kdsr	-	no
10090.ENSMUSP00000010044	Wnt3a	-	no
10090.ENSMUSP00000009790	Pla2g12b	-	no
10090.ENSMUSP00000009774	Ppp2cb	-	no
10090.ENSMUSP00000009538	Syn2	-	no
10090.ENSMUSP00000009530	Timp1	-	no
10090.ENSMUSP00000009425	Rarres2	-	no
10090.ENSMUSP00000009219	Cabp7	-	no
10090.ENSMUSP00000009157	Dynll1	-	no
10090.ENSMUSP00000009003	Rala	-	no
10090.ENSMUSP00000008991	Sptbn2	-	no
10090.ENSMUSP00000008987	Cldn13	-	no
10090.ENSMUSP00000008684	Mgst1	-	no
10090.ENSMUSP00000008451	1700109H08Rik	-	no
10090.ENSMUSP00000008350	Cers4	-	no
10090.ENSMUSP00000007602	M6pr	-	no
10090.ENSMUSP00000007433	Kiss1	-	no
10090.ENSMUSP00000007216	Ap2m1	-	no
10090.ENSMUSP00000007130	Ctnnb1	-	no
10090.ENSMUSP00000006912	Pip4k2a	-	no
10090.ENSMUSP00000006898	Gmnn	-	no
10090.ENSMUSP00000006893	Kiaa0319	-	no
10090.ENSMUSP00000006718	Wnt10a	-	no
10090.ENSMUSP00000006716	Wnt6	-	no
10090.ENSMUSP00000006703	Itih4	-	no

10090.ENSMUSP00000006697	Itih3	-	no
10090.ENSMUSP00000006669	Pdk1	-	no
10090.ENSMUSP00000006629	Sptbn1	-	no
10090.ENSMUSP00000006626	Actn3	-	no
10090.ENSMUSP00000006614	Epha2	-	no
10090.ENSMUSP00000006565	Cdc20	-	no
10090.ENSMUSP00000006508	Ggt1	-	no
10090.ENSMUSP00000006467	Arpc2	-	no
10090.ENSMUSP00000006397	Epor	-	no
10090.ENSMUSP00000006235	Ctsb	-	no
10090.ENSMUSP00000006221	Vps54	-	no
10090.ENSMUSP00000006181	Napa	-	no
10090.ENSMUSP00000006137	Trap1	-	no
10090.ENSMUSP00000006046	Trh	-	no
10090.ENSMUSP00000006005	Pth1r	-	no
10090.ENSMUSP00000005976	Tnfsf14	-	no
10090.ENSMUSP00000005889	Vav1	-	no
10090.ENSMUSP00000005860	Pvalb	-	no
10090.ENSMUSP00000005815	Kit	-	no
10090.ENSMUSP00000005791	Cabp5	-	no
10090.ENSMUSP00000005719	Adcy9	-	no
10090.ENSMUSP00000005671	Igf1r	-	no
10090.ENSMUSP00000005669	Cyp2b13	-	no
10090.ENSMUSP00000005611	Myl10	-	no
10090.ENSMUSP00000005601	Il27ra	-	no
10090.ENSMUSP00000005548	Hmox1	up	no
10090.ENSMUSP00000005509	Stx1a	-	no
10090.ENSMUSP00000005452	Fgfr4	-	no
10090.ENSMUSP00000005364	G6pc2	-	no
10090.ENSMUSP00000005292	Prdx2	-	no
10090.ENSMUSP00000005233	Eif2ak4	-	no
10090.ENSMUSP00000005164	Prkacb	-	no
10090.ENSMUSP00000005066	Map2k1	-	no
10090.ENSMUSP00000004990	Mapk14	-	no
10090.ENSMUSP00000004986	Mapk13	-	no
10090.ENSMUSP00000004949	Traf6	-	no
10090.ENSMUSP00000004913	Pgf	-	no
10090.ENSMUSP00000004622	Gab2	-	no
10090.ENSMUSP00000004565	Ralb	-	no

10090.ENSMUSP00000004456	Gpx5	-	no
10090.ENSMUSP00000004453	Gpx6	-	no
10090.ENSMUSP00000004392	Irf5	-	no
10090.ENSMUSP00000004377	Ptpn6	-	no
10090.ENSMUSP00000004330	Ikbkg	-	no
10090.ENSMUSP00000004214	Cacna1e	-	no
10090.ENSMUSP00000004172	Hmox2	-	no
10090.ENSMUSP00000004140	Gstm1	-	no
10090.ENSMUSP00000004137	Gstm7	-	no
10090.ENSMUSP00000004136	Gstm3	-	no
10090.ENSMUSP00000004134	Gstm5	-	no
10090.ENSMUSP00000003981	Il7r	-	no
10090.ENSMUSP00000003964	Gys1	-	no
10090.ENSMUSP00000003947	Nqo1	up	no
10090.ENSMUSP00000003754	Calb2	-	no
10090.ENSMUSP00000003640	Fosb	-	no
10090.ENSMUSP00000003575	Tpm4	-	no
10090.ENSMUSP00000003574	Cyp4f3	-	no
10090.ENSMUSP00000003550	Ncstn	-	no
10090.ENSMUSP00000003442	Cacnb3	-	no
10090.ENSMUSP00000003370	Hck	-	no
10090.ENSMUSP00000003345	Amph	-	no
10090.ENSMUSP00000003318	Dvl3	-	no
10090.ENSMUSP00000003284	Irf3	-	no
10090.ENSMUSP00000003154	Efna2	-	no
10090.ENSMUSP00000003137	Cyp2c29	-	no
10090.ENSMUSP00000003121	Rab8a	-	no
10090.ENSMUSP00000003115	Cdkn1b	-	no
10090.ENSMUSP00000003079	Prkar2b	-	no
10090.ENSMUSP00000003038	Ap2a2	-	no
10090.ENSMUSP00000003027	Map2k7	-	no
10090.ENSMUSP00000003017	Tbxas1	-	no
10090.ENSMUSP00000002979	Lamb1	-	no
10090.ENSMUSP00000002891	Top3a	-	no
10090.ENSMUSP00000002883	Sfrp4	-	no
10090.ENSMUSP00000002855	Kdelr1	-	no
10090.ENSMUSP00000002839	Ppp2r5d	-	no
10090.ENSMUSP00000002818	Ykt6	-	no
10090.ENSMUSP00000002708	Shh	-	no

10090.ENSMUSP00000002678	Tgfb1	-	no
10090.ENSMUSP00000002677	Axl	-	no
10090.ENSMUSP00000002588	Tiam1	-	no
10090.ENSMUSP00000002436	Snx9	-	no
10090.ENSMUSP00000002398	Adcy4	-	no
10090.ENSMUSP00000002320	Ppard	up	no
10090.ENSMUSP00000002101	Cd3g	-	no
10090.ENSMUSP00000002064	Blvra	-	no
10090.ENSMUSP00000002044	Map3k3	-	no
10090.ENSMUSP00000002011	Esam	up	no
10090.ENSMUSP00000001989	Uba1	-	no
10090.ENSMUSP00000001927	Ltbp1	-	no
10090.ENSMUSP00000001882	Folr1	-	no
10090.ENSMUSP00000001792	Il16	down	no
10090.ENSMUSP00000001790	Cldn15	-	no
10090.ENSMUSP00000001780	Akt1	-	no
10090.ENSMUSP00000001713	Gstt1	-	no
10090.ENSMUSP00000001566	Tubb5	-	no
10090.ENSMUSP00000001548	Itga3	-	no
10090.ENSMUSP00000001534	Sost	-	no
10090.ENSMUSP00000001479	Kpnb1	-	no
10090.ENSMUSP00000001452	Cct3	-	no
10090.ENSMUSP00000001402	Fbxo9	-	no
10090.ENSMUSP00000001327	Itgb7	-	no
10090.ENSMUSP00000001202	Ocrl	-	no
10090.ENSMUSP00000001156	Cfp	-	no
10090.ENSMUSP00000001055	Icam2	-	no
10090.ENSMUSP00000001036	Tyk2	-	no
10090.ENSMUSP00000001027	Aox1	-	no
10090.ENSMUSP00000001008	Ccl3	-	no
10090.ENSMUSP00000000939	Hip1r	-	no
10090.ENSMUSP00000000828	Txnrd3	-	no
10090.ENSMUSP00000000808	Il12rb1	-	no
10090.ENSMUSP00000000776	Tubgcp3	-	no
10090.ENSMUSP00000000769	Serpinf1	-	no
10090.ENSMUSP00000000767	Rpa1	-	no
10090.ENSMUSP00000000746	Dnmt3l	up	no
10090.ENSMUSP00000000642	Hk2	-	no
10090.ENSMUSP00000000574	Adora3	-	no

10090.ENSMUSP00000000505	Mcm7	-	no
10090.ENSMUSP00000000500	Pdgfb	-	no
10090.ENSMUSP00000000476	Pdgfra	-	no
10090.ENSMUSP00000000451	Raf1	-	no
10090.ENSMUSP00000000445	Myf5	-	no
10090.ENSMUSP00000000365	Mcts1	-	no
10090.ENSMUSP00000000329	Alox12	-	no
10090.ENSMUSP00000000326	Bcl6b	-	no
10090.ENSMUSP00000000299	Itgb2	-	no
10090.ENSMUSP00000000220	Ins2	-	no
10090.ENSMUSP00000000199	Ncs1	-	no
10090.ENSMUSP00000000194	Ccl12	-	no
10090.ENSMUSP00000000193	Ccl2	up	no
10090.ENSMUSP00000000187	Fgf6	-	no
10090.ENSMUSP00000000186	Fgf23	-	no
10090.ENSMUSP00000000161	Itgb2l	-	no
10090.ENSMUSP00000000137	Actr2	-	no
10090.ENSMUSP00000000127	Wnt3	-	no
10090.ENSMUSP00000000122	Ngfr	-	no
10090.ENSMUSP00000000049	Apoh	-	no
10090.ENSMUSP00000000028	Cdc45	-	no

Table 4. Hub nodes related to the input genelist and associated to AMG treatment

Cluster	Size	Density	Internal weight	External weight	P-value	Members
1	36	0,6141	386,9	162,3	10^{-20}	Wnt7a Wnt7b Sfrp5 Sfrp4 Sfrp1 Sfrp2 Wnt8b Wnt8a Wnt9a Wnt9b Wnt10b Wnt10a Lrp5 Lrp6 Serpinf1 Fzd9 Fzd8 Fzd7 Fzd6 Fzd5 Fzd3 Fzd2 Fzd1 Fzd10 Wnt11 Wnt16 Wnt2b Wnt3a Wnt4 Wnt6 Wnt1 Wnt2 Wnt3 Bambi Wnt5b Sost
2	172	0,8076	1,19E+04	3772	10^{-20}	Grm8 Ccl21a Ppbp Gpr18 Gpr17 Hcar2 App P2ry12 P2ry14 Nms Nmu Gnai1 Npy2r Tas2r140 Gper1 Ccl27a Oxgr1 Ccr1l1 Sst Adora3 Adora1 Galr1 Galr2 Rxfp4 Rxfp3 Sucnr1 Adra2c C5ar1 Oprd1 Aplnr

						Casr Ccl25 Ccl28 Fpr-rs4 Fpr-rs7 Gabbr2 Cnr2 Cnr1 Ppy S1pr4 S1pr5 S1pr1 S1pr2 S1pr3 Agtr2 Gpr55 Nmur1 Npy1r Ccr10 Ccl19 Ccl12 Ccl9 Ccl5 Ccl4 Ccl7 Ccl6 Ccl3 Ccl2 Tas2r125 Hebp1 Penk Ackr3 Ackr2 Fpr2 Fpr1 Htr5a Tas2r106 Tas2r107 Tas2r104 Tas2r103 Tas2r109 Anxa1 Kng1 Tas2r105 Kng2 Rln3 Cort Mtnr1a C3ar1 Tas2r110 Tas2r113 Tas2r115 Tas2r114 Tas2r117 Tas2r116 Grm3 Grm2 Grm7 Grm6 Chrm2 Chrm4 Hrh3 Pomc Insl5 Npy4r Ccl20 Cxcl16 Cxcl12 Cxcl13 Cxcl10 Tas2r129 Tas2r124 Tas2r120 Tas2r123 Gnat3 Gm2564 Npy5r Tas2r136 Tas2r131 Pmch Fpr-rs3 Lpar3 Htr1b Htr1a Htr1f Htr1d Pyy Gnai2 Gabbr1 Oprk1 Apln Cx3cr1 Npbwr1 Hrh4 Npw Npy Npb Fpr-rs6 Pf4 Ccr9 Ccr8 Ccr7 Ccr6 Ccr5 Ccr4 Ccr3 Ccr2 Ccr1 Ptgdr2 Lpar1 Lpar2 Cxcr4 Cxcr5 Cxcr1 Cxcr2 Cxcr3 Oprl1 Gal Gnai3 Cxcr6 C3 Xcr1 Oprm1 P2ry4 Bdkrb2 Bdkrb1 Pnoc Gpsm1 Cxcl9 Cxcl5 Cxcl2 Cxcl3 Nmur2 Cxcl1 Sstr4 Sstr5 Sstr2 Sstr3 Sstr1 Drd3 Drd2 Drd4
3	58	0,5812	960,7	569,5	10^{-20}	Kdelr1 Rab1b Spta1 Tmed9 Tmed2 Tmed3 Tmed7 Arcn1 Gosr1 Gosr2 Napa Sptan1 Cope Copa Gorasp1 Copb2 Copb1 Folr1 Cd59b Cd59a Tgfa Bet1l Uso1 Bet1 Rab36 Golga5 Sptbn1 Sptbn2 Sptbn4 Ank3 Ank1 Tmem115 Copg1 Copg2 Ykt6 Golgb1 Copz2 Copz1 Rab33b Ins2 Ins1 Tmed10 Nsf Ctsc Scfd1 Cd55 Golim4 Stx18 Cog4 Rab30 Golga3 Cog5 Cog6 Cog7 Cog1 Cog2 Cog3 Cog8
4	89	0,9002	3525	526	10^{-20}	Atg7 Siah1a Lmo7 Ube2a Unkl Dtx3l Znrf1 Ubr2 Fbxw24 Fbxw26 Fbxw21 Fbxw22 Fbxw28 Fbxw14 Fbxw11 Herc6 Fbxw13 Fbxo9 Fbxo7 Fbxo6 Fbxo4 Fbxo2 Smurf2 Rnf213 Rnf217 Fbxo27 Fbxo21 Fbxo22 Rnf114 Trim69 Mylip Fbxo32 Fbxo31 Fbxo30 Rnf19a Rnf19b Fbxw19 Fbxw18 Fbxw15 Fbxw16 Fbxw10 Hectd2 Siah2 Fbxl7 Fbxl4 Fbxl5 Fbxl3 Fbxl8 Rnf144b Skp2 Fbxo17 Fbxo10 Znrf2 Rbbp6 Gm5819 Huwe1 Cul1 Wsb1 Fbxw4 Fbxo40 Fbxo41 Fbxw7 Fbxw5 Fbxw9 Fbxw8 Fbxl22 Fbxl20 Fbxl13 Trip12 Spsb1 Lonrf1 Fbxl18 Fbxl19 Fbxl16

						Fbxl14 Fbxl15 Fbxl12 Rnf115 Btrc Fbxw20 Uba1 Uba3 Uba5 Uba7 Uba6 Rlim Trim36 Rbck1 Ccnf
5	27	0,7977	280	16,37	10^{-20}	Tjp1 Cldn24 Esam Cldn20 Cldn22 Cldn23 Ocln Cldn7 Cldn6 Cldn5 Cldn4 Cldn3 Cldn1 Cldn8 Cldn19 Cldn18 Cldn15 Cldn17 Cldn11 Cldn34c4 Cldn14 Cldn16 Cldn10 Cldn13 Cldn34d Cldn2 Cldn9
6	35	0,8613	512,5	513,1	10^{-20}	Gsto1 Hpgds Mgst1 Mgst3 Mgst2 Ggt7 Ggt6 Ggt1 Gstt1 Gstt2 Ggt5 Gsta3 Gsta2 Gsta1 Gsta4 Gsr Gss Gstm7 Gstm6 Gstm5 Gstm4 Gstm3 Gstm2 Gstm1 Gstp1 Gstp2 Gsto2 Gstk1 Gpx8 Gpx6 Gpx7 Gpx5 Gpx2 Gpx3 Gpx1
7	35	0,8081	480,8	271,1	10^{-20}	Rxra Hist1h2bh Dnmt3b Hist1h2bm Hist1h2bp Hist2h2bb H2afy2 Dnmt3l H2afj Hist1h2bk Hist1h2ba Hist2h2be Hdac1 Hist2h2ac Hist2h2ab Pcgf1 Rbbp4 Rbbp7 Jun Hist1h2af Hist1h2ak Hist1h2ah Hdac2 Hist2h2aa2 Hist2h2aa1 Ttf1 Hist1h2bb Hist3h2a Dnmt3a H2afz H2afy H2afx H2afv Ncor1 Hist3h2ba
8	177	0,409	6371	2004	10^{-20}	Psmd12 Sem1 Psmd13 Psmd10 Psmd11 Psmd14 Ccne1 Ccne2 Tnks Gtse1 Gm4858 Ppp2cb Ppp2ca Ube2c Brcc3 Ccnd1 Anapc7 Anapc4 Anapc5 Anapc2 Anapc1 Axin1 Axin2 Cdc20 Cdc23 Cdc26 Cdc27 Mpnd Gmnn Gm10696 Ctnnb1 Fbxo5 Tnfsf14 Tnfsf11 Tnfsf12 Cdc16 Ehmt1 Cops2 Anapc10 Anapc11 Anapc16 Anapc15 Cd40 Mysm1 Cdkn1a Cdkn1b Mapk6 Ccna1 Ccna2 Numb Cks1brt Cop1 Gm4778 Klhl12 Hecw1 Orc1 Gm973 Bub1b Adrm1 Amer1 Spred1 Traf3 Traf2 Aurkb Aurka Cdc6 Ltbr Bap1 Birc2 Skp2 Ublcp1 Psmc6 Psmc5 Psmc4 Psmc3 Psmc2 Psmc1 Tdpoz4 Tdpoz2 Tdpoz3 Nfkbie Nfkbia Nfkbib Pomp Wee1 Tnf Rnf146 Tnfrsf1b Psmb1 Psmb2 Psmb3 Psmb4 Psmb5 Psmb6 Psmb7 Psmb8 Psmb9 Tnks2 Spop Hnrnpd Ube2e1 Ppp2r1b Shh Nfkb2 Nfkb1 Nfkbiz Oaz1 Oaz2 Cdc25a Psma8 Psma5 Psma4 Psma7 Psma6 Psma1 Psma3 Psma2 Bub3 Gm9774 Tnfsf13b Plk1 Cul3 Cul1 Tnfrsf11a Ube2d1 Gli1 Gli3 Gli2 Ehmt2 Lta Ltb Psmb10 Psmb11 Rela Relb Pttg1 Nf1 Gm5286 Ubfd1 Psmg2 Map3k14 Prickle1 Gm9125 Tnfrsf13c Uchl5 Dvl1 Dvl3

						Fzr1 Psmf1 Cdk2 Cdk1 Gsk3b Odc1 Ppp2r5c Ppp2r5b Ppp2r5a Ppp2r5e Ppp2r5d Tnfrsf12a Psme1 Psme3 Psme4 Usp14 Itch Cd40lg Psmd2 Psmd3 Psmd1 Psmd6 Psmd7 Psmd4 Psmd5 Psmd8 Psmd9 Mad2l1 Sufu Cebpb
9	96	0,8366	3815	838,3	10^{-20}	Tmem216 Cep192 Cdk5rap2 Pafah1b1 Cc2d2a Tuba1a Dctn1 Dctn3 Dctn2 Cetn2 Odf2 Cep78 Cep72 Cep70 Cep76 Mapre1 Dync1h1 Haus1 Haus3 Haus2 Haus5 Haus4 Haus7 Haus6 Haus8 Rab11a Cep250 Nde1 Cep57 Actr1a Hsp90aa1 Nek2 Cenpj Cep41 Tpx2 B9d1 B9d2 Prkaca Ninl Aurka Hmmr Sfi1 Tuba4a Fbf1 Fgfr1op Dynll1 Ssna1 Cep97 Dync1i2 Pcm1 Ywhae Ywhag Cep83 Cep89 Nedd1 Ppp2r1a Plk4 Plk1 Optn Tubg2 Tubg1 Rab8a Cep135 Cep131 Ccp110 Bora Tubgcp6 Tubgcp5 Tubgcp4 Tubgcp3 Tubgcp2 Nphp4 Sept2 Cntrl Tubb4a Tubb4b Prkar2b Rpgrip1l Tctn1 Tctn3 C2cd3 Csnk1e Csnk1d Iqcb1 Kif24 Cdk1 Cep152 Sdccag8 Tubb5 Ajuba Mark4 Sclt1 Cep63 Mks1 Cep162 Ttbk2
10	39	0,7361	545,5	329,6	10^{-20}	Rad9a Nbn Rad9b Topbp1 Ube2b Timeless Zbtb32 Kat5 Clspn Brca1 Blm Exo1 Pcna Chek1 Atm Brip1 Rad1 Rbbp8 Tipin Dna2 Rad17 Rpa3 Rpa1 Bard1 Pold4 Pold2 Pold1 Usp1 Rfc2 Rfc3 Rfc4 Rfc5 Dtl Atrip Hus1 Rmi2 Rmi1 Top3a Wrn
11	112	0,4079	2535	708,6	10^{-20}	Aldh1a1 Aldh1a2 Aldh1a7 Aldh2 Aldh7a1 Ugt2b34 Cyp2c38 Cyp2u1 Cyp2c39 Cyp2c37 Cyp4f14 Cyp4f13 Cyp2c40 Alox5 Alox8 Aldh3a2 Pla2g4d Pla2g4e Pla2g4f Pla2g4a Pla2g4b Pla2g4c Pla2g3 Pla2g5 Pla2g6 Cyp2c54 Bco1 Cyp2c55 Plb1 Cyp2c66 Cyp2c65 Cyp2c68 Aox4 Aox3 Aox2 Aox1 Dhrs3 Dhrs4 Cyp2j9 Cyp2j8 Cyp2j5 Cyp2j6 Alox12b Alox12e Pla2g2f Pla2g2d Pla2g2e Pla2g2c Ugt2b35 Ugt2b37 Ugt2b36 Ugt2b38 Cyp2c70 Cyp4a32 Awat2 Aldh9a1 Ugt1a1 Ugt1a7c Pla2g10 Pla2g16 Ugt1a9 Pla2g1b Cyp7b1 Lrat Alox12 Alox15 Hsd3b2 Hsd3b1 Hsd3b6 Hsd3b5 Hsd3b4 Ugt1a10 Cyp2b23 Cbr2 Pla2g12a Pla2g12b Ptgs1 Ptgs2 Pld2 Pld1 Cyp2b19 Cyp2b13 Cyp2b10 Cyp11a1

						Ugt2a2 Ugt2a3 Ugt1a2 Ugt1a5 Cyp4a10 Cyp4a14 Cbr3 Cbr1 Dhrs9 Cyp4a12b Cyp4a12a Cyp2j13 Cyp2j12 Cyp2j11 Cyp17a1 Dgat1 Cyp2b9 Retsat Blvra Blvrb Ugt2b1 Cyp2e1 Aldh1b1 Sult2b1 Cyp26a1 Ugt1a6b Cyp2c29 Cyp2c23
12	49	0,345	405,7	283,4	10^{-20}	Prlr Ghr Il6ra Stat3 Il6st Il23r Ifngr1 Ifngr2 Osm Il9r Mpl Il20ra Socs3 Il7 Il6 Ctf1 Ifnar1 Il21r Ifnar2 Il15ra Crlf2 Il11 Osmr Il10ra Jak1 Jak3 Jak2 Il27ra Csf3r Il10rb Cntfr Epor Il12rb2 Il12rb1 Il13ra1 Ifnlr1 Il7r Il12a Il12b Lifr Lepr Il20rb Il13ra2 Il22ra1 Il22ra2 Tyk2 Il11ra2 Il11ra1 Lif
13	45	0,5587	553,1	382,8	10^{-20}	Smdt1 Pkd1l1 Rasgrp2 Rasgrp1 Rasgrp4 Rasgrp3 Cacna2d4 Cacna2d1 Cacna2d2 Ncam1 Micu1 Micu2 Mcub Hspa2 Catsper3 Catsper2 Catsper1 Catsper4 Catsperb Catsperd Ptpa Mcu Pkd2l1 Trpc5 Trpc4 Ppp2r2b Ppp2r2c Ppp2r2d Cacnb4 Cacnb3 Catsperg2 Fkbp1b Cacnb1 Cacnb2 Cacna1s Cacna1g Cacna1f Cacna1e Cacna1d Cacna1b Cacna1a Cacna1i Cacna1h Pde4d Ryr2
14	74	0,9007	2433	856,7	10^{-20}	Itih3 Itih4 Srgn Ecm1 Selenop Serpina3b Maged2 Serpina3j Serpina3i Fermt3 Ola1 Actn4 Actn1 Actn2 Gas6 Sccpdh Rarres2 F13a1 Apool Pdgfb Spp2 Lgals3bp F8 Timp1 F5 Timp3 Tex264 Fam3c Serpinf2 Islr Ctsw Orm2 Orm1 Serping1 Qsox1 A2m Pcyox1l Plg Clu Aldoart2 Aldoart1 Tmsb4x Fn1 Hrg Sparc Vegfb Vegfc Vegfa Vegfd Cdc37l1 Fam49b A1bg Ahsg Serpina3f Serpina3c Cfd Serpina3a Serpina3m Serpina3k Apoh Igf2 Gtpbp2 Hgf Tgfb2 Tgfb1 Nhlrc2 Pros1 Tor4a Fgb Fga Fgg Alb Lefty1 Lefty2
15	75	0,883	2450	1215	10^{-20}	Glp1r Gpr150 Sct Pth Lhcgr Gpr15 Pth2 Pth2r Gpr25 Gpr20 Pth1r Rxfp2 Rxfp1 Mc3r Gip Iapp Gpr45 Avpr2 Gnal Gnas Calcrl Ptger2 Ptger4 Ptgir Mc1r Gpr84 Gpr83 Gpbar1 Adrb3 Adrb2 Adrb1 Gipr Adcyap1r1 Vipr1 Vipr2 Htr4 Htr7 Htr6 Adm Sctr Ptgdr Ghrh Taar1 Adora2b Adora2a Fshr Fshb Calca Calcr Crhr1 Gpr27 Mc4r Hrh2 Cga Ramp3 Ramp2 Ramp1 Glp2r Gpr176 Crh Adm2 Tshr Vip Ghrhr Adcyap1 Mc2r Adcy9 Adcy8 Adcy3

						Adcy1 Adcy7 Adcy5 Adcy4 Drd1 Drd5
16	78	0,7712	2316	1412	10^{-20}	Epn1 Sgip1 Slc2a8 Bin1 Aak1 Fcho1 Fcho2 Usp46 Tgoln1 Gapvd1 Avpr2 Necap1 Scarb2 Cltc Htt Clta Actr3 Ap2a2 Hip1r Hspa8 Hip1 Cttn Actr2 Lrp2 Ap2s1 Adrb2 Reps1 Ap2b1 Synj2 Picalm Snx9 Fnbp1 Cftr Dnajc6 Fzd4 Pacsin2 Rab5a Ocrl Arpc4 Arpc5 Arpc1a Arpc2 Arpc3 Tfrc Ldlrap1 Ston2 Apob Ap2a1 Arrb1 Arrb2 Eps15 Usp35 Usp38 Igf2r Cd3g Cd3d Gak Dvl2 Dnm2 Cd4 Wasl M6pr Ap2m1 Wnt5a Usp12 Vamp8 Vamp7 Vamp4 Vamp2 Vamp3 Agfg1 Itsn1 Ldlr Cbl Amph Sh3gl2 Syt1 Syt9
17	121	0,9015	6545	4237	10^{-20}	Tac1 Cck Gpr17 P2ry10 Opn4 Nmb Nms Nmu Qrfp Gast Gprc6a Ltb4r2 F2 Npffr1 Npffr2 C130060K24Rik Hcrtr2 Hcrtr1 Casr Edn2 Edn3 Edn1 Fpr-rs4 Fpr-rs7 Cysltr1 Cysltr2 Gna11 Gna15 Gna14 Gnaq Agtr1a Agtr1b Tbxa2r Nmur1 Prok2 Prok1 Ccl9 Ccl6 Prokr2 Prokr1 Ptger1 Fpr2 Gpr68 Gpr65 Htr2a Anxa1 Uts2r Uts2b Nmbr Ptafr Ptgfr Nts Npff Grk2 Ffar1 Hcrt Ffar2 Grm1 Grm5 Chrm1 Chrm3 Chrm5 Oxtr Avp Ntsr1 Ntsr2 Xcl1 Gpr4 Gnrhr Gpr132 Ghrl Npsr1 Pmch Fpr-rs3 Gcgr Lpar3 Gcg F2rl1 F2rl2 F2rl3 Trio Ghsr Grp Uts2 Hrh1 Gnrh1 Nps Fpr-rs6 Cckar Trhr Lpar4 Lpar6 Lpar1 Lpar2 Adra1d Adra1a Trh Ednrb Ednra Grpr Cckbr F2r Golt1a Kiss1 P2ry6 P2ry1 P2ry2 Bdkrb2 Bdkrb1 Htr2b Htr2c Kiss1r Kalrn Oxt Tacr1 Tacr2 Tacr3 Ffar3 Nmur2 Avpr1a Avpr1b
18	44	0,6272	593,3	704	1,43E-08	Cdipt Mtmr4 Mtmr7 Pikfyve Mtm1 Plcb4 Plcb3 Plcb2 Plcb1 Mtmr3 Plcd1 Pi4ka Pi4kb Mtmr6 Inpp4a Inpp4b Pik3c2g Pik3c2a Pik3c3 Mtmr1 Mtmr2 Plcz1 Inpp5e Inpp5b Plcg2 Synj1 Pip4p1 Pip4p2 Plcd3 Plcd4 Plce1 Pip4k2b Pip4k2c Pip4k2a Pik3c2b Pi4k2a Pi4k2b Mtmr14 Pten Rock2 Gsn Pip5k1a Pip5k1b Pip5k1c
19	22	0,4622	106,8	27,79	7,18E-08	G6pc3 G6pc2 Galm Glb1 G6pc Gnpda1 Amdhd2 Mpi Lct Gnpnat1 Gla Dcxr Sord Gfpt2 Gfpt1 Gck Hk2 Hk1 Hkdc1 Akr1b8 Hk3 Gnpda2
20	18	0,6836	104,6	56,3	4,14E-07	Dtx1 Dtx2 Dtx4 Psen1 Psen2 Dner Ncstn Psenen Mfng Lfng Aph1a Aph1b Aph1c Notch3 Notch2

						Notch1 Notch4 Rfng
21	17	0,7691	104,6	71,38	8,39E-07	Acvr2b Bmp2 Acvr2a Smad3 Smad2 Smad1 Smad7 Smad6 Smad5 Smad4 Smad9 Zfyve16 Bmpr2 Bmpr1b Bmpr1a Acvr1 Ube2d3
22	79	0,3064	943,9	1187	1,02E-06	Epn2 Eps15l1 Klk1b4 Tek Epha2 Gab1 Kl Pdgfd Pdgfc Pdgfa Flrt1 Cblb Cblc Csf1 Efna1 Efna3 Efna4 Efna5 Efna2 Rnf41 Angpt4 Angpt1 Angpt2 Fgf18 Flt1 Flt4 Mdm2 Kit Epn3 Shc3 Shc2 Shc1 Shc4 Irs1 Fgfr3 Fgfr2 Fgfr4 Sh3glb1 Met Igf1r Kdr Sh3glb2 Ntrk1 Nedd4 Nedd4l Igf1 Ngf Pgf Csf1r Fgf1 Fgf2 Fgf3 Fgf4 Fgf5 Fgf6 Fgf7 Fgf8 Fgf9 Insr Wwp1 Pdgfra Pdgfrb Fgfr1 Fgf14 Fgf15 Fgf16 Fgf17 Fgf10 Fgf11 Fgf12 Fgf13 Sh3kbp1 Fgf21 Fgf20 Fgf23 Fgf22 Sh3gl3 Ngfr Sos2
23	19	0,5632	96,3	36,19	3,62E-06	Acer2 Acer1 Sgpl1 Plpp2 Kdsr Plpp3 Acer3 Sphk1 Sphk2 Sgpp1 Sgpp2 Asah2 Asah1 Cers1 Cers3 Cers2 Cers5 Cers4 Cers6
24	9	0,875	31,5	0,9	6,65E-05	Pofut2 Spon1 Adamts7 Adamts5 Adamtsl4 Adamtsl1 Cfp Adamts13 B3glct
25	48	0,3607	406,9	446,5	6,73E-05	Bcar1 Pxn Itgb8 Itgb6 Itgb7 Itgb4 Itgb5 Itgb2 Itgb3 Itgb1 Actn3 Lamc1 Lamc2 Col18a1 Thbs1 Lamb3 Lamb1 Hspg2 Bcan Tln1 Tln2 Bsg Sema7a Plxnc1 Mmp3 Icam1 Icam2 Itga2b Cd36 Itgal Itga7 Itga6 Itga5 Itga4 Itga3 Itga2 Itga1 Itga9 Itga8 Itgav Sdc4 Sdc1 Itga11 Itga10 Mmp13 Mmp14 Lama3 Lama1
26	9	0,6611	23,8	0	7,03E-05	Txnrd1 Sephs1 Txnrd3 Txnrd2 Scly Sephs2 Cth Kyat3 Kyat1
27	11	0,6202	34,11	11,1	7,66E-05	Nlrp1b Casp4 Nlrp1a Aim2 Naip2 Naip6 Naip5 Nlrc4 Pycard Nlrp3 Casp1
28	29	0,3936	159,8	194,6	0,000169492	Calml3 Eif2s1 Ppp1ca Ppp1cc Ppp1cb Gys2 Epm2a Gys1 Phka2 Phka1 Rps6ka6 Rps6ka3 Rps6ka2 Rps6ka1 Nhlrc1 Ppp1r3a Ppp1r3c Ppp1r3e Ppp1r3f Phkb Ppp1r3b Ppp1r3d Eif2ak4 Eif2ak2 Eif2ak3 Eif2ak1 Calm4 Phkg1 Phkg2
29	16	0,5366	64,39	86,52	0,000794959	Gys2 Epm2a Gys1 Phka2 Phka1 Rps6ka6 Nhlrc1 Ppp1r3a Ppp1r3c Ppp1r3e Ppp1r3f Phkb Ppp1r3b Ppp1r3d Phkg1 Phkg2
30	10	0,8986	40,44	28,88	0,000872598	Dtx4 Zbp1 Nlrp4b Tbk1 Tmem173 Nlrp4e Nlrp4f Nlrp4a Nlrp4c Irf3
31	24	0,6618	182,7	218,3	0,00117289	Mbd3 Gatad2b Brpf1 Chd3 Taf1d Taf1b Sirt1 Hdac1 Taf1c Rbbp4 Rbbp7 Ing5 Chd4 Pml Tbp Ehmt2

						Ttf1 Mta3 Mta2 Meaf6 Mta1 Csnk2a1 Brd7 Ercc6
32	10	0,7807	35,13	30,47	0,00125347	Atg5 Mfn2 Atg12 Mterf3 Map1lc3a Pink1 Mfn1 Prkn Vdac1 Sqstm1
33	13	0,7705	60,1	63,35	0,00136332	Ptpn12 Fscn1 Sh3pxd2a Sh3pxd2b Lcp1 Lpxn Tpm3 Tpm4 Tpm3-rs7 Vcam1 Gsn Kif9 Dbnl
34	6	0,83	12,45	9,241	0,0024233	Masp2 C4b Masp1 C2 Mbl1 Mbl2
35	18	0,8037	123	207,2	0,00361825	Stx6 Dhrs11 Arfrp1 Rgp1 Vps54 Vps51 Vps53 Tmf1 Rab6a Arl1 Rab43 Vps52 Golga1 Golga4 Ric1 Vti1a Gcc1 Stx16
36	5	0,8227	8,227	0	0,00364518	Mafk Maff Hbb-bh1 Mafg Nfe2
37	6	0,3	4,5	1,708	0,00444082	Gata3 Zfpm2 Gata2 Gata5 Gata6 Gata1
38	11	0,8377	46,07	49,61	0,00500049	Try10 Gm10334 Prss2 Prss3 Prss1 Sspo Gm5771 Try4 Try5 Mmp9 Mmp13
39	5	0,815	8,15	4,5	0,00520889	Fnip2 Rragc Fnip1 Rragd Flcn
40	7	0,4643	9,75	5,3	0,00817357	Igkv4-62 Fnip2 Rragc Fnip1 Rragd Flcn Lcn2
41	7	0,3876	8,14	5,01	0,00926279	Rps24 Denr Eif2s1 Eif3c Mcts1 Rps17 Mcts2
42	4	0,5582	3,349	0,9	0,0265039	Adgrl2 Tenm2 Shank1 Shank3
43	7	0,8663	18,19	23,78	0,0275087	Ppard Pdha1 Pdk1 Dld Pdhb Pdhx Dlat
44	3	0,8667	2,6	2,7	0,0296732	Mgll Gk2 Gk
45	3	0,5333	1,6	0	0,0296732	Selplg Sele Glg1
46	3	0,8667	2,6	0	0,0296732	Heph Slc40a1 Cp
47	14	0,455	41,4	73,44	0,0383875	Rxra Rxrb Rxrg Fabp5 Ppard Med1 Pdha1 Pdk1 Thra Thrb Dld Pdhb Pdhx Dlat
48	22	0,8382	193,6	339	0,0410554	Clspn Orc1 Orc3 Orc2 Orc5 Orc4 Chek1 Dbf4 Mcm10 Cdc7 Cdc6 Cdc45 Rpa3 Rpa1 Usp28 Mcm8 Mcm2 Mcm3 Mcm4 Mcm6 Mcm7 Atrip
49	18	0,7361	112,6	125,1	0,0414074	Dcaf10 Dcaf17 Dcaf11 Dcaf12 Dcaf13 Trpc4ap Cul4b Cul4a Dcaf5 Dcaf6 Dcaf7 Glmn Dcaf8 Ddb1 Ddb2 Crbn Ercc8 Dtl
50	5	0,3237	3,237	3,247	0,0631897	Srxn1 Prdx1 Prdx2 Prdx3 Prdx4
51	13	0,3283	25,61	48,89	0,0674411	Col18a1 Ctss Ctsl Ctsk Twnk Ctsf Ctso Birc3 Col15a1 Ctsb Sept4 Ctsd Xiap
52	17	0,55	74,79	161,8	0,0740005	Stx6 Cplx1 Dhrs11 Stx7 Stx3 Vps45 Snap29 Snap23 Napb Syn2 Vti1b Snx4 Snap25 Stx16 Stx17 Stx12 Stx1a
53	8	0,35	9,8	20,13	0,0741319	Dcxr Sord Rbp2 Mgll Gk2 Akr1b8 Dhdh Gk
54	3	0,9	2,7	2,7	0,0983528	Nqo1 Ggcx Vkorc1l1
55	14	0,5312	48,34	94,81	0,129783	Ctnna2 Ctnna1 Cdon Tcf3 Mef2a Mef2c Myod1 Bnip2 Cdh2 Cdh15

						Spag9 Myf6 Myf5 Myog
56	3	0,5805	1,742	0,9	0,130577	Il33 Il1rl1 Gata3
57	4	0,6058	3,635	7,375	0,148742	Cyp7b1 Ch25h Hsd3b7 Cyp27a1
58	10	0,4688	21,1	32,42	0,153472	Arg1 Arg2 Asl Ass1 Azin2 Oat Otc Gatm Acy1 Gm853
59	3	0,8	2,4	4	0,318676	Slc8a3 Slc8a2 Slc8a1
60	3	0,8	2,4	9,315	0,318676	Mmp3 Mmp1b Mmp1a
61	3	0,9	2,7	2,7	0,318676	Bsg Slc3a2 Slc7a11
62	5	0,6201	6,201	27	0,335201	Hmox1 Hmox2 Blvra Blvrb Rfk
63	5	0,87	8,7	21,56	0,335687	Col18a1 Ctss Ctsl Col15a1 Ctsb
64	9	0,4097	14,75	60,44	0,447177	Tbpl2 Tbpl1 Ets1 Ets2 Srf Thbs1 Ltbp1 Tbp Id1
65	11	0,3212	17,67	147,2	0,447595	Tbpl2 Tbpl1 Ets1 Runx1 Ets2 Srf Gata4 Mapk3 Tbx3 Tbp Id1
66	10	0,3002	13,51	43,13	0,468812	Ctsk Ctsh Twnk Ctsf Ctso Birc3 Ctsb Sept4 Ctsd Xiap
67	6	0,8933	13,4	24,2	0,532837	Ptges2 Ptgis Fam213b Ptgds Ptges Tbxas1
68	14	0,6199	56,41	171,9	0,536745	Myl6b Myl10 Myl9 Myl7 Myl6 Tln1 Sema7a Plxnc1 Tpm4 Rock2 Mylpf Itga1 Myl12a Myl12b
69	30	0,2635	114,6	306,1	0,544152	Ikbkb Ikbkg Diablo Ube2n Ripk2 Glipr1 Map2k4 Map2k7 Bcl10 Htra2 Tlr4 Tlr5 Map3k8 Ube2v1 Traf6 Traf5 Birc3 Traf1 Tnip2 Chuk Rnf31 Card11 Cyld Myd88 Map3k7 Map3k1 Map3k3 Malt1 Ripk1 Bcl3
70	19	0,4865	83,2	415,4	0,55807	Cdc37 Erbin Lrig1 Erbb2 Rnf41 Erbb4 Erbb3 Nrg4 Nrg1 Hsp90b1 Ereg Memo1 Btc Trap1 Diaph1 Ttc28 Hbegf Ptk6 Egf
71	8	0,6929	19,4	34,51	0,562909	Bco1 Dhrs3 Dhrs4 Awat2 Lrat Dhrs9 Dgat1 Retsat
72	3	0,8337	2,501	5,002	0,603926	Dkk4 Dkk1 Dkk2
73	5	0,3515	3,515	35,61	0,73519	Ppat Gart Stat3 Flt3 Hr
74	5	0,825	8,25	16,81	0,73582	Tbpl2 Tbpl1 Ets1 Ets2 Srf
75	46	0,3008	311,3	964,4	0,88026	Ikbkb Ikbkg Diablo Ube2n Ripk2 Tnfsf14 Tnfsf11 Tnfsf12 Glipr1 Map2k4 Map2k7 Bcl10 Cd40 Htra2 Tlr4 Map3k8 Ube2v1 Traf6 Traf5 Traf3 Traf2 Ltbr Birc2 Birc3 Traf1 Chuk Tnf Tnfrsf1b Rnf31 Card11 Tnfsf13b Cyld Tnfrsf11a Myd88 Lta Ltb Map3k7 Map3k1 Map3k3 Malt1 Ripk1 Map3k14 Tnfrsf13c Sqstm1 Tnfrsf12a Cd40lg
76	6	0,5024	7,536	49,73	0,885117	Hsp90ab1 Cdc37 Hsp90b1 Nlrp3 Trap1 Ttc28
77	6	0,7958	11,94	31,81	0,913257	Srf Gata4 Nfatc4 Nfatc3 Nfatc2 Nfatc1
78	4	0,8	4,8	12,02	0,916825	Runx1 Mecom Ctbp2 Ctbp1
79	43	0,3027	273,3	976,9	0,926618	Rhobtb2 Rhobtb1 Hsp90ab1 Mpig6b Rac3 Rac2 Plxna1 Trem2

						Vav2 Vav3 Vav1 Pak2 Ptpn6 Cyba Cybb Pik3r6 Pdpn Plcg2 Pik3ap1 Txk Lat Nck2 Nck1 Lcp2 Sema6d Tyrobp Ncf4 Ncf1 Ncf2 Fyn Btk Fcer1g Rac1 Cd19 Clec1b Map3k1 Cd28 Lyn Mapk13 Nox3 Itk Syk Sos1
80	11	0,7359	40,47	103,3	0,942534	Ager Cyba Cybb Nox1 Ncf4 Ncf1 Ncf2 Mmp2 Mmp9 Vcam1 Nox3
81	9	0,5227	18,82	109,3	0,944112	Itgam Itgb2 Tln2 Msn Itgb2l Icam1 Icam2 Itgal Ezr
82	40	0,3006	234,4	921,7	0,945448	Rhobtb2 Rhobtb1 Hsp90ab1 Mpig6b Rac3 Rac2 Plxna1 Trem2 Vav2 Vav3 Vav1 Pak2 Ptpn6 Cybb Pik3r6 Pdpn Plcg2 Pik3ap1 Txk Lat Nck2 Nck1 Lcp2 Sema6d Tyrobp Fyn Btk Fcer1g Rac1 Ctla4 Cd19 Clec1b Map3k1 Map4k3 Cd28 Lyn Cdk5 Itk Syk Sos1
83	6	0,4809	7,214	44,89	0,954223	Plxna1 Trem2 Cables1 Sema6d Tyrobp Cdk5
84	7	0,4952	10,4	53,18	0,958758	Magi1 Magi2 Magi3 Rapgef6 Rapgef2 Id1 Rap1b
85	5	0,8	8	23,34	0,96268	Magi1 Magi2 Magi3 Rapgef6 Rapgef2
86	30	0,3169	137,9	550,8	0,967814	Epn2 Eps15l1 Cdc37 Erbin Egfr Lrig1 Erbb2 Cblb Cblc Rnf41 Erbb4 Erbb3 Epn3 Nrg4 Nrg1 Sh3glb1 Ereg Memo1 Sh3glb2 Ntrk1 Nedd4 Btc Nedd4l Diaph1 Wwp1 Hbegf Ptk6 Sh3kbp1 Lrrk2 Sh3gl3
87	8	0,9059	25,37	50,51	0,970425	Cct6b Tcp1 Cct5 Cct4 Cct7 Cct3 Cct2 Cct8
88	5	0,635	6,35	31,04	0,97111	Hspg2 Bcan Sdc4 Sdc1 Mmp14
89	12	0,3402	22,45	136,8	0,973451	Itgam Itgb2 Tln2 Msn Itgb2l Dcc Ntn1 Icam1 Icam2 Itgal Ezr Unc5c
90	5	0,3168	3,168	33,49	0,974553	Uba52 Usp46 Usp35 Usp38 Usp12
91	6	0,4628	6,942	41,47	0,984681	Tlr4 Tlr5 Tlr2 Myd88 Cd36 Hmgb1
92	68	0,2951	672,3	2206	0,98515	Gnb2 Gnb3 Gnb4 Gnb5 Plcb4 Plcb3 Plcb2 Plcb1 Gng7 Gngt1 Gngt2 Map2k1 Map2k2 Gnal Mapk8 Mapk1 Rps6ka5 Mapk3 Cyba Cybb Fos Prkacb Rasgrf2 Dusp10 Nox1 Mapk11 Prkcg Prkcb Prkca Gm5741 Jun Prex1 Myod1 Ncf4 Fosl1 Ncf1 Ncf2 Fosl2 Pgr Mmp2 Mmp9 Gnao1 Fosb Vcam1 Junb Prkg2 Mapk9 Cacna1s Cacna1f Cacna1d Cacna1b Cacna1a Gng8 Mapk13 Mapk12 Gng3 Gng4 Mapk14 Nox3 Mapk10 Myf5 Jund Myog Gng13 Gng12 Gng11 Gng10 Ezr
93	3	0,8833	2,65	18,53	0,985452	Rgl1 Ralb Rala
94	3	0,6	1,8	13,07	0,986587	Wee1 Cables1 Cdk5
95	3	0,8793	2,638	18,97	0,986587	Mpig6b Pdpn Clec1b

96	3	0,9157	2,747	16,86	0,986587	Ager S100b Hmgb1
97	6	0,7067	10,6	34,44	0,986816	Myl1 Myl3 Myl2 Myl4 Tnnc2 Tnnc1
98	3	0,8	2,4	11,23	0,990789	Keap1 Klhl13 Klhl9
99	4	0,8552	5,131	43,71	0,992931	Ocln Csnk2b Csnk2a1 Csnk2a2
100	4	0,85	5,1	45,25	0,9943	Gp1bb Gp1ba Gp5 Gp9
101	20	0,5924	112,6	429	0,996982	Bcar1 Pxn Dock1 Brk1 Pdcd10 Elmo2 Abi1 Cables1 Shb Nckap1 Elmo1 Abl1 Crk Wasf2 Cdk5 Ptk6 Nckap1l Cyfip2 Cyfip1 Baiap2
102	6	0,8165	12,25	116,6	0,998499	Pdgfd Pdgfc Pdgfa Insrr Tgfa Igf1
103	21	0,3033	63,69	328,5	0,998836	Rasgrp2 Rasgrp1 Rasgrp4 Rasgrp3 Magi1 Rapgef6 Rasgrf2 Rgl1 Rapgef2 Rras Rras2 Rasa1 Tiam1 Nras Cacna1g Cacna1e Cacna1i Cacna1h Rap1b Mras Sos2
104	10	0,4056	18,25	148,3	0,99892	Ccl12 Ccl4 Ccl7 Ccl3 Ccl2 Ackr2 Cx3cr1 Cxcr4 Xcr1 Irf5
105	13	0,69	53,82	237	0,998956	Csf2ra Csf2rb Inppl1 Sftpd Ptpn6 Csf2rb2 Inpp5d Il2rg Il2rb Il2ra Ctla4 Il3ra Il5ra
106	21	0,3062	64,31	323,1	0,999169	Ikbkb Ikbkg Diablo Socs3 Htra2 Traf6 Traf5 Irs3 Irs2 Irs1 Irs4 Prkce Chuk Rnf31 Cyld Map3k7 Map3k3 Malt1 Ripk1 Mtor Bcl3
107	21	0,3253	68,32	534,7	0,999742	Sem1 Brcc3 Mpnd Cops2 Mysm1 Gm973 Adrm1 Bap1 Pcgf1 Bcor Ublcp1 Psmc2 Pomp Psmb9 Bcl6b Gm9774 Ubfd1 Psmg2 Uchl5 Usp14 Bcl6

Literature References

1 Sorg, H., Tilkorn, D. J., Hager, S., Hauser, J. & Mirastschijski, U. Skin Wound Healing: An Update on the Current Knowledge and Concepts. *Eur Surg Res* **58**, 81-94, doi:10.1159/000454919 (2017).

2 Gurtner, G. C., Werner, S., Barrandon, Y. & Longaker, M. T. Wound repair and regeneration. *Nature* **453**, 314-321, doi:10.1038/nature07039 (2008).

3 Guo, S. & Dipietro, L. A. Factors affecting wound healing. *J Dent Res* **89**, 219-229, doi:10.1177/0022034509359125 (2010).

4 Falanga, V. Wound healing and its impairment in the diabetic foot. *Lancet* **366**, 1736-1743, doi:10.1016/S0140-6736(05)67700-8 (2005).

5 Landen, N. X., Li, D. & Stahle, M. Transition from inflammation to proliferation: a critical step during wound healing. *Cell Mol Life Sci* **73**, 3861-3885, doi:10.1007/s00018-016-2268-0 (2016).

6 Koh, T. J. & DiPietro, L. A. Inflammation and wound healing: the role of the macrophage. *Expert Rev Mol Med* **13**, e23, doi:10.1017/S1462399411001943 (2011).

7 Eming, S. A., Martin, P. & Tomic-Canic, M. Wound repair and regeneration: mechanisms, signaling, and translation. *Sci Transl Med* **6**, 265sr266, doi:10.1126/scitranslmed.3009337 (2014).

8 Gill, S. E. & Parks, W. C. Metalloproteinases and their inhibitors: regulators of wound healing. *Int J Biochem Cell Biol* **40**, 1334-1347, doi:10.1016/j.biocel.2007.10.024 (2008).

9 Gonzalez, A. C., Costa, T. F., Andrade, Z. A. & Medrado, A. R. Wound healing - A literature review. *An Bras Dermatol* **91**, 614-620, doi:10.1590/abd1806-4841.20164741 (2016).

10 <The Role of Myofibroblasts in Wound Healing, Contraction and its Clinical Implications in Cleft Palate Repair.pdf>.

11 Chitturi, R. T. *et al.* The role of myofibroblasts in wound healing, contraction and its clinical implications in cleft palate repair. *J Int Oral Health* **7**, 75-80 (2015).

12 Neve, A., Cantatore, F. P., Maruotti, N., Corrado, A. & Ribatti, D. Extracellular matrix modulates angiogenesis in physiological and

pathological conditions. *Biomed Res Int* **2014**, 756078, doi:10.1155/2014/756078 (2014).

13 Micallef, L. *et al.* The myofibroblast, multiple origins for major roles in normal and pathological tissue repair. *Fibrogenesis Tissue Repair* **5**, S5, doi:10.1186/1755-1536-5-S1-S5 (2012).

14 Falke, L. L., Gholizadeh, S., Goldschmeding, R., Kok, R. J. & Nguyen, T. Q. Diverse origins of the myofibroblast-implications for kidney fibrosis. *Nat Rev Nephrol* **11**, 233-244, doi:10.1038/nrneph.2014.246 (2015).

15 DiPietro, L. A. Angiogenesis and wound repair: when enough is enough. *J Leukoc Biol* **100**, 979-984, doi:10.1189/jlb.4MR0316-102R (2016).

16 Demidova-Rice, T. N., Durham, J. T. & Herman, I. M. Wound Healing Angiogenesis: Innovations and Challenges in Acute and Chronic Wound Healing. *Adv Wound Care (New Rochelle)* **1**, 17-22, doi:10.1089/wound.2011.0308 (2012).

17 Borena, B. M. *et al.* Regenerative Skin Wound Healing in Mammals: State-of-the-Art on Growth Factor and Stem Cell Based Treatments. *Cell Physiol Biochem* **36**, 1-23, doi:10.1159/000374049 (2015).

18 Brem, H. & Tomic-Canic, M. Cellular and molecular basis of wound healing in diabetes. *J Clin Invest* **117**, 1219-1222, doi:10.1172/JCI32169 (2007).

19 Payne, W. G. *et al.* Wound healing in patients with cancer. *Eplasty* **8**, e9 (2008).

20 Serena, T. E. A Global Perspective on Wound Care. *Adv Wound Care (New Rochelle)* **3**, 548-552, doi:10.1089/wound.2013.0460 (2014).

21 Takeo, M., Lee, W. & Ito, M. Wound healing and skin regeneration. *Cold Spring Harb Perspect Med* **5**, a023267, doi:10.1101/cshperspect.a023267 (2015).

22 Augustin, M. Cumulative life course impairment in chronic wounds. *Curr Probl Dermatol* **44**, 125-129, doi:10.1159/000350789 (2013).

23 Barrientos, S., Stojadinovic, O., Golinko, M. S., Brem, H. & Tomic-Canic, M. Growth factors and cytokines in wound healing. *Wound Repair Regen* **16**, 585-601, doi:10.1111/j.1524-475X.2008.00410.x (2008).

24 Grazul-Bilska, A. T. *et al.* Wound healing: the role of growth factors. *Drugs Today (Barc)* **39**, 787-800 (2003).

25 Barrientos, S., Brem, H., Stojadinovic, O. & Tomic-Canic, M. Clinical application of growth factors and cytokines in wound healing. *Wound Repair Regen* **22**, 569-578, doi:10.1111/wrr.12205 (2014).

26 Takeuchi, O. & Akira, S. Pattern recognition receptors and inflammation. *Cell* **140**, 805-820, doi:10.1016/j.cell.2010.01.022 (2010).

27 Cordeiro, J. V. & Jacinto, A. The role of transcription-independent damage signals in the initiation of epithelial wound healing. *Nat Rev Mol Cell Biol* **14**, 249-262, doi:10.1038/nrm3541 (2013).

28 Wang, Z. Transactivation of Epidermal Growth Factor Receptor by G Protein-Coupled Receptors: Recent Progress, Challenges and Future Research. *Int J Mol Sci* **17**, doi:10.3390/ijms17010095 (2016).

29 Caley, M. P., Martins, V. L. & O'Toole, E. A. Metalloproteinases and Wound Healing. *Adv Wound Care (New Rochelle)* **4**, 225-234, doi:10.1089/wound.2014.0581 (2015).

30 Penn, J. W., Grobbelaar, A. O. & Rolfe, K. J. The role of the TGF-beta family in wound healing, burns and scarring: a review. *Int J Burns Trauma* **2**, 18-28 (2012).

31 Finnson, K. W., McLean, S., Di Guglielmo, G. M. & Philip, A. Dynamics of Transforming Growth Factor Beta Signaling in Wound Healing and Scarring. *Adv Wound Care (New Rochelle)* **2**, 195-214, doi:10.1089/wound.2013.0429 (2013).

32 Wu, M. Y. & Hill, C. S. Tgf-beta superfamily signaling in embryonic development and homeostasis. *Dev Cell* **16**, 329-343, doi:10.1016/j.devcel.2009.02.012 (2009).

33 Poniatowski, L. A., Wojdasiewicz, P., Gasik, R. & Szukiewicz, D. Transforming growth factor Beta family: insight into the role of growth factors in regulation of fracture healing biology and potential clinical applications. *Mediators Inflamm* **2015**, 137823, doi:10.1155/2015/137823 (2015).

34 Moustakas, A. & Heldin, C. H. The regulation of TGFbeta signal transduction. *Development* **136**, 3699-3714, doi:10.1242/dev.030338 (2009).

35 Brunner, G. & Blakytny, R. Extracellular regulation of TGF-beta activity in wound repair: growth factor latency as a sensor mechanism for injury. *Thromb Haemost* **92**, 253-261, doi:10.1160/TH04-05-0324 (2004).

36 Li, B. & Wang, J. H. Fibroblasts and myofibroblasts in wound healing: force generation and measurement. *J Tissue Viability* **20**, 108-120, doi:10.1016/j.jtv.2009.11.004 (2011).

37 Darby, I., Skalli, O. & Gabbiani, G. Alpha-smooth muscle actin is transiently expressed by myofibroblasts during experimental wound healing. *Lab Invest* **63**, 21-29 (1990).

38 Shin, D. & Minn, K. W. The effect of myofibroblast on contracture of hypertrophic scar. *Plast Reconstr Surg* **113**, 633-640, doi:10.1097/01.PRS.0000101530.33096.5B (2004).

39 Glading, A., Chang, P., Lauffenburger, D. A. & Wells, A. Epidermal growth factor receptor activation of calpain is required for fibroblast motility and occurs via an ERK/MAP kinase signaling pathway. *J Biol Chem* **275**, 2390-2398 (2000).

40 Huang, C., Jacobson, K. & Schaller, M. D. MAP kinases and cell migration. *J Cell Sci* **117**, 4619-4628, doi:10.1242/jcs.01481 (2004).

41 Sabio, G. & Davis, R. J. TNF and MAP kinase signalling pathways. *Semin Immunol* **26**, 237-245, doi:10.1016/j.smim.2014.02.009 (2014).

42 Barr, R. K. & Bogoyevitch, M. A. The c-Jun N-terminal protein kinase family of mitogen-activated protein kinases (JNK MAPKs). *Int J Biochem Cell Biol* **33**, 1047-1063 (2001).

43 Pereira, A. M., Tudor, C., Kanger, J. S., Subramaniam, V. & Martin-Blanco, E. Integrin-dependent activation of the JNK signaling pathway by mechanical stress. *PLoS One* **6**, e26182, doi:10.1371/journal.pone.0026182 (2011).

44 Song, Q., Gou, Q., Xie, Y., Zhang, Z. & Fu, C. Periplaneta americana Extracts Promote Skin Wound Healing via Nuclear Factor Kappa B Canonical Pathway and Extracellular Signal-Regulated Kinase Signaling. *Evid Based Complement Alternat Med* **2017**, 5821706, doi:10.1155/2017/5821706 (2017).

45 Saika, S. *et al.* Role of p38 MAP kinase in regulation of cell migration and proliferation in healing corneal epithelium. *Invest Ophthalmol Vis Sci* **45**, 100-109 (2004).

46 Alexander, C. M. *et al.* Expression and function of matrix metalloproteinases and their inhibitors at the maternal-embryonic boundary during mouse embryo implantation. *Development* **122**, 1723-1736 (1996).

47 Parks, W. C., Wilson, C. L. & Lopez-Boado, Y. S. Matrix metalloproteinases as modulators of inflammation and innate immunity. *Nat Rev Immunol* **4**, 617-629, doi:10.1038/nri1418 (2004).

48 Xue, M. & Jackson, C. J. Extracellular Matrix Reorganization During Wound Healing and Its Impact on Abnormal Scarring. *Adv Wound Care (New Rochelle)* **4**, 119-136, doi:10.1089/wound.2013.0485 (2015).

49 Page-McCaw, A., Ewald, A. J. & Werb, Z. Matrix metalloproteinases and the regulation of tissue remodelling. *Nat Rev Mol Cell Biol* **8**, 221-233, doi:10.1038/nrm2125 (2007).

50 Yan, C. & Boyd, D. D. Regulation of matrix metalloproteinase gene expression. *J Cell Physiol* **211**, 19-26, doi:10.1002/jcp.20948 (2007).

51 Li, G. *et al.* c-Jun is essential for organization of the epidermal leading edge. *Dev Cell* **4**, 865-877 (2003).

52 Angel, P., Szabowski, A. & Schorpp-Kistner, M. Function and regulation of AP-1 subunits in skin physiology and pathology. *Oncogene* **20**, 2413-2423, doi:10.1038/sj.onc.1204380 (2001).

53 Borden, P. & Heller, R. A. Transcriptional control of matrix metalloproteinases and the tissue inhibitors of matrix metalloproteinases. *Crit Rev Eukaryot Gene Expr* **7**, 159-178 (1997).

54 Ozsolak, F. & Milos, P. M. RNA sequencing: advances, challenges and opportunities. *Nat Rev Genet* **12**, 87-98, doi:10.1038/nrg2934 (2011).

55 Wang, Z., Gerstein, M. & Snyder, M. RNA-Seq: a revolutionary tool for transcriptomics. *Nat Rev Genet* **10**, 57-63, doi:10.1038/nrg2484 (2009).

56 Vitali, F. *et al.* Developing a 'personalome' for precision medicine: emerging methods that compute interpretable effect sizes from single-subject transcriptomes. *Brief Bioinform*, doi:10.1093/bib/bbx149 (2017).

57 Ashburner, M. *et al.* Gene ontology: tool for the unification of biology. The Gene Ontology Consortium. *Nat Genet* **25**, 25-29, doi:10.1038/75556 (2000).

58 Conesa, A. *et al.* A survey of best practices for RNA-seq data analysis. *Genome Biol* **17**, 13, doi:10.1186/s13059-016-0881-8 (2016).

59 Robinson, M. D., McCarthy, D. J. & Smyth, G. K. edgeR: a Bioconductor package for differential expression analysis of digital gene expression data. *Bioinformatics* **26**, 139-140, doi:10.1093/bioinformatics/btp616 (2010).

60 Wang, L., Feng, Z., Wang, X., Wang, X. & Zhang, X. DEGseq: an R package for identifying differentially expressed genes from RNA-seq data. *Bioinformatics* **26**, 136-138, doi:10.1093/bioinformatics/btp612 (2010).

61 Tarazona, S. *et al.* Data quality aware analysis of differential expression in RNA-seq with NOISeq R/Bioc package. *Nucleic Acids Res* **43**, e140, doi:10.1093/nar/gkv711 (2015).

62 Li, Q. *et al.* N-of-1-pathways MixEnrich: advancing precision medicine via single-subject analysis in discovering dynamic changes of transcriptomes. *BMC Med Genomics* **10**, 27, doi:10.1186/s12920-017-0263-4 (2017).

63 Schissler, A. G. *et al.* Dynamic changes of RNA-sequencing expression for precision medicine: N-of-1-pathways Mahalanobis distance within pathways of single subjects predicts breast cancer survival. *Bioinformatics* **31**, i293-302, doi:10.1093/bioinformatics/btv253 (2015).

64 Li, Q. *et al.* kMEn: Analyzing noisy and bidirectional transcriptional pathway responses in single subjects. *J Biomed Inform* **66**, 32-41, doi:10.1016/j.jbi.2016.12.009 (2017).

65 Wang, H. *et al.* Individual-level analysis of differential expression of genes and pathways for personalized medicine. *Bioinformatics* **31**, 62-68, doi:10.1093/bioinformatics/btu522 (2015).

66 Liu, R. *et al.* Identifying critical transitions of complex diseases based on a single sample. *Bioinformatics* **30**, 1579-1586, doi:10.1093/bioinformatics/btu084 (2014).

67 Singer, A. J. & Clark, R. A. Cutaneous wound healing. *N Engl J Med* **341**, 738-746, doi:10.1056/NEJM199909023411006 (1999).

68 Pereira, R. F. & Bartolo, P. J. Traditional Therapies for Skin Wound Healing. *Adv Wound Care (New Rochelle)* **5**, 208-229, doi:10.1089/wound.2013.0506 (2016).

69 Hirsch, T. *et al.* Regeneration of the entire human epidermis using transgenic stem cells. *Nature* **551**, 327-332, doi:10.1038/nature24487 (2017).

70 Biswas, A., Bharara, M., Hurst, C., Armstrong, D. G. & Rilo, H. The micrograft concept for wound healing: strategies and applications. *J Diabetes Sci Technol* **4**, 808-819, doi:10.1177/193229681000400407 (2010).

71 Marcarelli, M., Trovato, L., Novarese, E., Riccio, M. & Graziano, A. Rigenera protocol in the treatment of surgical wound dehiscence. *Int Wound J* **14**, 277-281, doi:10.1111/iwj.12601 (2017).

72 Svolacchia, F., De Francesco, F., Trovato, L., Graziano, A. & Ferraro, G. A. An innovative regenerative treatment of scars with dermal micrografts. *J Cosmet Dermatol* **15**, 245-253, doi:10.1111/jocd.12212 (2016).

73 Lampinen, M. *et al.* Intraoperative processing and epicardial transplantation of autologous atrial tissue for cardiac repair. *J Heart Lung Transplant* **36**, 1020-1022, doi:10.1016/j.healun.2017.06.002 (2017).

74 Gottrup, F. Oxygen in wound healing and infection. *World J Surg* **28**, 312-315, doi:10.1007/s00268-003-7398-5 (2004).

75 von Mering, C. *et al.* STRING: known and predicted protein-protein associations, integrated and transferred across organisms. *Nucleic Acids Res* **33**, D433-437, doi:10.1093/nar/gki005 (2005).

76 Gene Ontology, C. Gene Ontology Consortium: going forward. *Nucleic Acids Res* **43**, D1049-1056, doi:10.1093/nar/gku1179 (2015).

77 Vitali, F. *et al.* A Network-Based Data Integration Approach to Support Drug Repurposing and Multi-Target Therapies in Triple Negative Breast Cancer. *PLoS One* **11**, e0162407, doi:10.1371/journal.pone.0162407 (2016).

78 Sharan, R., Ulitsky, I. & Shamir, R. Network-based prediction of protein function. *Mol Syst Biol* **3**, 88, doi:10.1038/msb4100129 (2007).

79 Shannon, P. *et al.* Cytoscape: a software environment for integrated models of biomolecular interaction networks. *Genome Res* **13**, 2498-2504, doi:10.1101/gr.1239303 (2003).

80 Nepusz, T., Yu, H. & Paccanaro, A. Detecting overlapping protein complexes in protein-protein interaction networks. *Nat Methods* **9**, 471-472, doi:10.1038/nmeth.1938 (2012).

81 Wang, X., Ge, J., Tredget, E. E. & Wu, Y. The mouse excisional wound splinting model, including applications for stem cell transplantation. *Nat Protoc* **8**, 302-309, doi:10.1038/nprot.2013.002 (2013).

82 Martinez-Sarra, E. *et al.* Human dental pulp pluripotent-like stem cells promote wound healing and muscle regeneration. *Stem Cell Res Ther* **8**, 175, doi:10.1186/s13287-017-0621-3 (2017).

83 Liang, C. C., Park, A. Y. & Guan, J. L. In vitro scratch assay: a convenient and inexpensive method for analysis of cell migration in vitro. *Nat Protoc* **2**, 329-333, doi:10.1038/nprot.2007.30 (2007).

84 Szklarczyk, D. *et al.* The STRING database in 2017: quality-controlled protein-protein association networks, made broadly accessible. *Nucleic Acids Res* **45**, D362-D368, doi:10.1093/nar/gkw937 (2017).

85 Vitali, F. *et al.* Exploring Wound-Healing Genomic Machinery with a Network-Based Approach. *Pharmaceuticals (Basel)* **10**, doi:10.3390/ph10020055 (2017).

86 Sina, A., Lord-Dufour, S. & Annabi, B. Cell-based evidence for aminopeptidase N/CD13 inhibitor actinonin targeting of MT1-MMP-mediated proMMP-2 activation. *Cancer Lett* **279**, 171-176, doi:10.1016/j.canlet.2009.01.032 (2009).

87 Escuin-Ordinas, H. *et al.* Cutaneous wound healing through paradoxical MAPK activation by BRAF inhibitors. *Nat Commun* **7**, 12348, doi:10.1038/ncomms12348 (2016).

88 Monje, P., Hernandez-Losa, J., Lyons, R. J., Castellone, M. D. & Gutkind, J. S. Regulation of the transcriptional activity of c-Fos by ERK. A novel role for the prolyl isomerase PIN1. *J Biol Chem* **280**, 35081-35084, doi:10.1074/jbc.C500353200 (2005).

89 Murthy, S. *et al.* Evaluation of in vivo wound healing activity of Bacopa monniera on different wound model in rats. *Biomed Res Int* **2013**, 972028, doi:10.1155/2013/972028 (2013).

90 Yin, J., Xu, K., Zhang, J., Kumar, A. & Yu, F. S. Wound-induced ATP release and EGF receptor activation in epithelial cells. *J Cell Sci* **120**, 815-825, doi:10.1242/jcs.03389 (2007).

91 De Francesco, F. *et al.* A Regenerative Approach with Dermal Micrografts in the Treatment of Chronic Ulcers. *Stem Cell Rev* **13**, 139-148, doi:10.1007/s12015-016-9692-2 (2017).

92 Bullard, K. M. *et al.* Impaired wound contraction in stromelysin-1-deficient mice. *Ann Surg* **230**, 260-265 (1999).

93 Kyriakides, T. R. *et al.* Mice that lack matrix metalloproteinase-9 display delayed wound healing associated with delayed reepithelization and disordered collagen fibrillogenesis. *Matrix Biol* **28**, 65-73, doi:10.1016/j.matbio.2009.01.001 (2009).

94 Hattori, N. *et al.* MMP-13 plays a role in keratinocyte migration, angiogenesis, and contraction in mouse skin wound healing. *Am J Pathol* **175**, 533-546, doi:10.2353/ajpath.2009.081080 (2009).

95 Ayuk, S. M., Abrahamse, H. & Houreld, N. N. The Role of Matrix Metalloproteinases in Diabetic Wound Healing in relation to Photobiomodulation. *J Diabetes Res* **2016**, 2897656, doi:10.1155/2016/2897656 (2016).

96 Zhang, W. & Liu, H. T. MAPK signal pathways in the regulation of cell proliferation in mammalian cells. *Cell Res* **12**, 9-18, doi:10.1038/sj.cr.7290105 (2002).

97 Burotto, M., Chiou, V. L., Lee, J. M. & Kohn, E. C. The MAPK pathway across different malignancies: a new perspective. *Cancer* **120**, 3446-3456, doi:10.1002/cncr.28864 (2014).

98 Xia, Y. & Karin, M. The control of cell motility and epithelial morphogenesis by Jun kinases. *Trends Cell Biol* **14**, 94-101, doi:10.1016/j.tcb.2003.12.005 (2004).

99 Javelaud, D., Laboureau, J., Gabison, E., Verrecchia, F. & Mauviel, A. Disruption of basal JNK activity differentially affects key fibroblast functions important for wound healing. *J Biol Chem* **278**, 24624-24628, doi:10.1074/jbc.M301942200 (2003).

100 Cuevas, B. D. *et al.* MEKK1 regulates calpain-dependent proteolysis of focal adhesion proteins for rear-end detachment of migrating fibroblasts. *EMBO J* **22**, 3346-3355, doi:10.1093/emboj/cdg322 (2003).

101 Wortzel, I. & Seger, R. The ERK Cascade: Distinct Functions within Various Subcellular Organelles. *Genes Cancer* **2**, 195-209, doi:10.1177/1947601911407328 (2011).

102 Ding, J. & Tredget, E. E. The Role of Chemokines in Fibrotic Wound Healing. *Adv Wound Care (New Rochelle)* **4**, 673-686, doi:10.1089/wound.2014.0550 (2015).

Martina Balli
martina.balli01@universitadipavia.it

Università degli Studi di Pavia
via Ferrata, 3
27100 Pavia, Italy

MARTINA BALLI

UNVEILING THE MOLECULAR MECHANISM OF AUTOLOOGUS MICRO GRAFT-BASED THERAPY FOR SKIN REGENERATION THEOUGH A BIOINFORMATIC APPROACH

2019